THE SYNTHESIS AND EVALUATION OF N-METHYL-2-PHENYLMALEIMIDE ANALOGUES AS INHIBITORS OF MAO-B

Clarina I. Manley-King

BSc. (Hons) Chem.

Dissertation submitted in partial fulfillment of the requirements for

the degree

Magister Scientiae

in Pharmaceutical Chemistry at the North-West University,
Potchefstroom Campus, South Africa.

Supervisor:	Prof. J.J. Bergh
Co-supervisor:	Dr. J.P. Petzer
Assistant supervisor:	Dr. G. Terre'Blanche

2008

Potchefstroom

Dedicated to my Mum and sisters, for their continued love and encouragement throughout the years.

LET MY GATES BE OPENED

"Go in this strength and in this might, for as I was with Moses, so I will be with you" Joshua 1:5.

TABLE OF CONTENTS

LIST OF SCHEMES

LIST OF FIGURES

LIST OF TABLES

ABBREVIATIONS

AD	– Alzheimer's disease
CNS	– Central nervous system
CSC	– (E)-8-(3-Chlorostyryl)caffeine
DA	– Dopamine
DMSO	– Dimethylsulphoxide
EI-MS	– Electron ionization mass spectroscopy
FAD	– Flavin-adenine dinucleotide
MAO-A	– Monoamine oxidase A
MAO-B	– Monoamine oxidase B
$MMDP^+$	– 1-Methyl-4-(1-methylpyrrol-2-yl)-2,3-dihydropyridinium
MMP^+	– 1-Methyl-4-(1-methylpyrrol-2-yl)pyridinium
MMTP	– 1-Methyl-4-(1-methylpyrrol-2-yl)-1,2,3,6-tetrahydropyridine
Mp	– Melting point
$MPDP^+$	– 1-Methyl-4-phenyl-2,3-dihydropyridinium
MPP^+	– 1-Methyl-4-phenylpyridinium
MPTP	– 1-Methyl-4-phenyl-1,2,3,6-tetrahydropyridine
NMR	– Nuclear magnetic resonance spectroscopy
PD	– Parkinson's disease
SEM	– Standard Error of Mean
SN	– Substantia nigra
TLC	– Thin layer chromatography

ABSTRACT

We have recently demonstrated that 1-methyl-3-phenylpyrrole analogues are moderately potent competitive inhibitors of the enzyme monoamine oxidase B (MAO-B). The most potent analogue was 1-methyl-(4-trifluoromethylphenyl)pyrrole with an enzyme–inhibitor dissociation constant (K_i value) of 1.30 μM. The least potent inhibitor was 1-methyl-3-phenylpyrrole with a K_i value of 118 μM. Since 1-methyl-3-phenylpyrroles probably bind to the active site of MAO-B via hydrophobic interactions, we speculated that modification of the structure to include hydrogen bond acceptors may enhance binding affinity. An example of such a modified structure is N-methyl-2-phenylmaleimide, which may interact with MAO-B via both hydrogen bonding and hydrophobic burial, and hence may act as a more potent inhibitor. In this study we have prepared N-methyl-2-phenylmaleimide and selected phenyl ring substituted analogues. In order to test the merit of N-methyl-2-phenylmaleimides as potential MAO-B inhibitors, the chosen structures were modeled within the active site of human recombinant MAO-B. Results indicated that the carbonyl oxygens of the maleimide ring is stabilized by hydrogen bonding with amino acid residues and water molecules in the substrate cavity of the enzyme while the phenyl ring extends into the entrance cavity. Since similar interactions are not possible with 1-methyl-3-phenylpyrroles, we conclude that N-methyl-2-phenylmaleimides may inhibit MAO-B with enhanced potency compared to the pyrroles.

For the purpose of this study, seven N-methyl-2-phenylmaleimides analogues were synthesized and their enzyme–inhibitor dissociation constants (K_i values) for reversible interaction with MAO-B were determined. The most potent inhibitor among the oxidation products considered was the unsubstituted N-methyl-2-phenylmaleimide with a K_i value of 3.49 μM. The least potent inhibitor was found to be N-methyl-2-(3-trifluromethylphenyl)maleimide with a K_i value of 10.99 μM. The unsubstituted maleimide showed an approximately 30 fold increase in inhibition potency compared to the corresponding 1-methyl-3-phenylpyrrole. This may be in part due to the ability of the carbonyl oxygens of the maleimide ring to interact via hydrogen bonding with active site residues, an interaction which is impossible for the pyrroles.

OPSOMMING

Ons het onlangs aangetoon dat die 1-metiel-3-fenielpirroolanaloë matige potensie toon as kompeterende inhibeerders van die ensiem, monoamienoksidase B (MAO-B). Die mees potente van hierdie verbindings was 1-metiel-(4-trifluoormetielfeniel)pirrool met 'n dissosiasiekonstante vir ensieminhibisie (K_i-waarde) van 1.30 μM. Die swakste inhibeerder was 1-metiel-3-fenielpirrool met 'n K_i-waarde van 118 μM. Aangesien 1-metiel-3-fenielpirrole waarskynlik deur hidrofobiese interaksies aan die aktiewe setel van MAO-B bind, het ons gespekuleer ons dat indien dié strukture so gewysig word dat hulle waterstofbindingsakseptors bevat, bindingsaffiniteit mag verbeter. N-metiel-2-fenielmaleïenimied is 'n voorbeeld van so 'n gemodifiseerde struktuur wat met MAO-B interaksie kan ondergaan deur waterstofbinding sowel as hidrofobiese insluiting en wat dus sodoende sterker inhibisie mag vertoon.

In hierdie studie is 'n reeks N-metiel-2-fenielmaleïenimied-analoë gesintetiseer met geselekteerde substituente op die fenielring. Hierdie gekose strukture is in die aktiewe setel van menslike rekombinante MAO-B gepas om vas te stel of die N-metiel-2-fenielmaleïenimiede belofte toon as MAO-B-inhibeerders. Die resultate het aangedui dat die karbonielsuurstofatome van die maleïenimiedring gestabiliseer word deur waterstofbinding met aminosuurresidue en watermolekules in die substraatsetel van die ensiem en dat die fenielring tot in die ingangsetel strek. Aangesien soortgelyke interaksies nie met die 1-metiel-3-fenielpirrole moontlik is nie, het ons gepostuleer dat die N-metiel-2-fenielmaleïenimiede meer potente MAO-B-inhibeerders sal wees as die pirrole.

Vir hierdie studie is sewe N-metiel-2-fenielmaleïenimied-analoë gesintetiseer waarna hul dissosiasiekonstantes vir ensieminhibisie (K_i-waardes) vir omkeerbare interaksie met MAO-B bepaal is. Die mees potente inhibeerder onder die oksidasieprodukte wat getoets is, was die ongesubstitueerde N-metiel-2-fenielmaleïenimied wat 'n K_i-waarde van 3.49 μM gehad het. Die swakste inhibeerder was N-metiel-2-(3-trifluoormetielfeniel)maleïenimied waarvan die K_i-waarde 10.99 μM was. Die ongesubstitueerde maleïenimied was 30 maal meer potent as die ooreenstemmende 1-metiel-3-fenielpirrool. Dit mag gedeeltelik toegeskryf word aan die vermoë van die karbonielkoolstofatome van die maleïenimiedring tot waterstofbinding met die aktiewe setels op die residue – 'n tipe interaksie wat nie by die pirrole moontlik is nie.

ACKNOWLEDGEMENTS

I am most grateful to God, Almighty, for His unending faithfulness and for honoring His Word in my life.

Deepest love and appreciation goes to my family, for their continued love, encouragement and prayerful support during academic pursuit, you have always been there.

I am deeply indebted to my supervisors;

Professor Kobus Bergh, for his professional guidance throughout my journey and studies in South Africa.

Dr. Jacques Petzer, for his professional supervision, assistance, advice and encouragement throughout the entire research, you deserve my sincere thanks for always being available.

Dr. (Mrs) Gisella Terre'Blanche for her invaluable assistance, warmth and support during my studies.

My gratitude goes to André Joubert, Johan Jodaan and Louis Fourie of the SASOL Centre for Chemistry and staff of the Analytical Technology Laboratory, North West University, who recorded the NMR and MS spectra.

I am very much thankful to all the members of the Pharmaceutical Chemistry department, the School of Pharmacy and CENQAM, North West University, for the invaluable support, warmth, kindness that has contributed to my success and stay in South Africa.

I am deeply indebted to my colleagues at the Laboratory Services, Ministry of Health & Sanitation, Freetown, Sierra Leone, especially my boss Dr Aurthur C. Williams, and Mr Hudson, H. Lawson, who have supported and encouraged me over the years and contributed immensely to my personal career development as an analyst and a researcher. We have indeed come a long way.

I highly acknowledge the financial assistance for this study from the Third World Organization for Women in Science, National Research Foundation and Medical Research Council.

CHAPTER 1.

INTRODUCTION AND OBJECTIVES

1.1 Parkinson's disease

Parkinson's disease is a neurodegenerative disorder characterized pathologically by a marked loss of dopaminergic nigrostriatal neurons and clinically by disabling movement disorders (Jenner, 1998) and is currently the most common degenerative disorder of the ageing brain after Alzheimer's dementia. Parkinson's disease is one of the most widespread neurodegenerative disorders and in North America alone, it affects about 1 million people. It is a multifactorial disorder caused by genetic, various biological and environmental factors. Since it is not clear whether a single entity causes the disease, it is also referred to as the "idiopathic parkinsonism" (Calne, 1989; Calne, 1994). Parkinson's disease is a gradual progressive central neurodegenerative disorder that affects body movement (Ballard *et al.*, 1985). There are four primary symptoms characterizing the disease: tremor, rigidity, bradykinesia and postural instability (Ballard *et al.*, 1985). The motor disabilities characterizing Parkinson's disease are primarily due to the loss of dopaminergic neurons in the substantia nigra, resulting in a dramatic decrease in the dopamine (**1**, DA) levels in the brain (Jenner, 1998). Once dopaminergic neuronal cell death reaches the critical level of 85-90%, the neurological symptoms of Parkinson's disease appear (Reiderer *et al.*, 2004). This disorder has been found to generally affect older people above 50 years. Parkinson's disease is a chronic disease and also progressive (Reiderer *et al.*, 2004). The progressive nature of Parkinson's disease means that it may ultimately lead to severe disability.

The current treatment for Parkinson's disease is the systematic administration of levodopa, a precursor to DA which enters the brain via a carrier mediated transport system where it is converted to DA by the enzyme, L-aromatic amino acid decarboxylase (L-AAAD) (Jenner, 1998; Birkmayer *et al.*, 1975). Since the discovery in the 1960's, that striatal dopamine is deficient in Parkinson's disease and that its replacement with high dosages of levodopa could ameliorate the symptoms of parkinsonism, research on Parkinson's disease has increased dramatically. Although this is still used to treat Parkinson's disease, several problems usually develop during the chronic use of levodopa (Jenner, 1998). With time and disease progression, however, dopamine replacement becomes less efficacious and new adverse effects, including increased oxidative load in the substantia nigra and involuntary movement appear (Reiderer & Youdim, 1986; Youdim & Bakhle, 2006). In order to enhance the efficacy of levodopa treatment, this drug is frequently combined with carbidopa, an L-aromatic amino acid decarboxylase inhibitor, and (R)-deprenyl (**2**),

a monoamine oxidase B (MAO-B) inhibitor. Carbidopa delays the peripheral conversion of levodopa into dopamine until it reaches the brain (Jenner, 1998), while (R)-deprenyl blocks the central metabolism of dopamine (Youdim & Bahkle, 2006).

1.2 The role of MAO-B in Parkinson's disease

Monoamine oxidase (MAO) is a flavin adenine dinucleotide (FAD)-containing enzyme attached to the mitochondrial outer membrane of neuronal, glial, and other cells. Its roles include regulation of the levels of biogenic and xenobiotic amines in the brain and the peripheral tissues by catalyzing their oxidative deamination (Youdim & Bakhle, 2006). On the basis of their substrate and inhibitor specificities, two types of MAO (A and B) have been described. MAO-A preferentially deaminates serotonin and norepinephrine and is irreversibly inhibited by low concentrations of clorgyline (**3**). MAO-B preferentially deaminates arylalkylamines such as benzylamine (**4**) and is irreversibly inhibited by (R)-deprenyl (**2**) (Waldmeier, 1987). Both isoforms utilize dopamine as substrate (Youdim & Bakhle, 2006). Due to their role in the metabolism of catecholamine neurotransmitters, MAO-A and –B have long been of considerable pharmacological interest and reversible and irreversible inhibitors of MAO-A and -B have been used clinically to treat neurological disorders including depression and Parkinson's disease (PD) (Youdim & Bakhle, 2006). MAO-B has also been implicated in neurodegenerative processes resulting from exposure to xenobiotic amines. For example, the first step of the bioactivation of the parkinsonian inducing pro-neurotoxin, 1-methyl-4-phenyl-1,2,3,6-tetrahydropyridine (**5**, MPTP) is catalyzed by MAO-B (Chiba *et al.*, 1984).

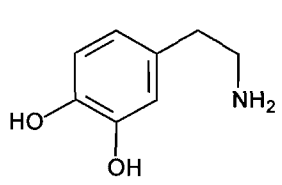

Dopamine (**1**)

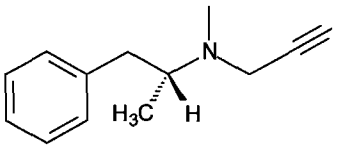

(R)-Deprenyl (**2**)

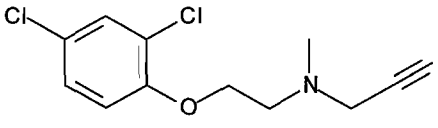

Clorgyline (**3**)

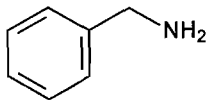

Benzylamine (**4**)

Figure 1.The structures of dopamine (**1**), (R)-deprenyl (**2**), clorgyline (**3**) and benzylamine (**4**).

MAO-A and –B are therefore important targets for the development of new drugs. We are particularly interested in the therapeutic role of MAO-B inhibitors in Parkinson's disease. Since the MAO-B isoform appears to be predominantly responsible for dopamine metabolism in the basal ganglia (Youdim *et al.*, 1972), inhibition of this enzyme in the brain may conserve the depleted supply of dopamine and inhibitors are frequently used in combination with levodopa as dopamine replacement therapy in patients diagnosed with early Parkinson's disease (Birkmayer *et al.*, 1975). For example, MAO-B inhibitors have been shown to elevate dopamine levels in the striatum of primates treated with levodopa (Finberg *et al.*, 1998). Furthermore, in the catalytic cycle of MAO, one mole of dopaldehyde and H_2O_2 is produced for each mole of dopamine oxidized. Both these catabolic products may be neurotoxic, if not rapidly inactivated by centrally located aldehyde dehydrogenase (ADH) (Gesi *et al.*, 2001) and glutathione peroxidase (Flohe, 1978), respectively. Thus inhibitors of MAO-B may also exert a neuroprotective effect by stoichiometrically decreasing aldehyde and H_2O_2 production in the brain. Inhibitors that have been demonstrated to be of clinical value include the mechanism-based inactivators (R)-deprenyl (Ebadi *et al.*, 2006) and rasagiline (**6**) (Rabey *et al.*, 2000) and reversible inhibitors such as lazabemide (Dingemanse *et al.*, 1997) and safinamide (Chazot, 2001).

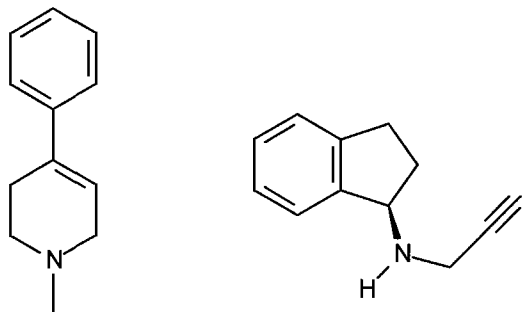

MPTP (**5**) Rasagiline (**6**)

Figure 2. The structures of MPTP (**5**) and rasagiline (**6**).

From a safety point of view, reversible inhibitors may be therapeutically more desirable than inactivators since MAO-B activity can be regained relatively quickly following withdrawal of the reversible inhibitor. In contrast, return of enzyme activity following treatment with inactivators requires *de novo* synthesis of the MAO-B protein which may require several weeks (Thebault *et al.*, 2004). For this reason, several studies are currently underway to develop reversible inhibitors of MAO-B (Gnerre *et al.*, 2000). These inhibitors act in a competitive manner while retaining selectivity towards MAO-B.

1.3 Hypothesis of this study

We have recently demonstrated that 1-methyl-3-phenylpyrrole analogues are moderately potent competitive inhibitors of the enzyme monoamine oxidase B (MAO-B) (Ogunrombi *et al.*, 2008). The most potent analogue was 1-methyl-(4-trifluoromethylphenyl)pyrrole (**7**) with an enzyme–inhibitor dissociation constant (K_i value) of 1.30 μM. The least potent inhibitor was 1-methyl-3-phenylpyrrole (**8**) with a K_i value of 118 μM (Figure 3). Since 1-methyl-3-phenylpyrroles probably bind to the active site of MAO-B via hydrophobic interactions, we speculate that modification of the structure to include hydrogen bond acceptors may enhance binding affinity. An example of such a modified structure is N-methyl-2-phenylmaleimide (**9a**), which may interact with MAO-B via both hydrogen bonding and hydrophobic burial, and hence may act as a more potent inhibitor.

To test this hypothesis in this study, we prepared a series of selected N-methyl-2-phenylmaleimides and evaluated them as inhibitors of MAO-B. The results from this study may aid in the identification of new reversible MAO-B inhibitors with exceptional potent action.

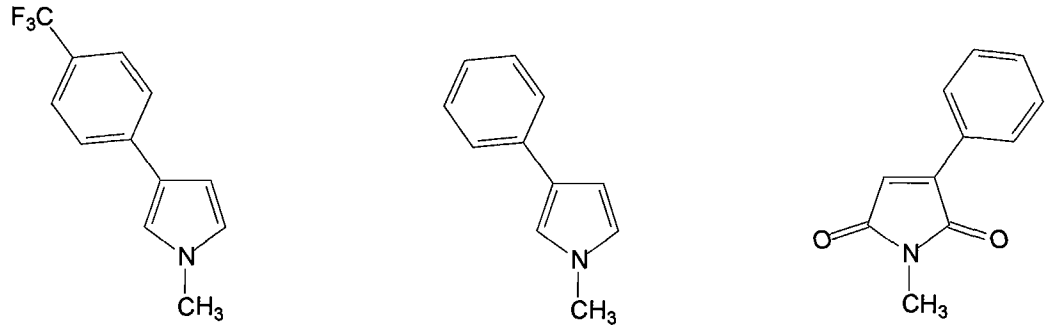

Figure 3. The structures of 1-methyl-(4-trifluoromethylphenyl)pyrrole (**7**), 1-methyl-3-phenylpyrrole (**8**) and N-methyl-2-phenylmaleimide (**9a**).

1.4 Objectives of this study

The objectives of this study can be summarized as follows:

a. A series of N-methyl-2-phenylmaleimide analogues will be synthesized according to procedures described in the literature. In this study, the chosen structures differed from N-methyl-2-phenylmaleimide only by substitution at C-3 of the phenyl ring. These structures (**9a–g**) are illustrated in Figure 4.

b. The N-methyl-2-phenylmaleimide analogues (**9a–g**) were evaluated as inhibitors of MAO-B. For this purpose we aimed to establish whether the mode of inhibition is reversible and competitive, and determined the enzyme–inhibitor dissociation constants (K_i values).

c. In an attempt to gain additional insight into the binding modes of the inhibitors to the active site of MAO-B, molecular docking of selected N-methyl-2-phenylmaleimide analogues (**9a–g**) within the active site of human MAO-B was performed. Results from these studies afforded information about the spatial location, main interactions and highlighted the structural features of the N-methyl-2-phenylmaleimide analogues that are important for MAO-B inhibition. This will assist in the rational design of MAO-B reversible inhibitors with enhanced potency. For this, LigandFit application of the molecular docking software, Discovery Studio 1.7 was employed.

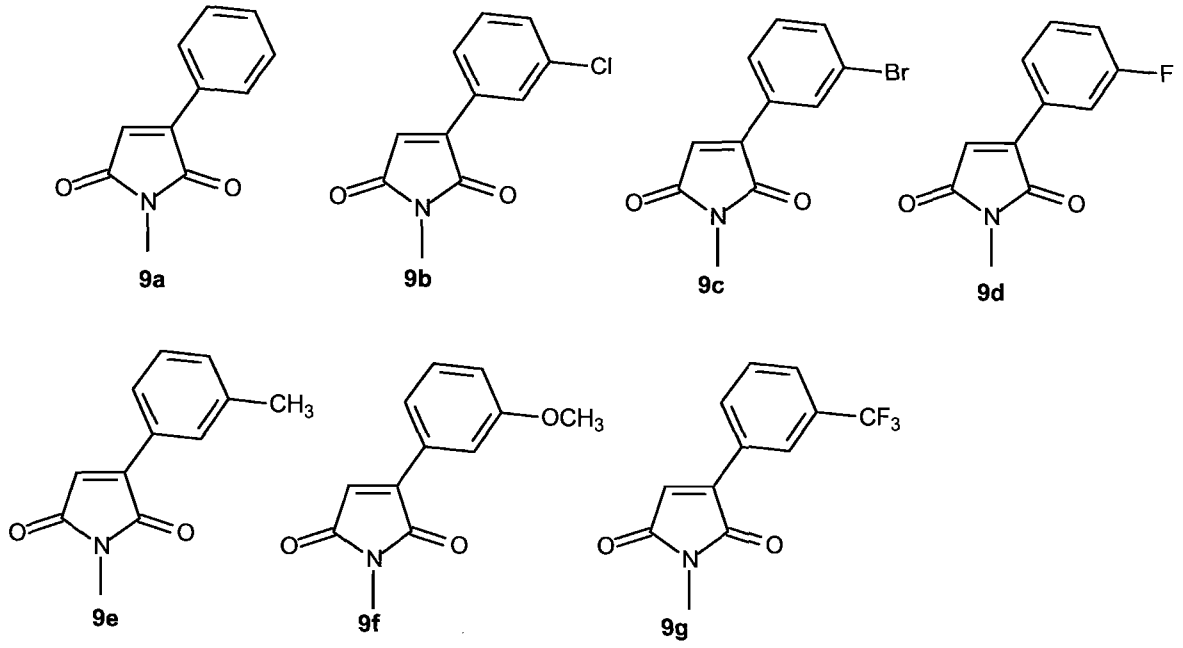

Figure 4. The structures of the N-methyl-2-phenylmaleimide analogues (**9a–g**) that were investigated as potential MAO-B inhibitors in the current study.

CHAPTER 2.

LITERATURE OVERVIEW

2.1 Parkinson's disease

Parkinson's disease is a chronic, progressive movement disorder that results from degeneration of the neurons of the substantia nigra in the midbrain. This causes the loss of dopamine (DA) from the striatum (Jenner, 1998) and the disruption of the neural circulatory that controls movement (Ballard *et al.*, 1985). Molecularly, this condition results when the majority of dopaminergic nerve cells in the substantia nigra die, or are impaired, automatically causing the levels of dopamine in the brain to decrease (Reiderer & Youdim, 1986).

2.1.1 General background

Parkinson's disease is a widespread neurodegenerative, multifactorial disorder, believed to be caused by ageing (Jenner & Olanow, 1996), genetic mutations (Lee *et al.*, 2001) and various biological and environmental factors such as exposure to herbicides and pesticides like rotenone and paraquat (Talpade *et al.*, 2000).

The four primary symptoms characterizing the disease are tremor, rigidity and postural instability (Ballard *et al.*, 1985). The profound deficit in brain dopamine levels, primarily attributed to the loss of dopaminergic neurons of the nigrostriatal dopaminergic pathway (Bernheimer *et al.*, 1973), causes depigmented neurons (due to decreased number of neuromelanin-containing neurons located in the midbrain substantia nigra pars compacta (SNpc) (Marsden,1983), gliosis and the presence of Lewy bodies (figure 5) (Dauer & Przedborski, 2003). The degree of terminal loss in the striatum was found to be more pronounced than SNpc dopaminergic neuron loss, which showed that it was the primary target of the degenerative process and suggested that neuronal death resulted from a "dying back" process (Bernheimer *et al.*, 1973). For example, Wu *et al.* (2003) showed that protecting the striatal terminals prevented loss of SNpc dopaminergic neurons in MPTP treated mice.

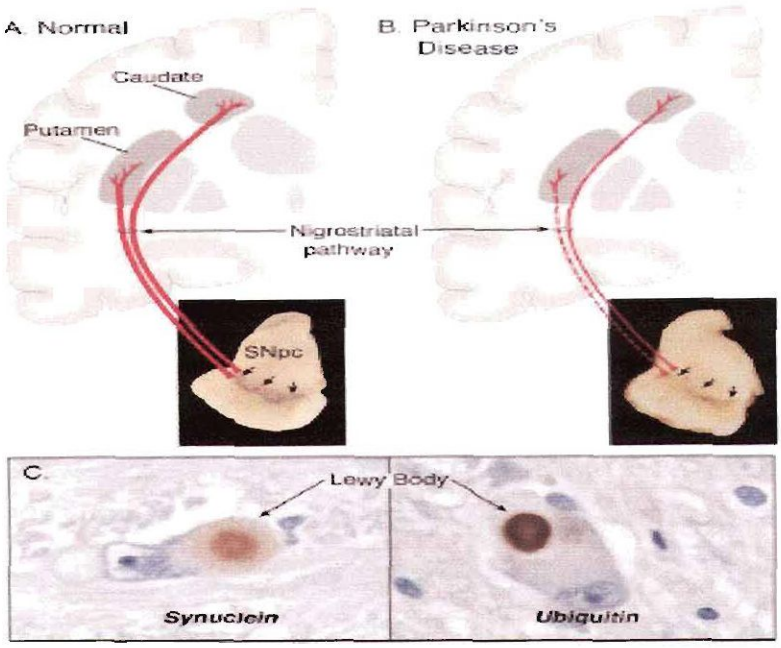

Figure 5. Neuropathology of Parkinson's disease (**A**) showing a normal nigrostriatal pathway, (**B**) a diseased nigrostriatal pathway with depigmentation of the SNpc as the the nigrostriatal pathway degenerates and (**C**) immunohistochemical labelling of intraneuronal inclusions, termed Lewy bodies, in a SNpc dopaminergic neuron (Daeur & Przedborski, 2003).

2.1.2 Treatment

At present there exists no cure for Parkinson's disease, however several therapeutic strategies provide relief from symptoms. The current treatment for Parkinson's disease is the systematic administration of levodopa (L-DOPA), a precursor to DA which enters the brain via a carrier-mediated transport system where it is converted to DA by the enzyme, L-aromatic amino acid decarboxylase (L-AAAD) (Jenner, 1998; Birkmayer *et al.*, 1975).

Levodopa is frequently combined with the L-aromatic amino acid decarboxylase inhibitor, carbidopa. Carbidopa blocks the metabolic conversion of levodopa to dopamine in the peripheral tissues, resulting in enhanced amounts of levodopa available for uptake into the brain. The MAO-B inhibitor, (R)-deprenyl is also frequently used as adjunct to levodopa therapy. (R)-Deprenyl inhibits the central oxidative metabolism of dopamine and therefore may conserve the depleted supply of dopamine. For example, MAO-B inhibitors have been shown to elevate dopamine levels in the striatum of primates treated with levodopa (Finberg *et al.*, 1988). Furthermore, in the catalytic cycle of MAO, one mole of dopaldehyde and H_2O_2 is produced for each mole of dopamine oxidized. Both these catabolic products may be neurotoxic if not rapidly inactivated by

centrally located aldehyde dehydrogenase (ADH) (Gesi *et al.*, 2001) and glutathione peroxidase (Flohe, 1978), respectively. Thus inhibitors of MAO-B may also exert a neuroprotective effect by stoichiometrically decreasing aldehyde and H_2O_2 production in the brain.

Other treatments include gene therapy (Stacy & Jankovic, 1993), deep brain stimulation, often used for non response to drugs, (Stacy & Jankovic, 1993) and restorative surgery (Hamani & Lozano, 2003).

2.1.3 Neuroprotection

Agents that have neuroprotective or neuro-restorative activities aim to prevent disease progression by targeting the mechanisms involved in the pathogenesis of the disease. Reversible and irreversible inhibitors of MAO-B have been used clinically to treat neurological disorders, including depression and Parkinson's disease (Youdim & Bahkle, 2006) as they are reported to possess neuroprotective properties.

As mentioned above, the MAO-B catalyzed oxidation of dopamine yields as secondary products H_2O_2, as well as dopaldehyde (**10**) and inhibitors of MAO-B stoichiometrically decrease aldehyde and H_2O_2 production in the brain and thus offer neuroprotection. Another source of H_2O_2, however, is the autoxidation of dopamine, which generally results in a one-step reduction of oxygen to the superoxide radical and the formation of hydrogen peroxide (H_2O_2), (Jenner & Olanow, 1996).

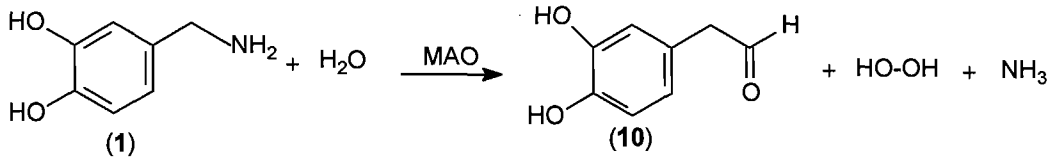

(**1**) (**10**)

Scheme 1. MAO catalyzed oxidation of DA (**1**) to 2-(3,4-dihydroxyphenyl)acetaldehyde (**10**) and hydrogen peroxide.

2.2 Monoamine oxidase

The enzyme monoamine oxidase (MAO) is of crucial interest to scientists because of its unique importance as a catalyst in major inactivation pathways of catecholamine neurotransmitters, dopamine, adrenaline and noradrenaline (Youdim, 1988).

2.2.1 General background

Monoamine oxidase (MAO) is a flavin adenine dinucleotide (FAD)–containing enzyme located on the outer mitochondrial membrane of certain cells of mammals, birds, fish, and a variety of lower animals and some fungi. Two isoforms, MAO-A and MAO-B, are found in humans and other mammals (Youdim, 1988). Their primary role includes the regulation of biogenic and xenobiotic amines in the brain and the peripheral tissues by catalyzing their oxidative deamination (Youdim *et al.*, 2006). MAO-A is composed of 527 amino acids whilst MAO-B is composed of 520 amino acids. The two isoforms have 70% sequence identity as deduced from their cDNA clones (Kearney *et al.*, 1971) and for each, the FAD cofactor is covalently attached to a conserved cysteinyl residue via an 8-R-S-thioether linkage. These two forms of the enzyme can be distinguished by differences in substrate preference, inhibitor specificity, tissue distribution, immunological properties, and amino acid sequences. The active forms of the enzymes are homodimers with subunit molecular weights, determined from their cDNA structure, of 59,700 and 58,800, respectively. The genes for both MAO-A and MAO-B have very similar structures, with both consisting of 15 exons and exhibit identical exon-intron organization, which has suggested that MAO-A and MAO-B are derived from duplication of the same ancestral gene (Weyler *et al.*, 1990). On the basis of their substrate and inhibitor specificities, MAO-A preferentially deaminates serotonin and norephinephrine and it is irreversibly inhibited by low concentrations of clorgyline (**3**). MAO-B deaminates arylalkyamines such as benzylamine (**4**) and β-phenylethylamine and is irreversibly inhibited by (R)-deprenyl (**2**) (Waldmeier, 1987; Kalgutkar *et al.*, 1995). Both forms however utilize dopamine (**1**) as substrate (Youdim & Bahkle, 2006).

2.2.2 Biological function of MAO-A and –B

As mentioned above, MAO-A and MAO-B are located on the outer mitochondrial membrane of various cell types including neuronal and glial cells in the brain (Youdim, 1988). Their primary role is the regulation of biogenic and xenobiotic amines in the brain and the peripheral tissues by catalyzing their α-carbon oxidation (Youdim *et al.*, 2006). Among the MAO substrates are neurotransmitters such as serotonin, norephinephrine and dopamine (**1**). This suggests that MAO plays a critical role in regulating the concentrations of these neurotransmitters in the central nervous system and therefore in modulating neurotransmission.

Oxidation of monoamine neurotransmitters by MAO leads to the corresponding imines, with the reduction of O_2 to hydrogen peroxide (H_2O_2). The dissociated imine product is then nonenzymatically hydrolyzed to the corresponding aldehyde (Silverman, 1980; Edmonson *et al.*, 2004). The primary product of MAO acting on a monoamine is therefore an aldehyde, which are reactive toxic species, if not rapidly reduced either to an alcohol or further oxidized by aldehyde dehydrogenase (ADH) to a carboxylic acid, the final excreted metabolite. This metabolic sequence is illustrated using dopamine (Scheme 1). Dopamine (**1**) is oxidized either by MAO-A or MAO-B, to the corresponding imine product which is rapidly hydrolyzed to dopaldehyde (**10**) (Olanow, 1990). As illustrated, for each mole of dopamine oxidized, one mole of H_2O_2 is produced by the reduction of molecular oxygen (O_2). Via the action of centrally located aldehyde dehydrogenase (ADH) (Gesi *et al.*, 2001), and glutathione peroxidase (Flohe *et al.*, 1978), respectively, dopaldehyde is further oxidized to 3,4-dihydroxyphenylacetic acid (DOPAC).

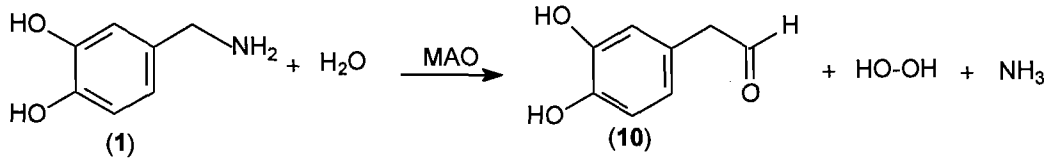

Scheme 1. The MAO catalyzed oxidation of DA.

2.2.3 The role of MAO-B in Parkinson's disease

The MAO catalytic oxidation of biogenic amines, plays an important role in their biological inactivation *in vivo*. Inhibition of MAO-A increased brain levels of the biogenic amines including noradrenaline and serotonin, which are generally low in depression patients. Reversible MAO-A inhibitors are therefore used in the treatment of depression. Selective inhibition of the B form preferentially decreased the deamination of dopamine, thus conserving the depleted supply of dopamine in the brain. Inhibitors of MAO-B are frequently used in combination with levodopa in the treatment of Parkinson's disease (Birkmayer *et al.*, 1975) and has been reported to enhance dopamine levels in the striatum of primates treated with levodopa compared to central dopamine of animals treated with levodopa alone (Finberg *et al.*, 1988).

The oxidation of primary amine substrates by MAO may, through its toxic metabolites, dopaldehyde and H_2O_2 lead to the promotion of neurodegenerative diseases such as Parkinson's disease. Indeed, enhanced MAO-B activity is associated with the ageing process and since Parkinson's disease is found in the elderly, MAO-B in particular has been suggested to play a role in the neurotoxic processes associated with this disease (Youdim & Green, 1975). MAO-B

inhibitors may therefore be indicated as neuroprotective agents for the treatment of Parkinson's disease in addition to being adjuvant therapy to levodopa.

2.2.4 Irreversible inhibitors of MAO-B

Irreversible inhibitors (inactivators or poison enzymes) are compounds that produce irreversible inhibition of the enzyme by forming stable covalent complexes. This blocks the access of the substrate to the target amino acid residues of the active site (Rodwell, & Kennely, 2000). The process is not readily reversed either by removing the remainder of the free inhibitor or by increasing the substrate concentration and even dilution or dialysis of the solution does not dissociate the enzyme inhibitor complex and restore enzyme activity (Rodwell, & Kennely, 2000).

An example of irreversible inhibitors is (R)-deprenyl (**2**, selegiline) which is structurally related to phenylethylamine (PEA), a MAO-B substrate. (R)-Deprenyl is a highly potent and selective irreversible inhibitor of MAO-B and has been shown to inhibit the oxidative deamination of dopamine *in vivo* (Youdim & Green, 1975; Youdim & Bakle, 2006).

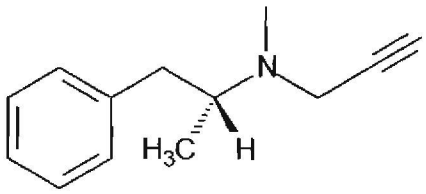

(R)-Deprenyl (**2**)

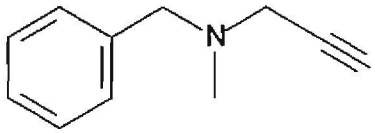

Pargyline (**11**)

Figure 6. The structures of the irreversible MAO inhibitors, (R)-deprenyl (**2**) and pargyline (**11**).

Pargyline (**11**), another irreversible inhibitor of MAO-B (Binda *et al.*, 2002), binds covalently with the FAD cofactor within the active site (Figures 7 and 8).

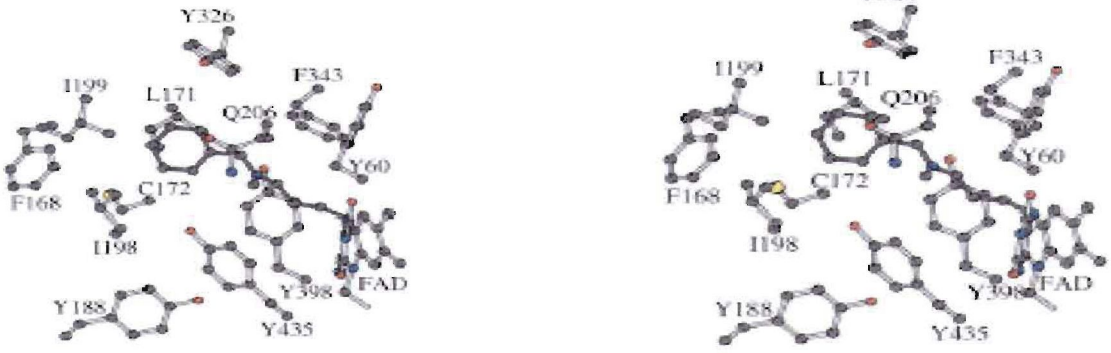

Figure 7. The substrate binding site of human MAO-B, showing the stereo view of pargyline inhibitor and residues lining the binding site at the re side of the flavin (Binda *et al.*, 2002).

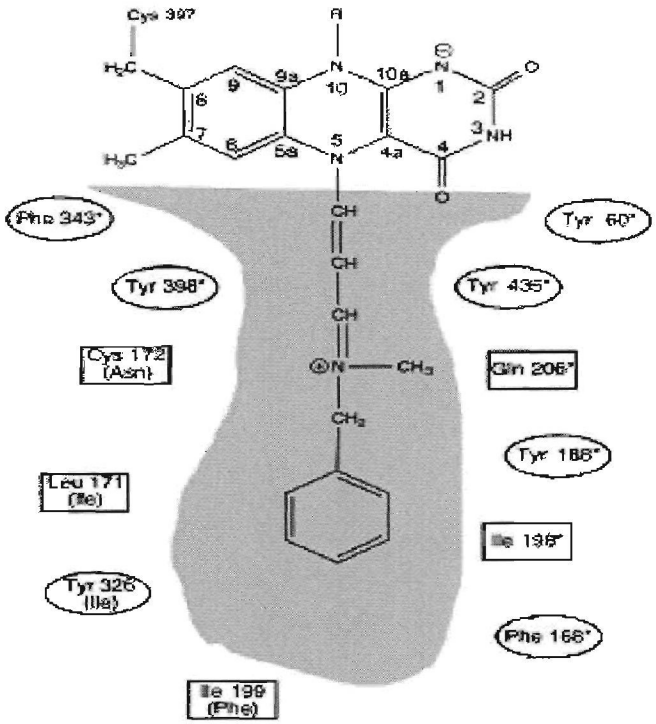

Figure 8. Schematic representation of pargyline forming a covalent bond with the FAD cofactor of MAO-B (Binda *et al.*, 2002).

2.2.5 Reversible inhibitors of MAO-B

Reversible inhibitors interact with enzymes mainly via hydrophobic interactions and hydrogen bonding (Binda *et al.*, 2003). This makes them therapeutically more desirable than inactivators since enzyme activity can be regained relatively quickly, following withdrawal of the reversible inhibitor. On the other hand, following inactivation of the enzyme, activity can only be regained via *de novo* synthesis of the enzyme protein (Thebault *et al.*, 2004). Several research groups are currently interested in discovering and characterizing new reversible inhibitors of MAO-B. Among the well-known reversible inhibitors are:

a. *Trans,trans-farnesol (**12**)*, a component of tobacco (Hubalek *et al.*, 2005) which has been found to be a moderately potent competitive inhibitor of human MAO-B with a K_i value of 2.3 μM. X-Ray crystal structures with human recombinant MAO-B in complex with *trans,trans*-farnesol have indicated that *trans,trans*-farnesol exhibits a dual binding mode that involves traversing both the entrance and substrate cavities of the enzyme (Hubalek *et al.*, 2005). The polar OH moiety is reported to be in close contact with the flavin, located in the substrate cavity where it is stabilized via hydrogen bonding (Hubalek *et al.*, 2005) while the aliphatic chain extends to the entrance cavity. The gate separating the two cavities is the side chain of Ile-199 which is shown to exhibit a

different rotamer conformation that allows for the fusion of the two cavities in order to accommodate *trans,trans*-farnesol (Binda *et al.*, 2003). The potency of MAO-B inhibition by *trans,trans*-farnesol may possibly be explained by dual mode of interaction.

b. *1,4-Diphenyl-2-butene* (***13***), a contaminant of polystyrene bridges used in the MAO-B crystallization process has been found to be a moderately potent competitive inhibitor of human MAO-B with a K_i value of 0.7 μM (Hubalek *et al.*, 2005). Based on X-Ray crystal structures 1,4-diphenyl-2-butene is also shown to bind to both the substrate and entrance cavities of MAO-B.

c. *(E)-8-(3-Chlorostyryl)caffeine* (***14***, *CSC*), an A_{2A} adenosine receptor antagonist (Chen *et al.*, 2001) has recently been found also to be an exceptionally potent MAO-B inhibitor with a K_i value of 0.128 μM for the inhibition of baboon liver MAO-B (Vlok *et al.*, 2006). Although the exact binding mode of CSC to the active site of MAO-B is unknown, its relatively large planar structure suggests that this inhibitor also traverses both the entrance and substrate cavities of the enzyme. This dual mode of binding may explain the potent action of CSC as MAO-B inhibitor.

d. *Isatin* (***15***) is a small molecule inhibitor which is reported to inhibit human MAO-B with a K_i value of 3 μM (Hubalek *et al.*, 2005). X-Ray crystal structures with human recombinant MAO-B in complex with isatin, have indicated that isatin binds within the substrate cavity and is stabilized via hydrogen bonding. The 2–oxo group and the pyrrole NH are hydrogen bonded to ordered water molecules present in the active site, whereas the 3-oxo group was not involved in any hydrogen bonding (Binda *et al.*, 2003). For this binding mode, the side chain of Ile-199 is rotated into its normal position, separating the entrance from the substrate cavity.

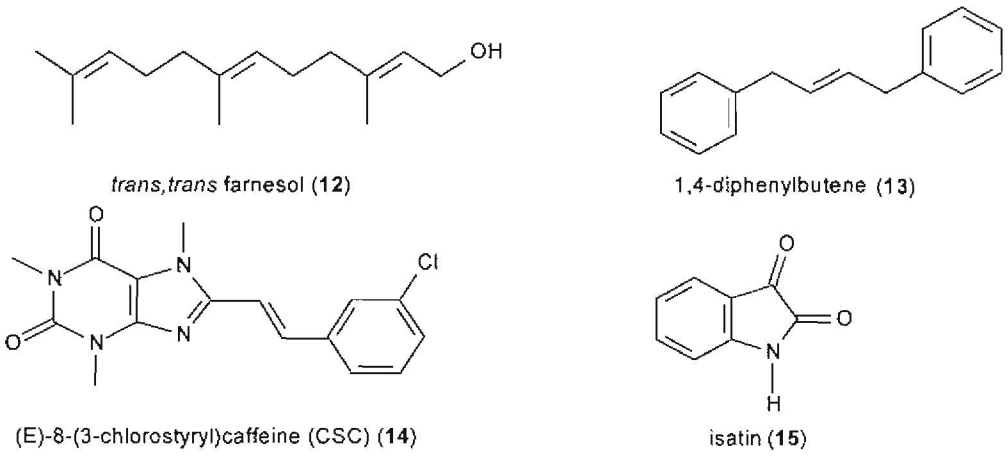

trans,trans farnesol (**12**) 1,4-diphenylbutene (**13**)

(E)-8-(3-chlorostyryl)caffeine (CSC) (**14**) isatin (**15**)

Figure 9. The structures of *trans,trans*-farnesol (**12**), 1,4-diphenyl-2-butene (**13**), (E)-8-(3-chlorostyryl)caffeine (**14**) and isatin (**15**).

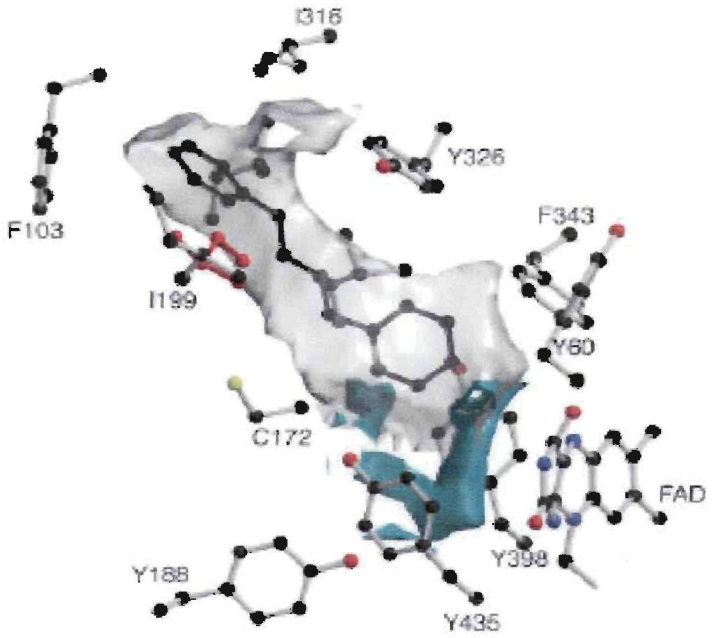

Figure 10. The structure of 1,4-diphenyl-2-butene complex with MAO-B. The inhibitor phenyl ring in contact with Phe-103, Ile-199, and Ile-316 occupies the entrance cavity space, whereas the inhibitor ring in contact with Tyr-398 and Tyr-435 occupies the substrate cavity space (Binda *et al.*, 2002).

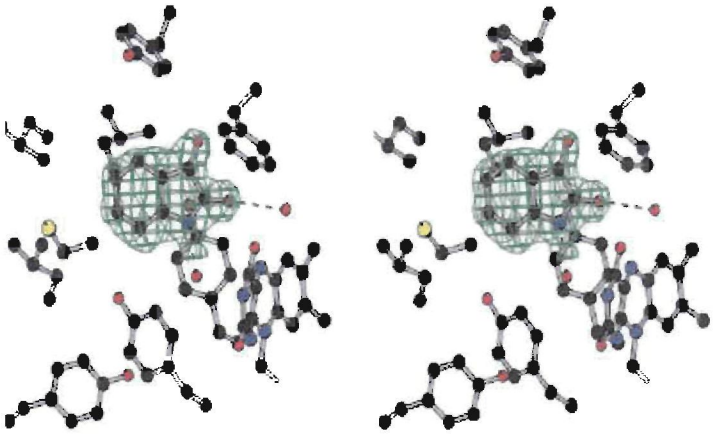

Figure 11. Stereoview of the isatin binding site in human recombinant MAO-B. Carbons are in black, nitrogens in blue, oxygens in red, and sulfurs in yellow. H-bonds involving inhibitor atoms are outlined by the dashed line (Binda *et al.*, 2002).

Of importance to this study was the recent discovery that a series of 1-methyl-3-phenylpyrrole derivatives exhibited MAO-B inhibition activity (Ogunrombi *et al.*, 2008). The most potent analogue was 1-methyl-(4-trifluoromethylphenyl)pyrrole (**7**) with an enzyme–inhibitor dissociation constant (K_i value) of 1.30 μM (Figure 3). The least potent inhibitor was 1-methyl-3-phenylpyrrole (**8**) with a K_i value of 118 μM. As stated in Chapter 1, modeling studies suggest that 1-methyl-3-phenylpyrroles binds to the active site of MAO-B via hydrophobic interactions. In this study we speculate that modification of the structure to include hydrogen bond acceptors may enhance binding affinity. An example of such a modified structure is N-methyl-2-phenylmaleimide (**9a**), which may interact with MAO-B via hydrogen bonding between the maleimide carbonyl oxygens and active site water and/or amino acid residues located in the substrate cavity.

2.2.6 Mechanism of action of MAO-B

Despite an extensive literature on these two enzymes, MAO-A and -B, the detailed mechanism by which they catalyze amine oxidation is not well-defined, although several mechanisms have been proposed. Studies into the structure and mechanism of both MAO-A (Miller & Edmonson, 1999) and MAO-B (Walker & Edmonson, 1994) gave some insight into the mechanism of these enzymes.

Enzymes have evolved to catalyse these reactions and these oxidoreductases can be grouped into the flavoprotein and quinoprotein families. The mechanism of amine oxidation catalysed by the quinoprotein amine oxidases is understood reasonably well and occurs through the formation of enzyme–substrate covalent adducts with TPQ (topaquinone), TTQ (tryptophan tryptophylquinone), CTQ (cysteine tryptophylquinone) and LTQ (lysine tyrosyl quinone) redox centres. However, the oxidation of amines by flavoenzymes is less well understood as the precise mechanism of this biotransformation is still unclear and it has been described by two currently debated pathways: (a) single electron transfer (SET) pathway and (b) nucleophilic (polar) pathway (Miller & Edmonson, 1999; Walker & Edmonson, 1994).

2.2.6.1 The SET pathway

The generally accepted mechanism for the MAO catalyzed α-carbon oxidation of amines according to Silverman (Silverman *et al.*, 1980) proceeds via an initial single electron transfer step (Scheme 2) from the nitrogen lone pair of the substrate (**A**) to the oxidized flavin FAD to generate an aminyl radical cation (**B**) and the flavin semiquinone FAD. α-Carbon deprotonation of **B** yields the α-amino radical (**C**). This α-amino radical transfers the second electron to the semiquinone to give the reduced flavin $FADH^-$ and the iminium ion (**D**).

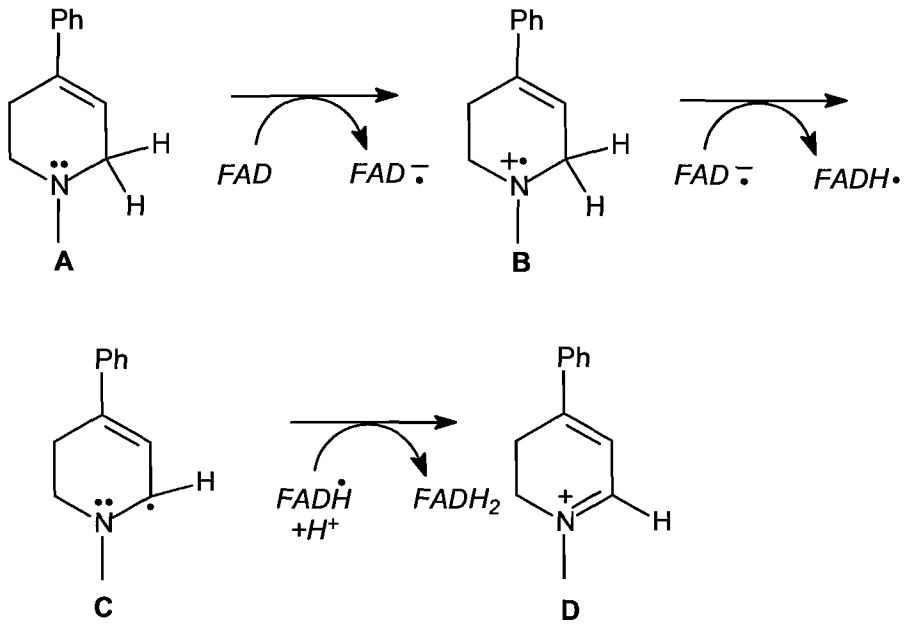

Scheme 2. The proposed SET oxidation pathways for MAO catalysis as illustrated with MPTP as substrate (Silverman *et al.*, 1980).

2.2.6.2 The polar nucleophilic pathway

An earlier proposal, based on flavin model reactions, suggested a polar nucleophilic mechanism which involved attack of the deprotonated amine substrate at the flavin C-4a position to form a substrate–flavin adduct (Scheme 3). This is followed by proton abstraction from the α-carbon of the amine-flavin adduct that occurs by an active site base on the enzyme. Formation of the protonated imine product results from its elimination from the reduced flavin. The reactivity at the flavin C-4a atom is considered additional evidence for this catalytic mechanism. In lieu of active site base, the highly basic N5 atom of the flavin, which is generated following nucleophilic attack of the substrate, may also act as base for the deprotonation of the substrate α-carbon (Miller & Edmondson, 1999).

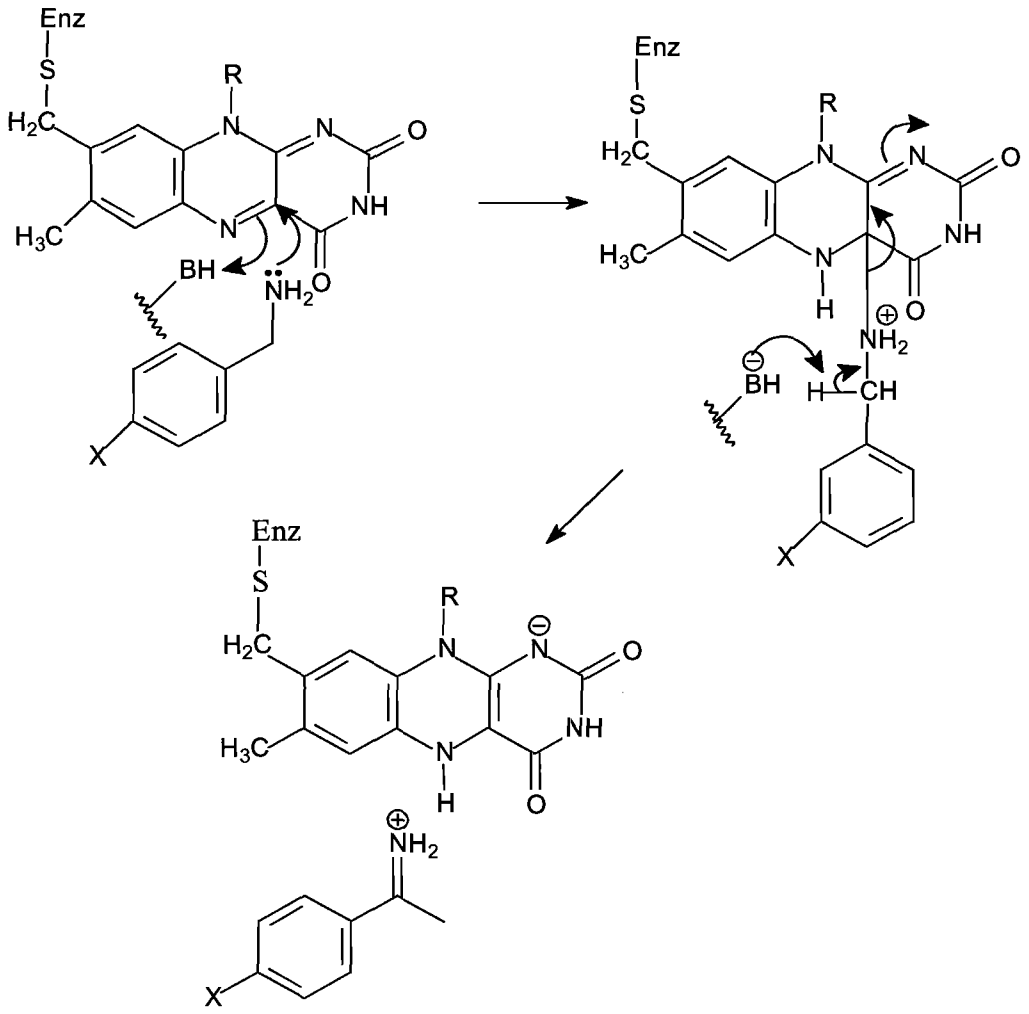

Scheme 3. The proposed polar nucleophilic mechanism for MAO catalysed oxidation of benzylamine (Miller & Edmondson, 1999).

2.2.7 Three dimensional structure of MAO-B

The human MAO-B structure was recently characterized to 3 Å resolution and the crystal structure showed the enzyme to be dimeric but not covalently linked, and it contained about 520 amino acids that folded into a compact structure (Binda *et al.*, 2002). The enzyme appears to be linked to the outer mitochondrial membrane via the C-terminal amino acids 461–515 which forms a transmembrane helix. The active site of the enzyme consists of a substrate binding cavity as well as an entrance cavity preceding it. Substrates and inhibitors must traverse the entrance cavity in order to gain access to the substrate cavity where catalysis takes place (Figure 12). The entrance cavity is lined with hydrophobic amino acids, Phe-103, Trp-119, Leu-164, Leu-167, Phe-168, Ile-316, creating a relatively lipophilic environment (Novaroli *et al.*, 2006). In contrast, the substrate cavity is relatively polar with the FAD cofactor forming the back wall of the cavity. In front of the

FAD are two tyrosine residues, Tyr-398 and Tyr-435, which together with the FAD and Phe-343 at the top of the cavity create an aromatic cage where catalysis takes place. The only hydrophobic patch in the substrate cavity is the area defined by Tyr-60, Phe-343 and Tyr-398 (Binda *et al.*, 2002, 2004). The substrate cavity has a volume of 420 $Å^3$, while the entrance cavity has a volume of 290 $Å^3$. The cavities are separated by Tyr-326, Ile-199, Leu-171 and Phe-168.

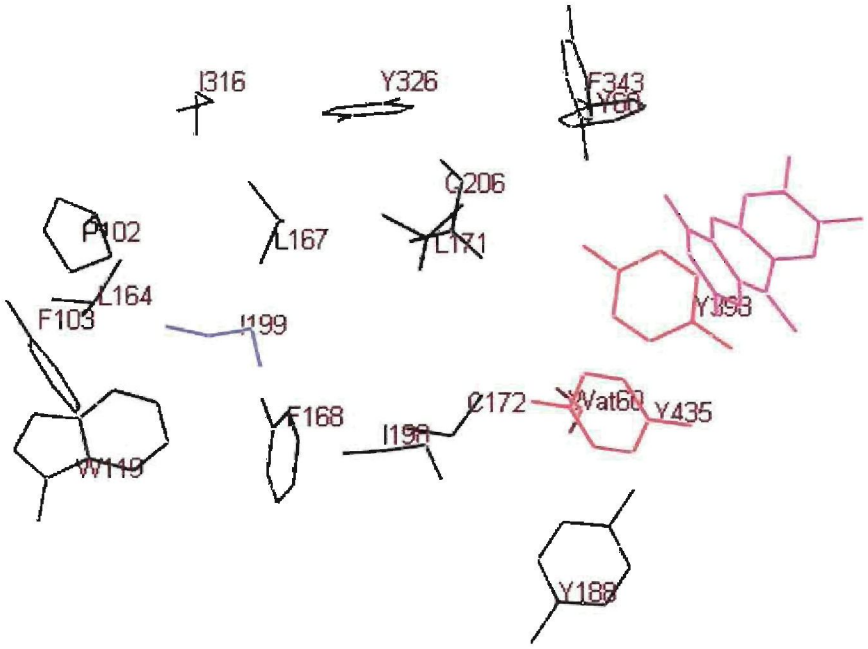

Figure 12. A model of the active site of human recombinant MAO-B. The residues Try 398, and Try 435, forming the aromatic cage are in red, Ile 199, the "gate" of the cavity is in blue and the FAD cofactor is in purple.

In order to gain access to the substrate cavity, an inhibitor of MAO-B must traverse the entrance cavity. This is true for small molecule inhibitors such as isatin (**15**) (Figure 9) that has been shown to bind within the substrate cavity of the enzyme (Binda *et al.*, 2003, 2004). A larger inhibitor such as the reversible inhibitor 1,4-diphenyl-2-butene (**13**) appears to exhibit a dual binding mode that involves traversing both the entrance and substrate cavities (Binda *et al.*, 2003). Another inhibitor, trans,trans-farnesol (**12**) is also reported to span both the entrance and substrate cavities with the polar OH moiety in close contact with the flavin located in the substrate cavity (Hubalek *et al.*, 2005). The gate separating the two cavities is the side chain of Ile-199 which is thought to exhibit different rotamer conformations that allows for the fusion of the two cavities in order to accommodate these larger inhibitors (Binda *et al.*, 2003). The potent action of many good MAO-B

inhibitors may possibly be explained by this binding that involves traversing both the entrance and substrate cavities (Binda *et al.*, 2003).

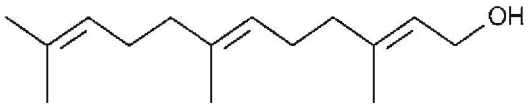

trans,trans farnesol (**12**)

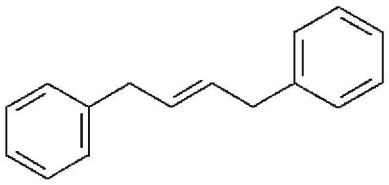

1,4-diphenylbutene (**13**)

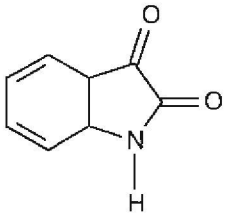

isatin (**15**)

Figure 13. The structures of *trans,trans*-farnesol (**12**) 1,4-diphenyl-2-butene (**13**) and isatin (**15**).

2.2.8 *In vitro* measurements of MAO-B activity

MAO-B activity measurements are most frequently conducted by directly measuring either the production of the enzyme catalyzed product or the consumption of the substrate amine or molecular oxygen (O_2). Occasionally the enzyme activity is measured indirectly which involves converting the enzyme catalyzed product into a more readily measured species.

2.2.8.1 Direct measurements

Oxygen consumption by the MAO-B catalytic cycle can be measured polarographically, using an oxygen sensitive electrode. This requires a well controlled assay environment and the method is unsuitable for the rapid processing of very large number of samples (Averill-Bates *et al.*, 1993). In another less frequently used method (Cotzias & Dole, 1997), the rate of ammonia production from the deamination of tryamine by MAO-B can also be measured. The detection of MAO-B generated hydrogen peroxide, by measuring its absorbance spectrophotometrically at 230 nm has also been reported. However, the sensitivity at a wavelength of 230 nm is often lost due to interferences from the absorbance of most biological and synthetic compounds (Stevanato *et al.*, 1995).

Radiometric detection of the MAO-B catalyzed oxidation products from ^{3}H-tyramine is also used. Usually radiometric methods are employed for small tissue samples and it involves the extraction of labelled products into an organic solvent. This assay is time consuming and less accurate in time dependent measurements, particularly with tritiated substrates.

The detection of the fluorescence of the oxidized monoamine product is most frequently used to measure MAO-B activity. This method however, is limited to experiments with only one substrate. The fluorescence product, 4-hydroxyquinoline, formed from the oxidation of kynuramine by MAO-B is an example of this method. Zhou *et al.* (1996) reported that kynuramine is slowly oxidatively deaminated and intramolecularly cyclized to form 4-hydroquinoline (Figure 14). 4-Hydroquinoline is fluorescent and can be easily quantified in the presence of non-fluorescence substrate.

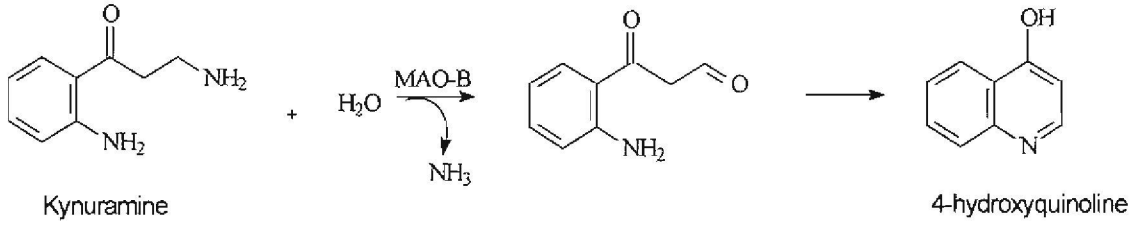

Figure 14. The oxidation of kynuramine by MAO-B and subsequent cyclization to yield 4-hydroxyquinoline.

In our laboratory we measure the rate of the MAO-B catalyzed oxidation of 1-methyl-4-(1-methylpyrrol-2-yl)-1,2,3,6-tetrahydropyridine (MMTP) (**16**) to the corresponding dihydropyridinium metabolite ($MMDP^+$) (**17**) (Scheme 4) spectrophotometrically (Vlok *et al.*, 2006). $MMDP^+$ production is measured at 420 nm, a wavelength at which the substrate does not absorb light. Because of the favourable chromophoric characteristics and *in vitro* chemical stability of $MMDP^+$ this assay is frequently used to measure activities of both MAO-A and -B.

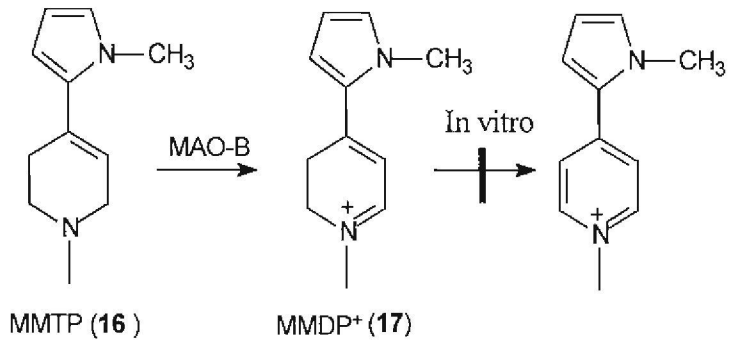

Scheme 4. The MAO catalyzed oxidation of MMTP (**16**) to the dihydropyridinium species, $MMDP^+$ (**17**).

We also utilize the selective MAO-B substrate benzylamine (**4**) (Figure 1) to measure MAO-B activity. When using purified MAO-B as enzyme source, which is relatively free from background interference, the concentration of the α-carbon oxidation product, benzaldehyde (**18**) (λ_{max} = 250 nm), may be measured spectrophotometrically. In contrast, background absorption in the near-UV wavelength range, when using the mitochondria as enzyme source, is too high to measure benzaldehyde concentrations by spectrophotometry. Even protein precipitation and subsequent centrifugation (the last two steps during a discontinuous assay) of the incubations do not solve this problem. For this reason the extent of benzylamine oxidation is measured by an HPLC-UV assay (Vlok *et al.*, 2006).

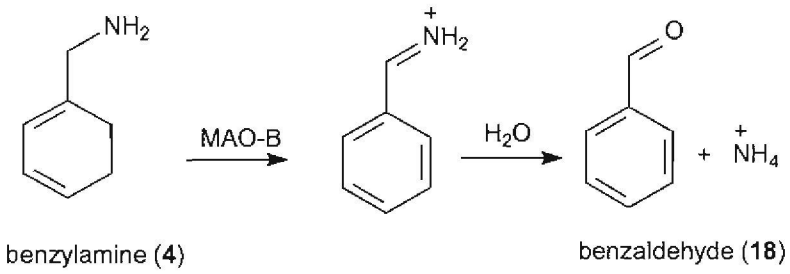

Scheme 5. The MAO-B catalyzed oxidation of benzylamine (**4**) to benzaldehyde (**18**).

2.2.8.2 Indirect measurements

Indirect measurements are based on the horseradish peroxidase (HRP) coupled reaction system, where MAO generated H_2O_2 is measured. For example, a one step fluorometric method for monoamine oxidase activity measurement was developed using a highly sensitive and stable H_2O_2 probe, N-acetyl-3,7-dihydroxyphenoxazine (Amplex Red) (Zhou & Panchuk-Voloshina, 1997). This method detected MAO activity in either end point or kinetic measurements and can screen for MAO inhibitors from a large number of compounds. The spectral properties of the oxidation product of Amplex Red, resorufin, makes it suitable for studies in crude preparations of cell lysate and tissue homogenates. The method was found to be both selective and sensitive for both MAO-A and –B and was able to measure concentrations as low as 200 μg protein.

Luminometric assay is based of measurement of the light produced from the peroxidase catalysed chemiluminescent oxidation of luminol. This assay is however, dependent on the amount of H_2O_2 produced in the MAO reaction (O'Brien *et al.*, 1993) and is highly sensitive as it enables the analysis of substances that are not readily detectable.

For *in vivo* measurements, monoamine oxidase (MAO) assay kits have been developed and are widely used. The monoamine oxidase (MAO) assay kit is intended for determination of MAO activity in patient serum or plasma samples. The technique is based on colorimetry and one such assay kit measures H_2O_2 production at wavelength 556 nm. This MAO-B assay is based on the enzymatic oxidation of the synthetic substrate benzylamine by MAO, to generate benzaldehyde, ammonia and H_2O_2. The latter is determined by a Trinder reaction coupled with a peroxidase and 4-aminoantipyrine. The reaction product, quinone dye, is monitored kinetically at 556 nm (Ono, 1975).

2.3 Enzyme kinetics

Enzymes are proteins that function as catalysts for biological reactions and the products of these reactions are organic compounds which show very little tendency for reactions outside the cell (Rodwell & Kennely, 2000). Enzymes are extremely efficient and display great catalytic power by accelerating the rates of reactions. Enzymes achieve this by providing a new reaction pathway with a lower energy of activation than the rate-determining step of the uncatalyzed reaction. Enzymes often need coenzymes which are smaller organic molecules or metallic cations possessing special chemical reactivities or structural properties (Rodwell & Kennely, 2000).

2.3.1 The FAD cofactor

Flavin coenzymes act as co-catalysts with enzymes in a large number of redox reactions, many of which involve O_2. Flavin adenine dinucleotide (FAD) and flavin mononucleotide (FMN) are the coenzymatically active forms of vitamin B2, riboflavin (Figure 15).

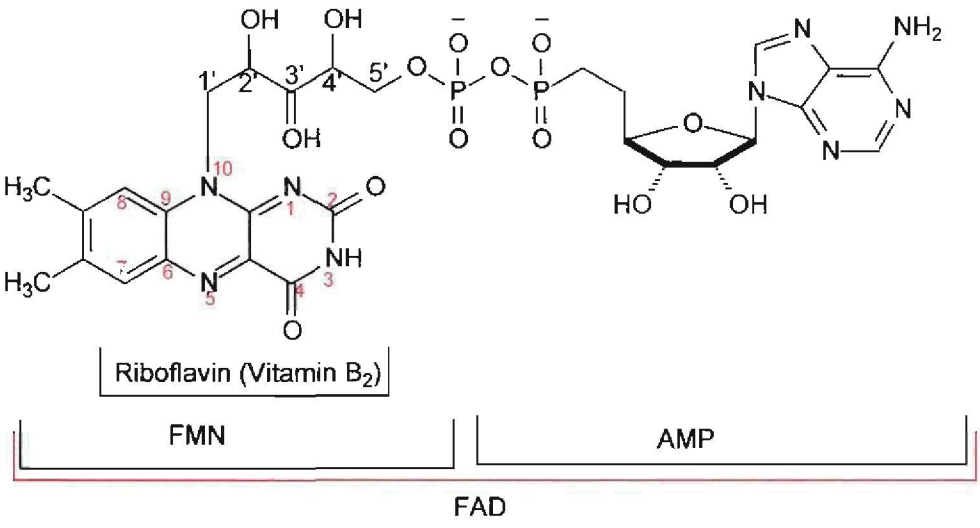

Figure 15. Structures of the vitamin riboflavin and the derived flavin coenzymes.

The catalytically functional portion of the coenzymes is the isoalloxazine ring, specifically the N-5 and C-4a positions, which is thought to be the immediate site of catalytic action. The flavin coenzymes exist in four spectrally distinguishable oxidation states that account in part for their catalytic functions (Scheme 6). They are the yellow oxidized form, the red or blue one-electron reduced form, and the colorless two-electron reduced form.

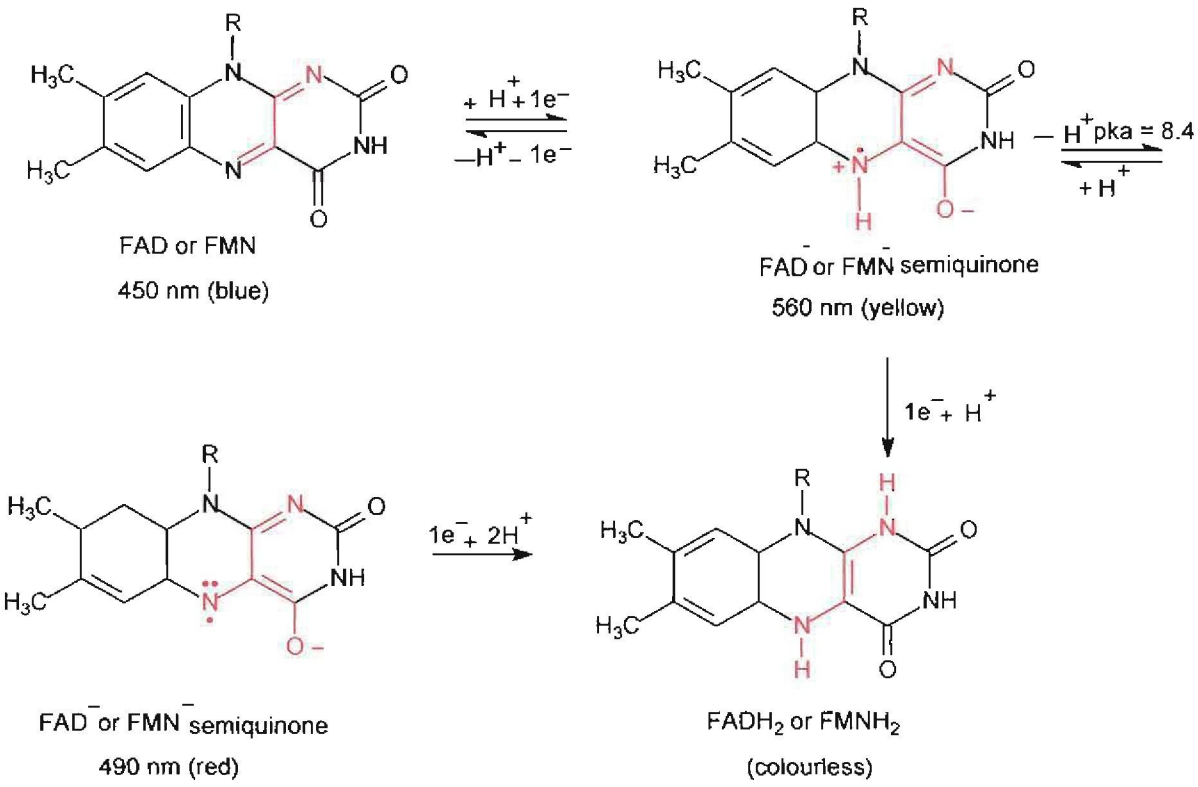

Scheme 6. The oxidation states of flavin coenzymes.

2.3.2 Michaelis-Menten kinetics

Enzymes have localized catalytic sites and the substrate (S) binds at the active site to form an enzyme-substrate complex (ES). Subsequent steps transform the bound substrate into product (P) and regenerate the free enzyme E, capable to interact with another molecule of S (Silverman, 1996).

$$E + S \underset{k_{-1}}{\overset{k_1}{\rightleftharpoons}} ES \underset{k_{-2}}{\overset{k_2}{\rightleftharpoons}} E + P$$

Scheme 7. Enzyme-catalyzed reaction.

Unlike a first order reaction where the rate of reaction is directly proportional to the substrate concentration, the rate of reaction for an enzyme catalyzed reaction initially increases with

increase in substrate concentration and then achieves a steady state where the rate is no longer dependent on increased substrate concentration and the overall speed of the reaction depends on the concentration of ES. Based on the steady-state kinetics analysis assumption, shortly after the enzyme and substrate are mixed, ES becomes approximately constant and remains so for a period of time, that is the steady state. The rate (V) of the reaction in the steady state usually has a hyperbolic dependence on the substrate concentration and is proportional to [S]. at low concentrations, but approaches a maximum (V_{max}) when the enzyme is fully occupied with substrate (Figure16).

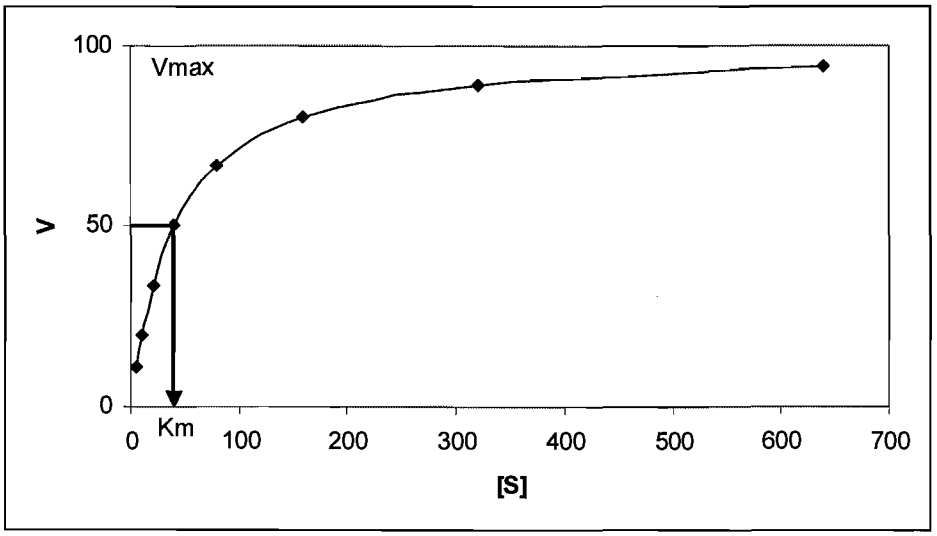

Figure 16. A graph of rate, V versus substrate concentration, [S] illustrating the Michaelis-Menten behaviour of enzymes.

This behaviour is described by the Michaelis-Menten equation:

$$V = \frac{V_{\max} \times [S]}{K_m + [S]}$$

$$V = \frac{k_{cat} \times [E]\ [S]}{K_m + [S]}$$

The maximum velocity (V_{max}), is obtained when all the enzyme is in the form of the enzyme-substrate complex. The Michaelis constant (K_m), is the substrate concentration at which the velocity is half maximal. If ES is in equilibrium with the free enzyme E and substrate S, K_m is equal to the dissociation constant for the complex (K_s). More generally, K_m depends on at least three rate constants and is larger than K_s. The turnover number (k_{cat}), represents the maximal catalytic

activity of the enzyme and is the maximum number of molecules of substrate converted to product per active site per unit time and it is V_{max} divided by the total enzyme concentration [E]. For the Michealis–Menten reaction, under conditions of initial velocity measurements, then $k_2 = k_{cat}$.

The specificity constant (k_{cat}/K_m), provides a measure of how rapidly an enzyme can work at low substrate concentration [S]. It is useful for comparing the relative abilities of different compounds to serve as substrates for the same enzyme. The larger this number, the better the substrate.

2.3.3 Measurement of kinetic parameters

Kinetic parameters are determined by measuring the initial reaction velocity as a function of the substrate concentration. The usual procedure for measuring the rate of an enzymatic reaction is to mix enzyme with substrate and observe the formation of product or disappearance of substrate as soon as possible after mixing, when the substrate concentration is still close to its initial value and the product concentration is small. From the hyperbolic shape of V versus S plots, V_{max} can only be determined by extrapolation of the asymptotic approach of V to limiting value of S as it increases indefinitely and this determination is usually approximate. Instead, the Michealis–Menten equation is transformed into a straight line equation which is similar to the equation for a straight line graph with a plot of 1/V versus 1/[S]:

$$1/V = (K_m / V_{\max})(1/[S]) + 1/V_{\max}$$

giving the intercept as $1/V_{max}$ and the slope as K_m/V_{max}.
Such a plot is known as the Lineweaver–Burke double reciprocal plot and K_m and V_{max} can readily be obtained from a plot of 1/V versus 1/[S] (Figure 17).

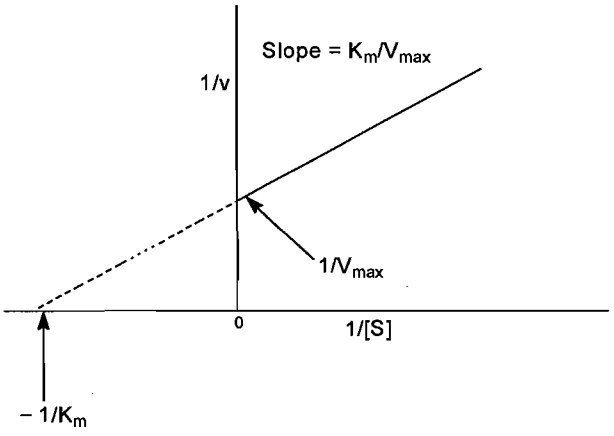

Figure 17. The Lineweaver-Burke double-reciprocal plot.

2.3.4 Competitive inhibition

Enzymes can be inhibited by agents that interfere with the binding of substrate or with conversion of the ES complex into products. There are two kinds of inhibitors: reversible and irreversible inhibitors (Silverman, 1996). Reversible inhibitor interacts with the enzyme through non covalent association or dissociation reactions. Reversible inhibitors among others include competitive, noncompetitive and uncompetitive inhibitors. A competitive inhibitor competes for the same binding site on the enzyme (the active site) as the substrate. Consequently, a sufficiently high concentration of substrate can eliminate the effect of a competitive inhibitor.

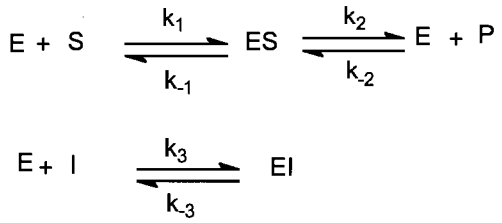

Scheme 8. Formation of enzyme complexes where I binds reversibly to the enzyme at the same site as the substrate.

Irreversible inhibitors (inactivators or poison enzymes) are compounds that produce irreversible inhibition of the enzyme by forming stable covalent complexes that block the access of the inhibitor to the target amino acid residues. These complexes can be characterized and they often provide information on the active site of the enzyme. They generally affect the chemical modification of the amino acid residues in the enzymes that play essential roles in catalysis. The process is not readily reversed either by removing the remainder of the free inhibitor or by increasing the substrate concentration. Dilution or dialysis of the solution does not dissociate the enzyme inhibitor complex and restore enzyme activity (Rodwell, & Kennely, 2000).

In this study we will however, focus on competitive inhibition as the compounds under investigation are expected to act in a reversible competitive manner. Competitive inhibition may be represented graphically by the Lineweaver-Burke plot (Figure 18). A higher concentration of a competitive inhibitor increases the slope of the straight line while the y-axis intercept remains unaffected and the intercept on the x-axis increases becomes less negative. Therefore a competitive inhibitor raises the apparent substrate K_m value while V_{max} remains unchanged. The Michaelis-Menten equation describing competitive inhibition is:

$$V_i = \frac{V_{max} \times \frac{[S]}{K_m}}{1 + \frac{[S]}{K_m} + \frac{[I]}{K_i}}$$

The inverse of this equation describes the double reciprocal plot in the presence of a competitive inhibitor:

$$\frac{1}{V_i} = \frac{K_m}{V_{max}}\left(1 + \frac{[I]}{K_i}\right) \times \frac{1}{[S]} + \frac{1}{V_{max}}$$

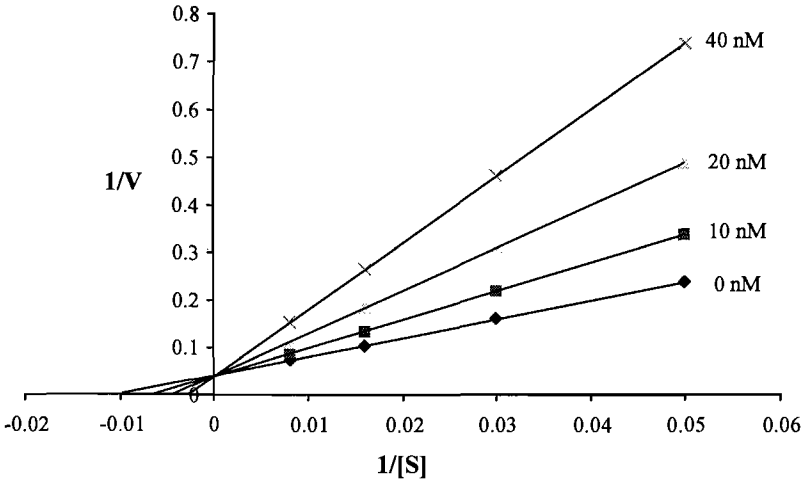

Figure 18. An example of a double reciprocal plot or Lineweaver-Burke plots in the presence of various concentrations of a competitive inhibitor.

The K_i value of a competitive inhibitor is the enzyme-inhibitor dissociation constant. For a series of competitive inhibitors, those with the lowest K_i values will cause the greatest degree of inhibition at a fixed concentration of inhibitor [I]. The K_i value for an inhibitor can be determined from the secondary plot in which the slope of each reciprocal plot is graphed vs. the corresponding inhibitor concentration (Figure 19). The x-axis value is equal to $-K_i$. In the presence of a concentration of inhibitor [I] that is approximately equal to K_i, the substrate concentration has to double to maintain the same initial velocity as in the absence of the inhibitor.

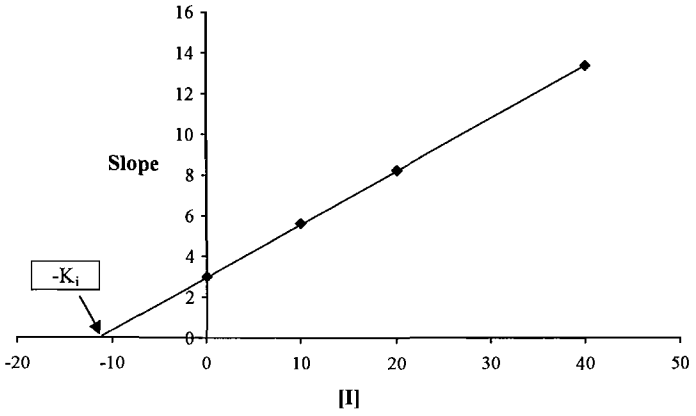

Figure 19. Graph of the slopes from the double reciprocal plot versus inhibitor concentration.

2.4 Animal models of Parkinson's disease

Since the majority of Parkinson's disease patients have no identifiable genetic mutation, important information regarding the pathophysiology of Parkinson's disease has been learnt through the study of animal models, by investigating the underlying mechanisms that lead to the development of experimental Parkinson's disease.

2.4.1 MPTP

2.4.1.1 General background

The 1-methyl-4-phenyl-1,2,3,6-tetrahydropyridine (**5**, MPTP) model of Parkinson's disease is the most frequently used experimental animal model employed by researchers (Salach *et al.*, 1984). Although MPTP was first identified as a parkinsonian agent in humans, it has been demonstrated to exert similar effects in a number of other primates (Jenner, 2003) as well as in cats, and in several rodents. In rodents, it was shown that only specific strains of mice were susceptible to MPTP neurotoxicity (Inoue *et al.*, 1999). MPTP is a thermal breakdown product of a meperidine–like narcotic analgesic that was used as a synthetic heroin. MPTP was shown to cause a permanent form of parkinsonism that closely resembles Parkinson's disease in humans (Ballard *et al.*, 1985) and also causes degeneration of the substantia nigra in monkeys (Przedborski & Vila, 2003).

The discovery of the toxic action of MPTP began when heroin addicts in California took an illicit street drug contaminated with MPTP and subsequently developed severe parkinsonism (Langston, 1985). This discovery of a toxic substance that damaged the brain and produced parkinsonian symptoms caused a dramatic breakthrough in parkinson's research. MPTP was first derived from 1-methyl-4-phenyl-4-propionoxypiperidine (**19**, MPPP), a meperidine (**20**) analogue (Langston *et al.*, 1983). In the synthesis of MPPP, higher reaction temperatures facilitate the dehydration reaction to yield MPTP (Scheme 9). Improper isolation and crystallization procedures, also appears to result in the elimination of propionic acid from MPPP (Scheme 9).

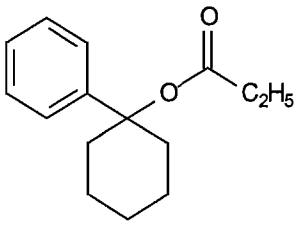

MPPP (**19**)

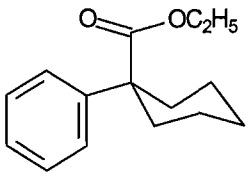

meperidine (**20**)

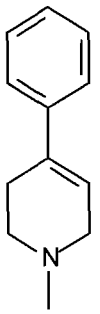

MPTP (**5**)

Figure 20. The structures of MPPP (**19**) meperidine (**20**) and MPTP (**5**).

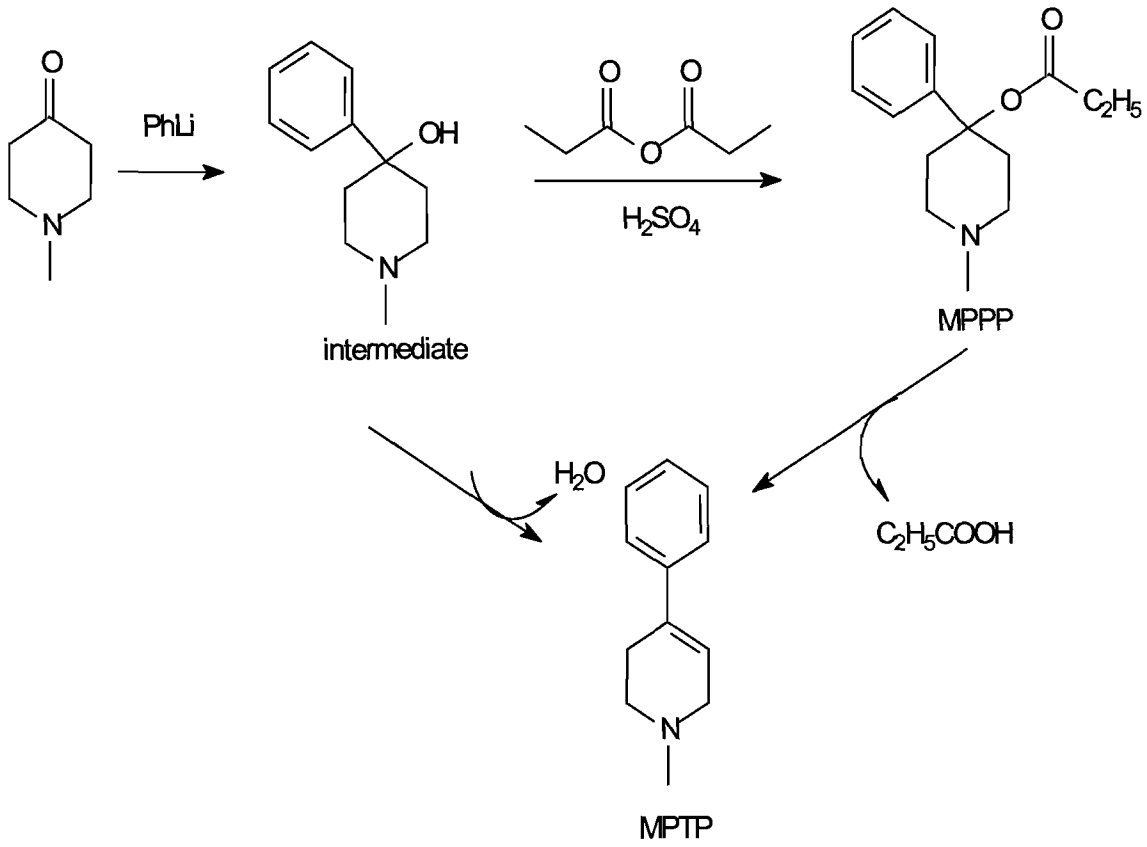

Scheme 9. The preparation of MPTP (**5**) from MPPP (**19**).

2.4.1.2 The mechanism of toxicity of MPTP

A considerable amount of work has been done towards elucidation of the mechanism of MPTP-induced neurotoxicity. MPTP (**5**) is firstly oxidised by the enzyme MAO-B to 1-methyl-4-phenyl-2,3-dihydropyridium (**21**, $MPDP^+$) (Scheme 10) (Nicklas *et al.*, 1985; Ramsay *et al.*, 1991; Singer *et al.*, 1988; Singer & Ramsay, 1990). The $MPDP^+$ metabolite is unstable and undergoes a further two electron-oxidation to form the corresponding toxic pyridinium species, MPP^+ (**22**) by a poorly defined pathway (Singer *et al.*, 1988). It was suggested the conversion of $MPDP^+$ to MPP^+ is enzyme mediated or occurred by a simple disproportionation mechanism to yield the toxic 1-methyl-4-phenylpyridinium ion (MPP^+) (Langston *et al.*, 1984; Castagnoli *et al.*, 1985; Singer & Ramsay, 1990).

The neurotoxicity of MPTP was found to be dependent on its conversion to the 1-methyl-4-phenylpyridinium species MPP^+ (Salach, 1984) and was mediated by MAO-B (Chiba *et al.*, 1984, 1985; Trevor *et al.*, 1987). This MAO-dependent formation of MPP^+ appeared to be a necessary

event in the neurotoxic process, as pretreatment of mice and monkeys with MAO-B inhibitors prevented the MAO-B-catalyzed oxidation of MPTP and its subsequent MPTP-induced neurotoxicity (Heikkila *et al.*; 1984; Langston *et al.*, 1984).

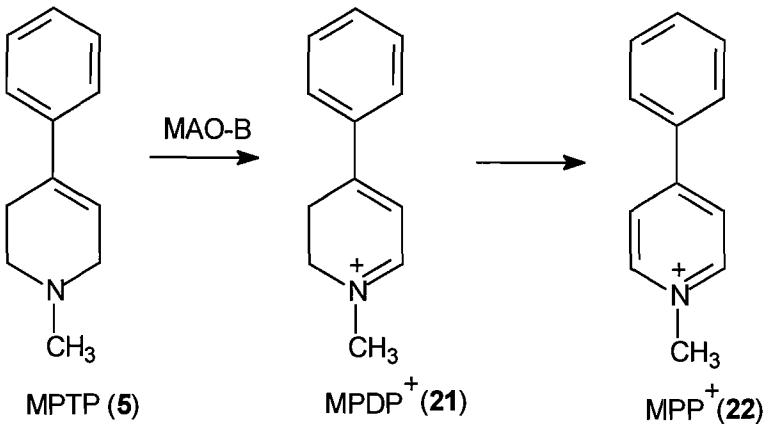

Scheme 10. The MAO catalyzed oxidation of MPTP (**5**) to the dihydropyridinium species, $MPDP^+$ (**21**) and the pyridinium MPP^+ (**22**).

The oxidation of MPTP is believed to take place in the glial cells from where the metabolites, $MPDP^+$ and MPP^+, are released by an unknown mechanism into the extracellular space (Figure 21), (Singer *et al.*, 1988).

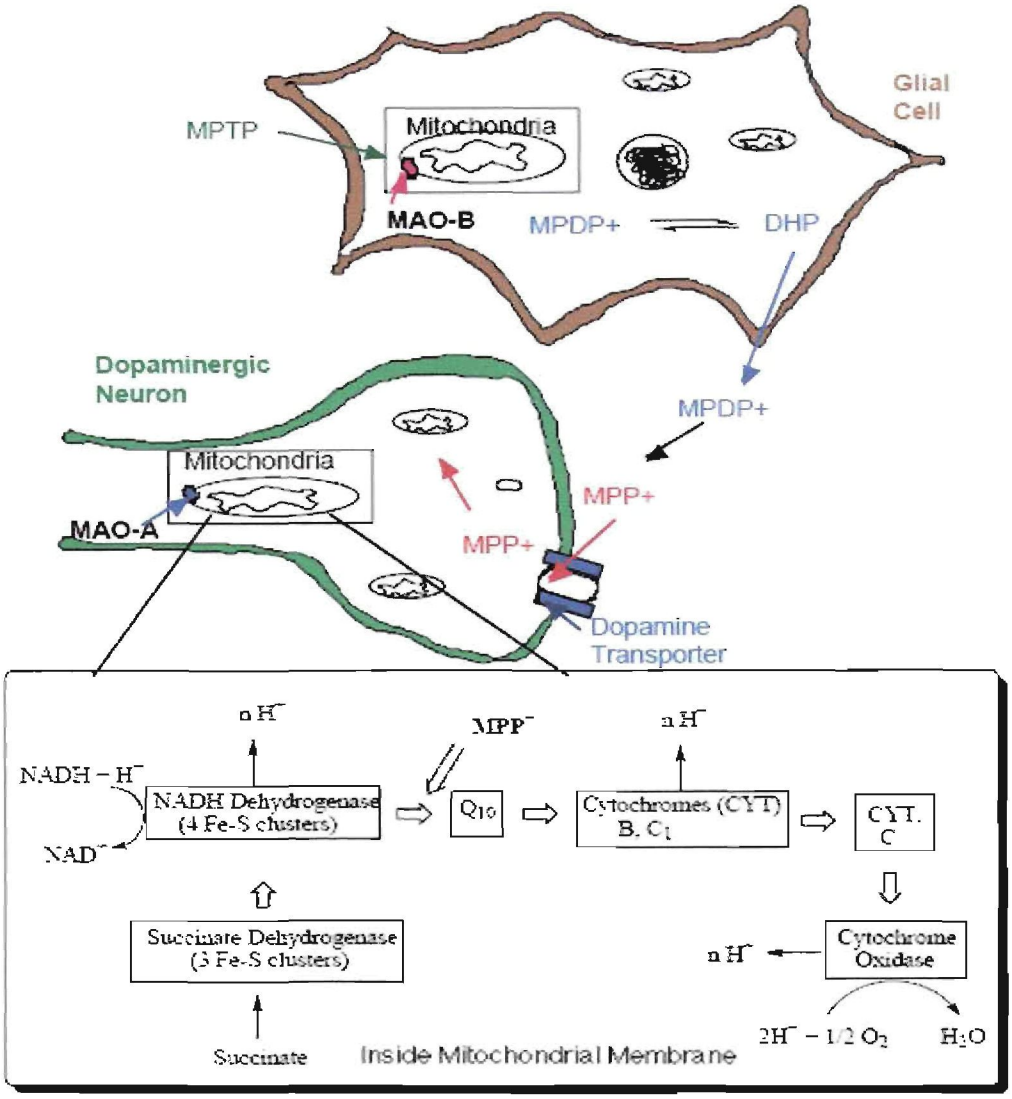

Figure 21. Schematic representation of the mechanism of MPTP-induced neurotoxicity (Javitch *et al.*, 1985).

MPP^+ is then concentrated into dopaminergic neurons via the dopamine transporter (DAT). Inside the neuronal cell, MPP^+ is concentrated within the mitochondria (Ramsay & Singer, 1986) and interrupts the transfer of electrons from complex I to ubiquinone (Figure 22). MPP^+ enters the mitochondria by the diffusion through the mitochondrial inner membrane (Nicklas *et al.*, 1985; Vyas & Heikkila, 1986). This action triggers a series of events, involving the production of toxic reactive oxygen species and decreased synthesis of cellular ATP leading to the eventual cell death (Ramsay *et al.*, 1986).

Although this appeared to be the major step in the blockade of mitochondrial function, studies have shown that MPP^+ also directly inhibited complexes III and IV of the electron transport chain (Mizuno *et al.*, 1988). Based upon the finding that MPP^+ depletes cellular energy due to interference with complex I–III, and as such was related to the etiology of human Parkinson's disease, the MPTP model has become the reference for most studies of toxin based models.

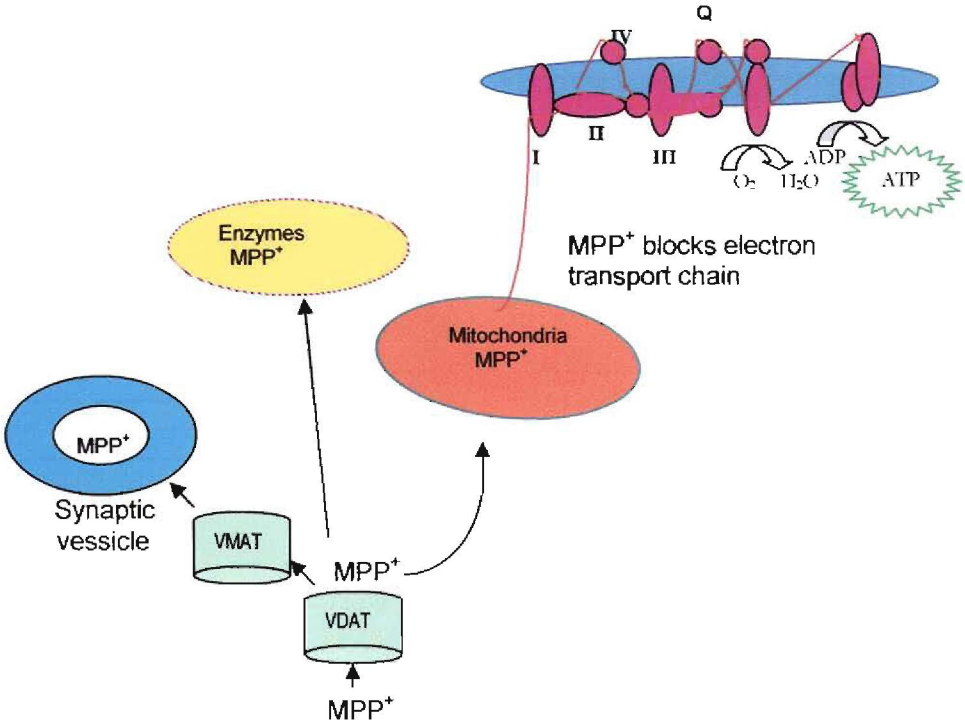

Figure 22. Schematic representation of the mechanism of MPP^+ (**22**) action inside dopaminergic neurons.

Despite the fact that inhibition of complex I by MPP^+ reduces energy production within dopaminergic neurons and causes loss of cellular energy with several deleterious consequences, it has been shown that this is not the immediate cause of the neuronal death. The exact mechanism leading to cell death is still not clear and it is thought to take place through a complicated pathway (Langston, 1990). One possibility is the production of increased free radicals due to complex I inhibition or via MPP^+-induced dopamine leakage from synaptic vesicles to the cytosol (Smeyne & Jackson-Lewis, 2005).

2.4.2 Hydroxydopamine (6-OHDA)

6-Hydroxydopamine (**23**, 6-OHDA), is a neurotoxin, that was used to study the first animal model of Parkinson's disease (Bove *et al.*, 2005). Although 6-OHDA-induced pathology differs from PD, it is still extensively used for both *in vitro* and *in vivo* investigations. Its failure to cross the blood-brain barrier (BBB), means it must be administered by local stereotaxic injection into the

substantia nigra or the striatum to target the nigrostriatal dopaminergic pathway. 6-OHDA-induced toxicity is relatively selective for monoaminergic neurons (Ungerstedt, 1968), possibly since it shares some structural similarities with dopamine and norepinephrine and exhibits a high affinity for several catecholaminergic plasma membrane transporters such as the dopamine (DAT) and norepinephrine transporters (NET) (Sauer & Oertel, 1994). Following accumulation in the cytosol, 6-OHDA generates hydrogen peroxide (H_2O_2) (Scheme 11) via the reduction of molecular oxygen. One mole of 6-OHDA may produce several equivalents of O_2 by redox cycling chemistry (Dauer *et al.*, 2003; Przedborski & Ischiropoulos, 2005).

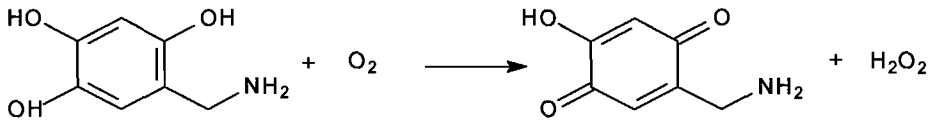

6-OHDA

Scheme 11. The redox cycling of 6-OHDA (**23**) produces H_2O_2 as a neurotoxin.

Unilateral 6-OHDA administration to experimental animals produces an asymmetric circling behaviour, the magnitude of which depends on the degree of the nigrostriatal lesion (Ungerstedt *et al.*, 1970). Because the unilateral lesion can be quantitatively measured; this model offers a notable advantage to assess the antiparkinsonian properties of new drugs and the benefit of transplantation or gene therapy to repair the damaged pathways.

2.4.3 Rotenone

Rotenone (**24**) is the most potent member of the rotenoids, a family of natural cytotoxic compounds extracted from tropical plants; widely used as an insecticide and pesticide (Figure 23) (Talpade *et al.*, 2000).

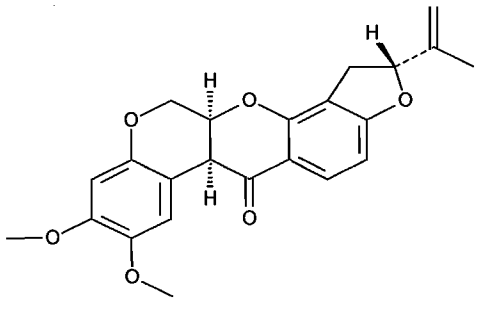

Rotenone (**24**)

Figure 23. The chemical structure of rotenone.

Rotenone is highly lipophilic and readily gains access to all organs including the brain, freely crosses all cellular membranes and can accumulate in subcellular organelles such as the mitochondria. The accessibility of rotenone to freely enter all cells have linked rotenone, an environmental toxin, with Parkinson's disease as it binds at the same site as MPP^+, the potent Parkinson-inducing agent. Like MPP^+, rotenone inhibits mitochondrial complex I (Betarbet *et al.*; 2000) activity (Talpade *et al.*; 2000). Aside from its action on mitochondrial respiration, rotenone also inhibits the formation of microtubules from tubulin (Brinkley *et al.*, 1974). Selective degeneration of nigrostriatal dopaminergic neurons (Alam & Schmidt, 2002) is observed in rats when administered low doses of intravenous rotenone (Greene & Greenmayre, 1996; Ferrante *et al.*, 1997).

2.4.4 Paraquat

The herbicide paraquat (**25**, N,N'-dimethyl-4-4'-bipyridinium) also induces a parkinsonian syndrome in animals. Paraquat is structurally similar to MPP^+ and is known to be present in the environment, at very low levels. Exposure to paraquat has been linked to an increased risk for Parkinson's disease (Dauer & Przedborski, 2003). The toxicity of paraquat is thought to be mediated by the formation of superoxide radicals (Scheme 12) (Day *et al.*, 1999).

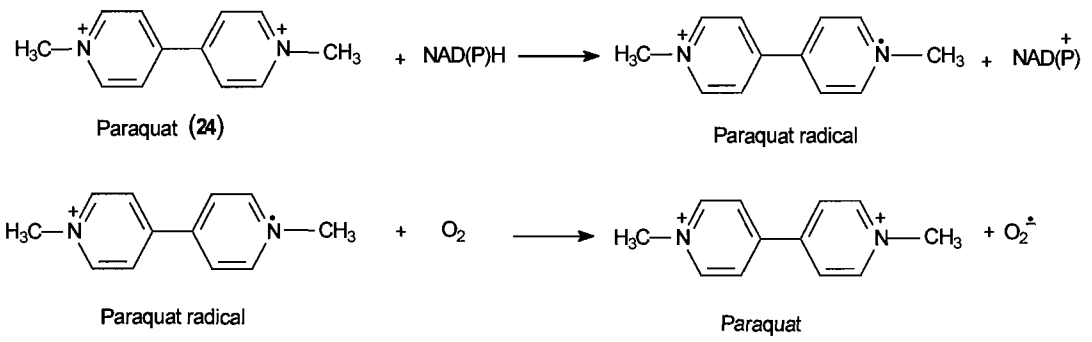

Scheme 12. The redox cycling reaction of paraquat.

The systemic administration of paraquat to mice leads to dopaminergic neuron degeneration (Manning-Bog *et al.*, 2002). Despite the apparent structural similarity to MPP^+ (Dauer & Przedborski, 2003), paraquat is neither a substrate nor an inhibitor of DAT and *in vivo* exposure to MPTP and rotenone, but not paraquat, inhibits complex I in brain mitochondria. It therefore exerts selective dopaminergic toxicity in a manner that is unique from rotenone and MPTP.

2.5 Biological importance of Maleimides

Cyclic imides such as succinimides, maleimides, pthalimides and their derivatives contain an imide ring and a general structure –CO-N(R)-CO- that confers hydrophobicity and neutral characteristics. These compounds are of scientific interest because they exhibit a diversity of biological activities such as antibacterial, antifungal, antinociceptitive, anticonvulsant and antitumor activities. However, in spite of these activities, much of their mechanisms of action at molecular levels remain to be elucidated.

Lima *et al.* (1999) found prominent antimicrobial activity in imidic compounds which were effective to inhibit the growth of Escherichia coli, Staphylococcus aureus, Candida albicans, Microsporum canis and Penicillium. Dantas *et al.* (2000) evaluated the sensitivity of Candida species and dermatophytes to maleimides, naftalimides and succinimides and noted that only maleimides showed promising results as Candida inhibitors, while the inhibition of Microsporum and Tricophyton was similar for the three assayed compounds.

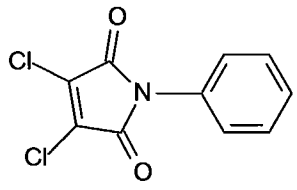

3,4-dichloro-N-phenylmaleimide

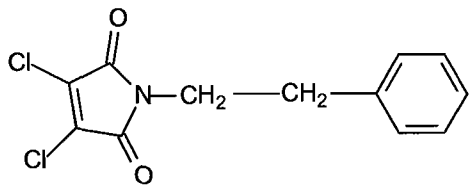

3,4-dichloro-N-phenyl-ethylmaleimide

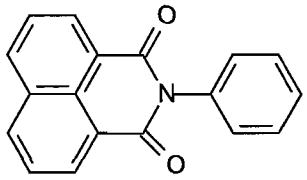

N-phenyl-corborneno-succinimide

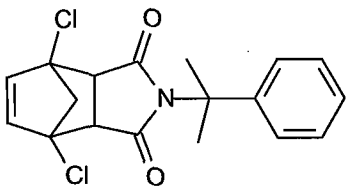

N-phenyl-naphtalimide

Figure 24. Examples of the structures of maleimides, succinimides and naftalimides.

Cechinel Filho *et al.* (1994) studied the antibacterial activity of cyclic imides, including N-phenylmaleimides and N-aryl-dichloromaleimides on S. aureus, Salmonella tiphymurium and E. coli and reported that maleimide derivatives showed activities which were approximately 30 times higher than the succinimides against Escherichia coli and Staphylococcus aureus. This suggests that the structural feature of the unsaturated bond of the maleimide ring is important for its activity.

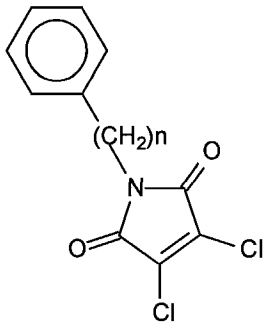

N-aril-dichloromaleimide

Figure 25. Structure of *N*-aril-dichloromaleimide.

Antifungical action of 3,4-dichloro-N-*substituted maleimides* (Figure 26) was further investigated by Pontes *et al.* (2007) who reported that *T. asahii* strains and *T. inkin* strains were largely inhibited by 3,4-dichloro-N-*substituted maleimides*. These results were compatible with those observed by (Dantas *et al.*, 2000) which showed that 3,4 dichloro-N-benzylmaleimide and 3,4-dichloro-*N*-phenylpropilmaleimide inhibited *Candida albicans* growth.

Gayoso *et al.* (2006) showed that maleimides inhibit the growth of onychomycosis, a fungal infection in which the nails are affected. These findings and the emergent necessity of developing new and efficient antifungical compounds could lead to a possible rational inclusion of these compounds in pharmaceutical compositions used for the anti-onychomycosis therapy.

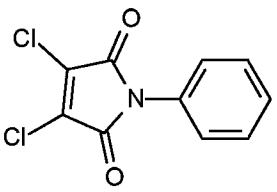

3,4-dichloro-N-phenylmaleimide

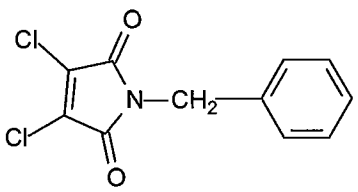

3,4-dichloro-N-benzylmaleimide

Figure 26. The structures of 3,4-dichloro-N-substituted maleimides.

The antimicrobial activity of maleimides may possibly be related to the double bond in the imidic ring or with the nitrogen atom, which could lead to electronic interactions between maleimides and microbial cells (Dantas *et al.*, 2000). Moreover, increasing electronic density on the nitrogen atom

of these compounds, suggests participation in the activation of redox cycles that play a major role for development of biological activities (Andricopulo *et al.*, 1998).

2.5.1 Metabolism of the maleimide derivative, Thalidomide

Maleimide derivatives such as thalidomide, are unstable in aqueous solutions and are believed to undergo spontaneous hydrolysis, to produce metabolites that exhibit enantiomeric, species as well as tissue specificity. Studies done on the hydrolysis of thalidomide show that hydrolysis can occur both in the glutaramide ring and the aromatic ring depending on the pH (Schumacher *et al.*, 1965a). Above pH 7, both rings undergo hydrolysis while below pH 7, only the pthalimide amide bond is hydroylsed. Metabolites of thalidomide present in urine, blood, plasma and tissue of various species have been studied extensively (Schumacher *et al.*, 1965b).

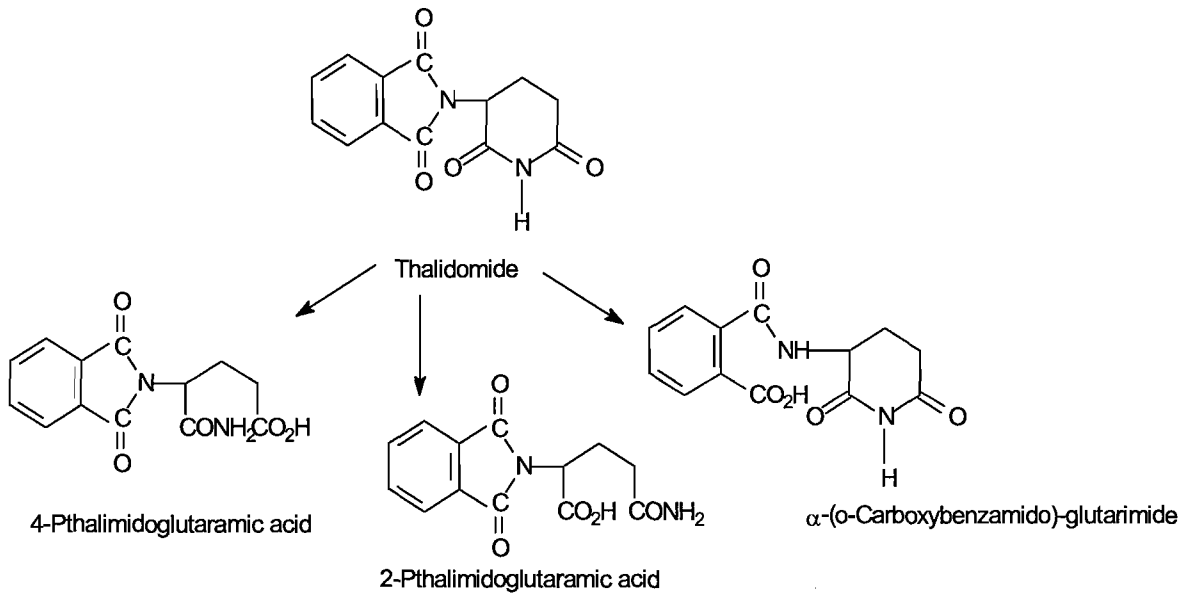

Scheme 13. Spontaneous hydrolysis of Thalidomide.

2.6 Summary

Parkinson's disease, a neurodegenerative disorder, is characterized mainly by a marked loss of dopamine nigrostriatal neurons which results in a disabling movement disorder. There are various therapeutic strategies available for the treatment of Parkinson's disease. Most of these provide relief from the symptoms of the disease while the underlying cause of neurodegeneration is left untreated. Dopamine replacement therapy with the dopamine precursor levodopa, is currently used as first line therapy. Levodopa is frequently combined with the MAO-B inhibitor (R)-deprenyl. Inhibition of MAO-B in the brain may conserve the already depleted supply of dopamine and also

stoichiometrically decreases the dopaldehyde and H_2O_2 production associated with dopamine in the brain. MAO-B inhibitors may therefore provide a neuroprotective effect in addition to symptomatic relief for Parkinson's disease patients.

Since maleimides are structurally related to thalidomide, they also may be unstable in aqueous solutions and undergo spontaneous hydrolysis to the carboxylic acid. If such drugs are absorbed, it is likely that they will spontaneously hydrolyse in the blood, into compounds that are more stable than the parent drug. Any study into the pharmacological and biochemical properties of maleimides must therefore take into account this instability.

CHAPTER 3.

PREPARATION OF SYNTHETIC TARGETS

3.1 Synthesis of N-methyl-2-phenylmaleimides

In this chapter we propose a possible synthetic route for the preparation of N-methyl-2-phenylmaleimide and selected phenyl ring substituted analogues (**9a–g**) (Figure 27). As is evident, these N-methyl-2-phenylmaleimides are structural analogues of a series of 1-methyl-3-phenylpyrroles (**8a–g**) (Figure 27), compounds that have been found recently to be moderately potent competitive inhibitors of MAO-B (William & Lawson, 1999; Ogunrombi *et al.*, 2008). In this study the MAO-B inhibition potencies of **9a–g** will be compared to that of **8a–g**.

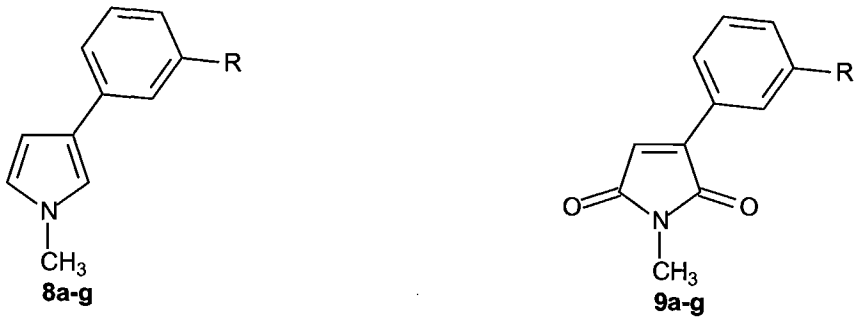

a: R=H
b: R=Cl
c: R=Br
d: R=F
e: R=CH_3
f: R=OCH_3
g: R=CF_3

Figure 27. The structures of 1-methyl-3-phenylpyrroles (**8a–g**) and N-methyl-2-phenylmaleimide (**9a–g**).

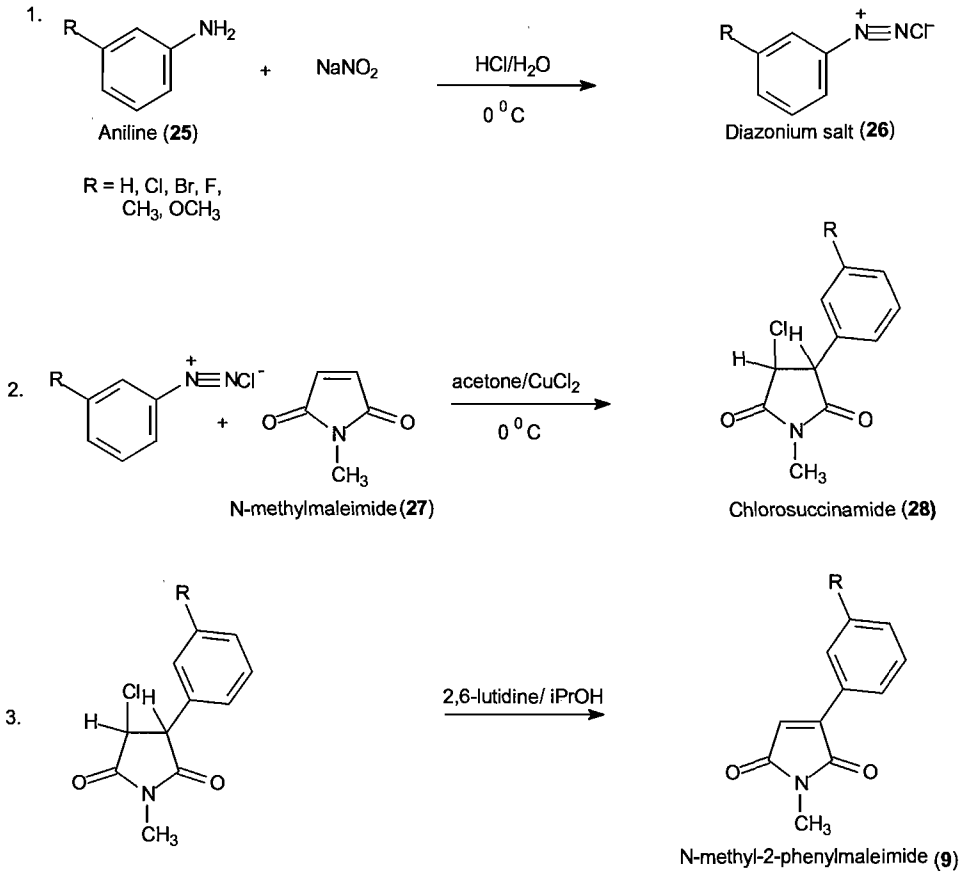

Scheme 14. The synthetic pathway proposed for the synthesis of N-methyl-2-phenylmaleimides (**9a–g**) (Mckenzie *et al.*, 1984).

A convenient synthetic route for the preparation of N-methyl-2-phenylmaleimide (**9a**) had been reported (Mckenzie *et al.*, 1984). This route is illustrated in Scheme 14. In the first step aniline (**25**) is diazotized at –10 °C with sodium nitrite. The resulting diazonium salt (**26**) is added at –10 °C to a stirred solution of N-methylmaleimide (**27**) in acetone. The final target N-methyl-2-phenylmaleimides (**9a–g**) may be obtained following dehydrohalogenation of the intermediate chlorosuccinimide (**28**).

Of note however, is the work of Epstein and co-workers (Epstein *et al.*, 1980), who reported the formation of a Diels-Alder dimer from this synthesis of N-methyl-2-(4-methylphenyl)maleimide (Scheme 15). This dimer possibly resulted from excessive heating during the 2,6-lutidine dehydrohalogenation of the intermediate chlorosuccinimide. It was however found that this side reaction could be suppressed by dilution of the lutidine with isopropyl alcohol and by reduction of the heating time.

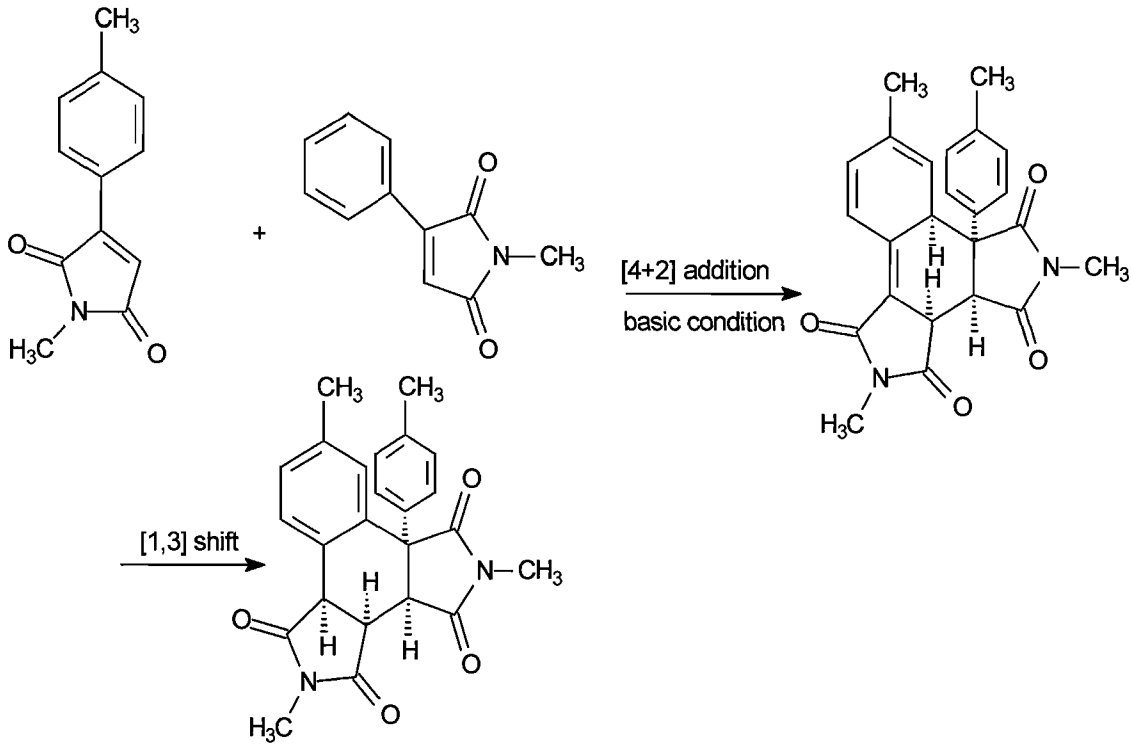

Diels-Alder dimer

Scheme 15. The formation of a Diels-Alder dimer during the synthesis of N-methyl-2-(4-methylphenyl)maleimide (Epstein *et al.*, 1980).

3.1.1 Materials and instrumentation

All starting materials, unless otherwise mentioned were obtained from Sigma-Aldrich and was used without purification. Proton and carbon NMR was recorded on a Varian Gemini 300 spectrophotometer. Proton (^{1}H) spectra was recorded in $CDCl_3$ at a frequency of 300 MHz and carbon (^{13}C) spectra at 75 MHz. Chemical shifts is reported in parts per million (δ) down field from the signal of tetramethylsilane added to the deuterated solvent. Spin multiplicities are given as s (singlet), d (doublet), t (triplet), q (quartet), dd (doublet of doublets) or m (multiplet) and the coupling constants (J) is given in Hertz (Hz). Direct insertion electron impact ionization (EIMS) and high resolution mass spectra (HRMS) was obtained on a VG 7070E mass spectrometer. Melting points (mp) were determined on a Gallenkamp melting point apparatus. All the melting points are uncorrected. Thin Layer Chromatography (TLC) was carried out using silica gel 60 (Machery-Nagel) or neutral alumina (Merck), both containing UV_{254} fluorescent indicator.

3.1.2 General synthetic procedure

Diazotization reaction: The appropriately C-3 substituted aniline derivative (20 mmol) was dissolved in a mixture of 12 N hydrochloric acid (12 ml) and water (4 ml) and then cooled in an ice–salt bath (–10 °C). Upon cooling, the aniline hydrochloric acid salt precipitated from solution. To this, a solution of sodium nitrite (22 mmol; 1.52 g) in 3.14 ml water was added dropwise over a period of 10 min while the mixture was being stirred vigorously. During this time, the reaction was not allowed to reach temperatures above 0 °C. The aniline derivative was completely diazotized, when the mixture completely dissolves, with the formation of the diazonium salt.

Meerwein reaction: N-methylmaleimide (20 mmol; 2.22 g) was dissolved in 15.69 ml of acetone and then cooled on an ice–salt bath (–10 °C). To this, the diazotized aniline was added over a period of 2 min. The pH of the reaction was adjusted to 3.0 with 12 g solid NaOAc and solid $CuCl_2.2H_2O$ (0.49 g) was added as a single portion. The reaction was stirred for a period of 3 hours in the ice–salt bath while the pH was periodically adjusted to 2.9. The reaction was allowed to heat to room temperature and was stirred for an additional 18 hours. If a precipitate forms, it was collected by filtration (**9b-9d, 9f, 9g**) while for an oil, the crude product was extracted to benzene (100 mL) (**9a, 9e**).

Dehydrohalogenation reaction: The crude product was combined with excess 2,6-lutidine (0.98 g) and isopropanol (4.9 ml) and the resulting solution was heated for 15 min in an oil bath at 100 °C to initiate dehydrohalogenation as more vigorous heating caused decomposition. For **9a** and **9e**, the crude product was extracted to benzene (100 ml) and purified on a short column (35 X 80 mm) by neutral aluminium oxide chromatography (Fluka 507C) to remove the substantial amounts of "diazo resins" which contaminated the product. Compounds **9b-9d, 9f, 9g** were directly applied to the neutral alumina column. The brown material stayed at the top of the column, while the fractions containing the pure product eluted as a clear yellow solution. Following removal of the solvent under reduced pressure, the yellow solid obtained was recrystallized twice from boiling ethanol to afford the target products **(9a-g)**.

All reactions were monitored using neutral alumina or silica gel TLC (mobile phase of Petroleum ether 80%: Ethylacetate 20%) and the plates were visualized with UV light (254 nm) and fluorescence at 366 nm.

3.1.3 Physical characterization

The structures and purity of the compounds were verified by ^{1}H-NMR and ^{13}C-NMR, as well as by nominal and high resolution mass spectrometry. For those compounds previously reported, the physical data and melting points were determined and compared to literature values. The UV-Vis absorption spectral properties of the synthesized compounds were also recorded.

3.2 Results

N-Methyl-2-phenylmaleimide (**9a**) was prepared from aniline (**25**) and N-methylmaleimide (**27**) in a yield of 39%: mp 146-148 °C (147-148 °C by capillary method); ^{1}H NMR ($CDCl_3$) δ 3.05 (s, 3H), 6.70 (s, 1H), 7.41-7.44 (m, 3H), 7.88-7.91 (m, 2H); ^{13}C NMR ($CDCl_3$) δ 23.78, 123.87, 128.51, 128.74, 130.51, 143.91, 170.34, 170.67; EI-MS *m/z;* 187 (M^{+}); HRMS calcd 187.063329, found 187.064037.

N-Methyl-2-(3-chlorophenyl)maleimide (**9b**) was prepared from appropriately substituted aniline (**25**) and N-methylmaleimide (**27**) in a yield of 6%: mp 113-115 °C (from ethanol); ^{1}H NMR ($CDCl_3$) δ 3.07 (s, 3H), 6.74 (s, 1H), 7.35-7.44 (m, 2H), 7.78-7.81 (m,1H), 7.98-7.90 (m,1H); ^{13}C NMR ($CDCl_3$) δ 23.94, 125.02, 126.64, 128.48, 130.62 (d), 135.04, 142.60, 169.92, 170.26; EI-MS *m/z;* 221 (M^{+}); HRMS calcd 221.024356, found 221.023664.

N-Methyl-2-(3-bromophenyl)maleimide (**9c**) was prepared from appropriately substituted aniline (**25**) and N-methylmaleimide (**27**) in a yield of 16%: mp 116-119 °C (from ethanol); ^{1}H NMR ($CDCl_3$) δ 3.05 (s, 3H), 6.73 (s, 1H), 7.55-7.58 (m, 1H), 7.82-7.85 (m, 1H), 8.03-8.04 (m, 1H); ^{13}C NMR ($CDCl_3$) δ 23.91, 123.00, 125.00, 127.07, 130.84 (d), 133.92, 142.42, 169.85, 170.19; EI-MS *m/z;* 264, *266* (M^{+}); HRMS calcd 264.973840, found 264.974289.

N-Methyl-2-(3-fluorophenyl)maleimide (**9d**) was prepared from appropriately substituted aniline (**25**) and N-methylmaleimide (**27**) in a yield of 31%: mp 155-158 °C (from ethanol); ^{1}H NMR ($CDCl_3$) δ 3.05 (s, 3H), 6.73 (s), 7.11-7.14 (m, 1H), 7.36-7.44 (m, 1H), 7.63-7.69 (m, 2H); ^{13}C NMR ($CDCl_3$) δ 23.87, 115.47 (d), 117.99 (d), 124.23 (d), 124.93, 130.50 (d), 142.61 (d), 161.12, 164.40, 169.93, 170.26; EI-MS *m/z;* 205 (M^{+}); HRMS calcd 205.053907, found 205.05318.

N-Methyl-2-(3-methylphenyl)maleimide (**9e**) was prepared from appropriately substituted aniline (**25**) and N-methylmaleimide (**27**) in a yield of 4%: mp 91-93 °C (from ethanol); ^{1}H NMR ($CDCl_3$) δ 3.05 (s, 3H), 6.68 (s, 1H), 7.24-7.34 (m, 2H), 7.68-7.70 (m, 2H); ^{13}C NMR ($CDCl_3$) δ 21.37, 23.78, 123.72, 125.71, 128.87, 131.88, 138.64, 144.14, 170.45, 170.76; EI-MS *m/z;* 201 ($M^{\cdot+}$); HRMS calcd 201.078979, found 201.078442.

N-Methyl-2-(3-methoxyphenyl)maleimide (**9f**) was prepared from appropriately substituted aniline (**25**) and N-methylmaleimide (**27**) in a yield of 15%: mp 145-148 °C (146-148 °C by capillary method); ^{1}H NMR ($CDCl_3$) δ 3.04 (s, 3H), 3.82 (s, 3H), 6.69 (s, 1H), 6.96-6.99 (m, 1H), 7.35-7.45 (m, 1H), 7.46-7.47 (m, 2H); ^{13}C NMR ($CDCl_3$) δ 23.78, 55.32, 113.05, 117.01, 120.95, 124.12, 129.10, 143.72, 159.78, 172.28, 170.61; EI-MS *m/z;* 217 ($M^{\cdot+}$); HRMS calcd 217.073893, found 217.073177.

N-Methyl-2-(3-trifluoromethylphenyl)maleimide (**9g**) was prepared from appropriately substituted aniline (**25**) and N-methylmaleimide (**27**) in a yield of 9%: mp 103-105 °C (from ethanol); ^{1}H NMR ($CDCl_3$) δ 3.07 (s, 3H), 6.81 (s, 1H), 7.20 (m, 1H), 7.55-7.71 (m, 1H), 8.07-8.16 (m, 2H); ^{13}C NMR ($CDCl_3$) δ 23.93, 121.82 (d), 125.28 (d), 125.41 (d), 127.50 (d), 129.48 (d), 130.91, 131.34, 131.78, 132.12 (q), 142.45, 160.75, 170.19; EI-MS *m/z;* 255 ($M^{\cdot+}$); HRMS calcd 255.050713, found 255.053127.

Table 1: Physical Properties of N-methyl-2-phenylmaleimides

Structure:

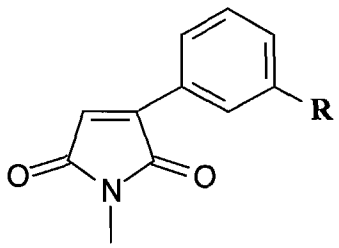

Compound	R	Mp °C	Yield %	Appearance	Formula
9a	H	146-148 °C Lit 147-148 °C	39	Light brown needle-like crystals	$C_{11}H_9NO_2$
9b	Cl	113-116 °C	6	Light brown needle-like crystals	$C_{11}H_8ClNO_2$
9c	Br	116-119 °C	16	Dark brown needle-like crystals	$C_{11}H_8BrNO_2$
9d	F	155-158 °C	31	Light brown needle-like crystals	$C_{11}H_8FNO_2$
9e	CH_3	91-93 °C	4	Bright yellow needle–like crystals	$C_{12}H_{11}NO_2$
9f	OCH_3	103-105°C	15	Light brown needle-like crystals	$C_{12}H_{11}NO_2$
9g	CF_3	145-148 °C Lit 146-148 °C	9	Bright yellow needle–like crystals	$C_{12}H_8F_3NO_2$

Table 2. The wavelengths of maximal light absorption (λ_{max}) of N-methyl-2-phenylmaleimide analogues (**9a-g**). The molar extinction coefficients (ε) at these wavelengths are also listed.

Concentration = 50 μM

Compound	(λ_{max})[a]	(ε M^{-1})
9a	269	9500
9b	266	10500
9c	269	10340
9d	267	11540
9e	273	9820
9f	275	13460
9g	263	12580

[a]All UV/Vis spectral measurements were conducted in isopropanol.

3.3 Summary

In this chapter, a synthetic route to the desired N-methyl-2-phenylmaleimide derivatives (**9a–g**) is described. One possible complication that may arise is the formation of dimers due to Diels-Alder reaction during one of the intermediary steps. This side reaction however, was suppressed by the dilution of the lutidine with isopropyl alcohol and by reduction of the heating time. The compounds (**9a–g**) were prepared using the method described, the yields were fairly low due to the double recrystallization procedure that was employed, but yielded crystals that were of high purity (**9a-g**).

CHAPTER 4.

ENZYMOLOGY

4.1 The MAO-B assay

This chapter will discuss the procedures for the determination of the enzyme-inhibitor dissociation constants (Ki values) for the reversible interaction of MAO-B with the N-methyl-2-phenylmaleimides.

4.1.1 General background

In our laboratory 1-methyl-4-(1-methylpyrrol-2-yl)-1,2,3,6-tetrahydropyridine (**16**, MMTP) is used as MAO-B substrate for the determination of enzyme-inhibitor dissociation constants (K_i values). The rate of the MAO-B catalyzed oxidation of MMTP to the corresponding dihydropyridinium metabolite (**17**, $MMDP^+$) is measured spectrophotometrically at a wavelength of 420 nm. At this wavelength neither the substrate nor the test inhibitors absorbs light, and therefore do not interfere with the spectrophotometry.

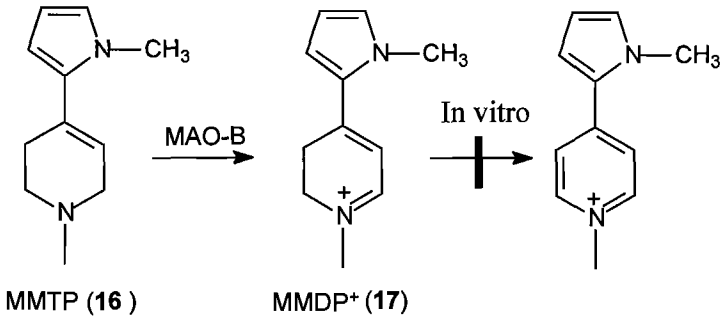

Scheme 4. The MAO-B catalyzed oxidation of MMTP (**16**) to the corresponding dihydropyridinium metabolite $MMDP^+$ (**17**) which can be conveniently measured via spectrophotometry (420 nm).

In order to prevent any contribution towards the oxidation of MMTP by MAO-A, the source of the MAO-B enzyme must either be devoid of any MAO-A activity or the oxidation of MMTP by MAO-A must be prevented. This can be achieved by inactivating MAO-A with the selective mechanism-based inactivator, clorgyline. The mitochondrial fraction obtained from baboon liver tissue was used as enzyme source, which exhibits a high degree of MAO-B catalytic activity while being devoid of MAO-A activity (Inoue *et al.*, 1999). Therefore, for the purpose of the current study, the assays were carried out in the absence of clorgyline pre-inactivation. The interaction of reversible

inhibitors with MAO-B obtained from baboon liver tissue appears to be similar to that of the human form of the enzyme since inhibitors are approximately equipotent with both enzyme sources (Petzer *et al.*, 2003). The MAO-B inhibitory properties of the compounds prepared was also investigated in order to determine whether these test inhibitors act as time dependent inactivators or as reversible inhibitors of the enzyme.

4.1.2 Materials and instrumentation

The oxalate salt of MMTP (Bissel *et al.*, 2002), a generous gift from the laboratory of Neal Castagnoli, Jr, was used. UV-Vis spectra were recorded on a Milton-Roy Spectronic 1201 spectrophotometer. Note that MMTP is a structural analogue of the nigrostriatal neurotoxin 1-methyl-4-phenyl-1,2,3,6-tetrahydropyridine (MPTP) and should be handled with care, using disposable gloves and protective eyewear. Procedures for the safe handling of MPTP have been described (Pitts *et al.*, 1986).

4.1.3 Experimental method for K_i determination

Mitochondria were isolated from baboon liver tissue as described by Salach and Weyler (Salach & Weyler, 1987) and stored at -70 °C in 300 µl aliquots. Following addition of an equal volume of sodium phosphate buffer (100 mM, pH 7.4) containing glycerol (50% w/v) to the aliquots, the protein concentration was determined by the method of Bradford using bovine serum albumin as reference standard (Bradford, 1976).

Since the mitochondrial fraction from baboon liver tissue is reported to be devoid of MAO-A activity (Inoue *et al.*, 1999), inactivation of this isoform was unnecessary. The MAO-A and MAO-B mixed substrate MMTP (K_m = 60.9 µM for baboon liver MAO-B) (Inoue *et al.*, 1999) was used as substrate for the inhibition studies. Incubations were carried out in sodium phosphate buffer (100 mM, pH 7.4) and contained MMTP (30-120 µM), the mitochondrial isolate (0.15 mg protein/mL) and various concentrations of the test inhibitor. The stock solutions of the inhibitors were prepared in DMSO and added to the incubation mixtures to yield a final DMSO concentration of 4% (v/v). DMSO concentrations higher than 4% are reported to inhibit MAO-B (Gnerre *et al.*, 2000). Following incubation at 37 °C for 10 minutes, the enzyme reactions were terminated by the addition of 10 µl perchloric acid (70%) and the samples centrifuged at 16 000g for 10 minutes. The MAO-B catalyzed production of $MMDP^+$ was found to be linear for the first 10 minutes of the reaction. (Inoue *et al.*, 1999). The supernatant fractions were removed and the concentrations of the MAO-B generated product, $MMDP^+$ were measured spectrophotometrically at a wavelength of 420 nm (ε = 25 000 M^{-1}) (Inoue *et al.*, 1999).

The initial rates of oxidation at four different substrate concentrations (30-120 μM) in the absence and presence of three different concentrations of inhibitor was calculated and the Lineweaver-Burke plots constructed. The slopes of the Lineweaver-Burke plots was plotted versus the inhibitor concentration [I] (Figure 28) and the Ki value was determined from the x-axis intercept (intercept = Ki). Linear regression analysis was performed using Sigma plot software package (Systat Software Inc).

4.1.4 Experimental method for reversibility determination

In order to determine whether the test inhibitor (**9a**) acts as a time-dependent inactivator or a reversible inhibitor of MAO-B, baboon liver mitochondrial fractions (0.3 mg of protein/ml) was preincubated with the test inhibitor (14 μM) for periods of 0, 15, 30, and 60 minutes at 37 °C (Inoue *et al.*, 1999). The solvent for this incubation is 100 mM sodium phosphate buffer (pH 7.4). The MAO-A and B mixed substrate, MMTP, at final concentration of 90 μM, was incubated at 37 °C for 15 minutes with 0.15 mg protein/ml of the preincubated mitochondria. The final volumes of these were 500 μl and final concentration of the test inhibitor 7 μM. Following termination of the reactions by the addition of 10 μl perchloric acid (70%), the concentrations of $MMDP^+$ were measured as outlined above. These experiments were done in triplicate.

If there is no decrease of MAO-B activity with increased preincubation time of the inhibitor with the enzyme, it can be concluded that the inhibitor interacts reversibly with the active site of the enzyme, MAO-B, otherwise, the inhibitor acts in a time dependent manner and is therefore an irreversible inactivator. A plot of the rate of inhibitor activity versus incubation time (Figure 30) was used to determine whether these compounds are reversible inhibitors of MAO-B or time dependent inactivators.

4.1.5 Experimental method for IC_{50} determination

Incubations were carried out in sodium phosphate buffer (100 mM, pH 7.4) and contained MMTP (50 μM), the mitochondrial isolate (0.15 mg protein/ml) and various concentrations of the test inhibitors (0.003–30 μM). The stock solutions of the inhibitors were prepared in DMSO and added to the incubation mixtures to yield a final DMSO concentration of 4% (v/v). Following incubations at 37 °C for 10 minutes, the enzyme reactions were terminated by the addition of 10 μl perchloric acid (70%) and the samples were centrifuged at 16000g for 10 minutes. The concentrations of $MMDP^+$ were measured as outlined above and these experiments were carried out in duplicate. The IC_{50} values were determined by plotting the initial rates of oxidation versus the logarithm of the inhibitor concentrations to obtain a sigmoidal dose-response curve (Figure 29). This kinetic data were fitted to the one site competition model incorporated into the Prism software package

(GraphPad Software Inc.). The IC_{50} values were determined in duplicate and are expressed as mean ± standard error of the mean (S.E.M).

4.1.6 Calculations

The initial velocity (V_i) for MAO-B catalytic oxidation of MMTP was calculated using the equation below. For the spectrophotometric determination of MAO-B activity, the equation is substituted with the measured absorbance (*Abs*) of the dihydropyridinium metabolite $MMDP^+$, the reported molar absorptivity (ε) for $MMDP^+$ (25 000 M^{-1}) and the protein concentration of the mitochondrial preparation used *[E]* (0.15 mg protein/ml), with the incubation time (*Time*) of 10 min. The dimension of V_i in this equation is mol/[mg protein.min] of the dihydropyridinium ($MMDP^+$) formed.

$$V_i = \frac{Abs}{\varepsilon} \times \frac{1}{[E]} \times \frac{1}{Time}$$

4.1.7 Results and Discussion

All of the N-methyl-2-phenylmaleimide analogues (**9a–g**) tested were found to be inhibitors of MAO-B. As demonstrated by example with N-methyl-2-(3-chlorophenyl)maleimide (**9b**) (Figure 28), the lines of the Lineweaver–Burke plots intersected at the y-axis, indicating the mode of inhibition to be competitive.

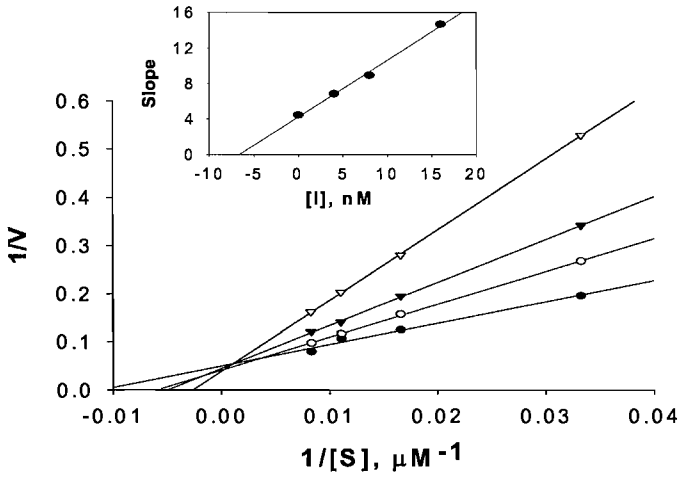

Figure 28. Lineweaver–Burke plots of the oxidation of MMTP by baboon liver MAO-B in the absence (filled circles) and presence of various concentrations of **9b** (open circles, 4 μM; filled triangles, 8 μM; open triangles, 16 μM). The concentration of the baboon liver mitochondrial isolate was 0.15 mg/mL and the rates are expressed as nmoles/min.mg protein of $MMDP^+$ formed. The inset is the replot of the slopes versus the inhibitor concentrations.

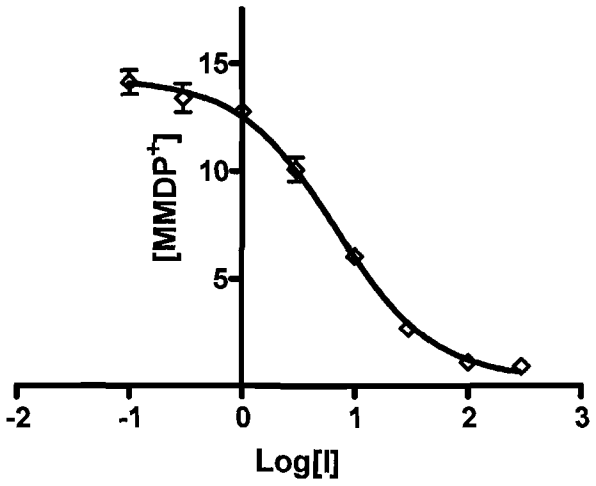

Figure 29. A plot of Log_{10} inhibitor concentration [I] versus product concentration [$MMDP^+$], μM. The inhibitor used was N-methyl-2-(3-chlorophenyl)maleimide (**9b**) with the IC_{50} value of 6.66 μM.

The IC_{50} values and the enzyme-inhibitor dissociation constants (K_i values) for the inhibition of MAO-B by the test compounds are presented in Table 3. In this study, we have determined both the IC_{50} and K_i values for the compounds under investigation as potential MAO-B inhibitors. The reason for this being that it is convenient to firstly determine IC_{50} values using a wide range of inhibitor concentrations. The IC_{50} value so obtained can then be used as an approximation of the K_i value, and a much narrower range of inhibitor concentrations can then be selected for the experimental determination of K_i. The most potent inhibitor among the N-methyl-2-phenylmaleimide analogues was found to be the unsubstituted N-methyl-2-phenylmaleimide **(9a)** with a K_i value of 3.49 μM (Table 3), approximately a 30 fold increase in potency compared to the unsubstituted N-methyl-3-phenylpyrrole which has a reported K_i value for the inhibition of baboon liver MAO-B of 118 μM (Ogunrombi *et al.*, 2008). The second most potent inhibitor evaluated in this study was N-methyl-2-(3-chlorophenyl)maleimide (**9b**), with a K_i value of 6.66 μM, also more potent than the lead pyrrole compound.

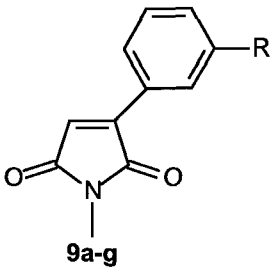

9a-g

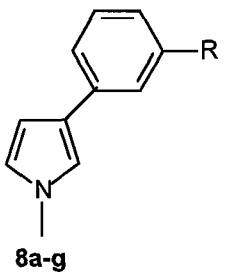

8a-g

Table 3. The IC_{50} and K_i values for the inhibition of MAO-B by N-methyl-2-phenylmaleimide analogues (**9a-g**) compared with the K_i values for the 1-methyl-3-phenylpyrrolyl derivatives (**8a-g**).

Compound	R	IC_{50} values[a] (9a-g)	K_i (μM) (R^2 values)[b] (9a-g)	K_i (μM)[c] (8a-g)
9a	H	7.01 ± 1.77	3.49 (R^2 = 0.994)	118
9b	Cl	12.87 ± 0.65	6.66 (R^2 = 0.995)	20.9
9c	Br	6.870 ± 0.41	6.99 (R^2 = 0.991)	14.3
9d	F	6.726 ± 1.53	5.73 (R^2 = 0.988)	38.9
9e	CH_3	11.72 ± 0.095	8.60 (R^2 =0.995)	56.0
9f	CF_3	17.41 ± 1.87	10.99 (R^2 = 0.995)	6.55
9g	OCH_3	9.52 ± 1.05	8.56 (R^2 =0.996)	41.7

[a]The concentration of MMTP used was 50 μM and the enzyme concentration was 0.15 mg mitochondrial protein /ml.

[b]The R^2 values shown here are those of the replot of the Lineweaver-Burke plots used to determine the K_i values.

[c]Values taken from (Ogunrombi *et al.*, 2008).

The MAO-B inhibitory properties of (**9a-g**) were investigated in order to determine whether the test inhibitors act as time–dependent inactivators or as reversible inhibitors of the enzyme. For this study, **9a** was selected as a representative test inhibitor. When baboon liver mitochondrial fractions were preincubated with **9a** (7 μM) for periods of 0, 15, 30 and 60 minutes, the rate of

MAO-B catalyzed oxidation of MMTP (90 μM) to $MMDP^+$ slightly increased. The slight increase in MAO-B catalytic activity with time, seen from the plot of rate versus incubation time (Figure 30), is probably due to the fact that maleimides, like thalidomide generally undergo hydrolysis in aqueous solutions, depending on the pH, to give carboxylic acids which are more stable.

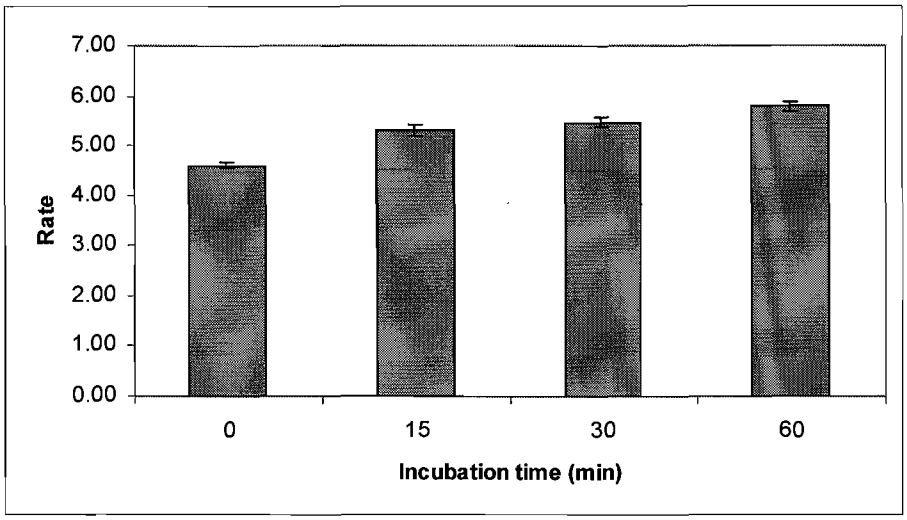

Figure 30. Time dependent inhibition of baboon liver MAO-B by N-methyl-2-phenylmaleimide (**9a**). Baboon liver mitochondria (0.3 mg/mL) were preincubated with the inhibitor (14 μM) at preincubation times of 0, 15, 30 and 60 minutes. The enzyme was added to the substrate to yield final [E] of 0.15 mg/mL, [I] of 7.0 μM and a final [S] of 90 μM. Incubations were carried out for 15 min at 37 °C.

4.2 Molecular docking studies

In this section we describe the modeling of N-methyl-2-phenylmaleimide (**9a**) within the active site of human recombinant MAO-B. The specific interactions between the ligand and the enzyme active site were identified. 1-Methyl-3-phenylpyrrole (**8a**) was also docked into MAO-B in order to compare the binding mode to that of **9a**.

4.2.1 General background

Docking is the procedure of fitting one molecule into another. In this study, it involves the fitting of a small molecule ligand into the active site of the MAO-B protein. Docking is a useful tool to determine the possibility of the ligand to bind to the enzyme active site before actually synthesizing the ligand. Of the many interactions that may occur between a ligand and the receptor molecule, we focused on hydrogen bonding interactions since the structures under

investigation (**9a–g**) differ mainly from the lead compound (**8a**) in their ability to interact with protein molecules via hydrogen bonding. Other interactions that may occur between a ligand and a receptor are: hydrophobic interactions, electrostatic interactions, charge transfer interactions and dipole interactions.

4.2.2 Method

Among the crystallographic structures of MAO-B deposited in the Brookhaven Protein Data Bank, the structure with *trans,trans*-farnesol bound to the enzyme (2BK3.pdb) (Hubalek *et al.*, 2005) was selected for the docking studies. The choice of this complex was based on the high resolution of the crystallographic structure and the observation that *trans,trans*-farnesol spans both the entrance and substrate cavities of the enzyme active site. As a result, the side chain of Ile-199, which acts as a "gate" separating the two cavities, is rotated out of its normal conformation to allow for the fusion of the two cavities and the accommodation of larger structures (Binda *et al.*, 2003).

All the computational studies were carried out in the Windows-based Discovery Studio 1.7 modeling and simulation environment (Accelrys Software Inc.). The ligands to be docked were constructed within DS Visualizer Pro and then prepared for the docking simulations using the Prepare Ligands application of Discovery Studio. The crystallographic structure of *trans,trans*-farnesol in complex with human MAO-B (2BK3.pdb) (Hubalek *et al.*, 2005) was retrieved from the Brookhaven Protein Data Bank (www.rcsb.org/pdb) and the co-crystallized inhibitor was manually deleted. Following typing of the receptor model with the CHARMm forcefield, the binding site was identified by the Ligandfit flood-filling algorithm. Automated docking was then carried out with the LigandFit application of Discovery Studio. This docking protocol employed total ligand flexibility whereby the final ligand conformations were determined by the Monte Carlo conformation search method set to a variable number of trial runs. The docked ligands were further refined using *in situ* ligand minimization with the Smart Minimizer algorithm. All the application modules within Discovery Studio were set to their default values and 10 docking solutions were allowed for each ligand.

4.2.3 Results and discussion

In order to test the merit of N-methyl-2-phenylmaleimides as potential MAO-B inhibitors, N-methyl-2-phenylmaleimide analogue (**9a**) was modeled within the active site of human recombinant MAO-B. As indicated in figure 31, the inhibitor (**9a**) traverse both the entrance and substrate cavity, with the C-5 carbonyl oxygen of the maleimide ring stabilized by hydrogen bonding with amino acid residues and water molecules in the substrate cavity of the enzyme, while the phenyl ring extends into the entrance cavity.

This orientation is highly favoured as it allows the C-5 carbonyl oxygen of the maleimide ring to interact with both Try–435 and Wat–60 molecules in the substrate cavity, forming specific H-bonds. This mode of binding is in complete reversal to that observed by the N-methyl-3-phenylpyrroles (Ogunrombi *et al.*, 2008) in which the pyrrolyl ring extends beyond the boundary of the entrance and substrate cavity, while the phenyl ring binds within the substrate cavity (Figure 32).

For 1-methyl-3-phenylpyrrole (**8a**), hydrogen bond interaction with the enzyme is not possible (Figure 32). This may be the reason why the pyrrole inhibitors are in general less potent than the corresponding maleimide analogues. The only exception is pyrrole **8f** (3-CF_3) which is slightly more potent than the corresponding maleimide **9f**. A possible explanation may be that the CF_3 of **8f** is involved in hydrogen bond interaction within the substrate cavity (Ogunrombi *et al.*, 2008), while the CF_3 of the maleimide is located in the entrance cavity which is largely hydrophobic, with no possibility of hydrogen bond formation. Since hydrogen bond interactions are not possible with 1-methyl-3-phenylpyrrole (**8a**), we conclude that hydrogen bonding is responsible for N-methyl-2-phenylmaleimide (**9a**) being a more potent inhibitor of MAO-B compared to the pyrroles. Interestingly, the observation that C-3 phenyl substitution of the N-methyl-2-phenylmaleimides does not enhance the MAO-B inhibition potency, may be explained by the deep protrusion of the inhibitor into the substrate cavity, which does not allow for stabilizing hydrophobic interactions between the phenyl substituents and the lipophilic environment of the entrance cavity.

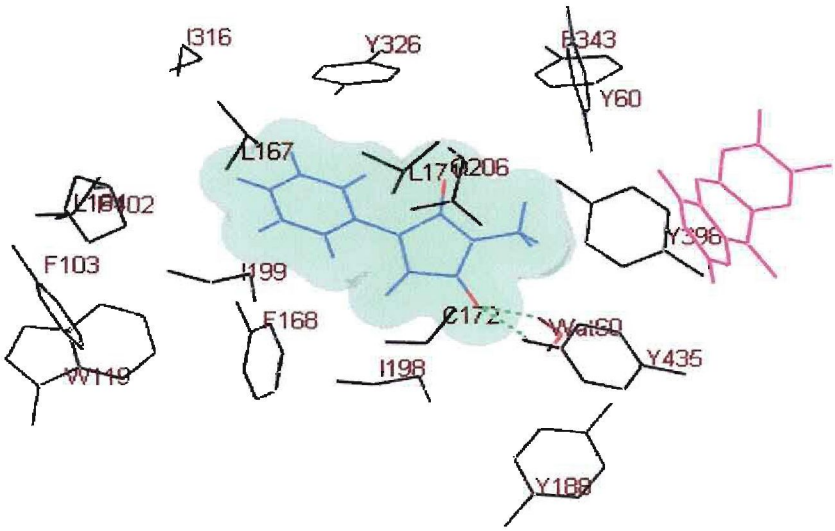

Figure 31. The binding mode of N-methyl-2-phenylmaleimide (**9a**) to the active site of MAO-B. Hydrogen bonding is indicated by the dotted lines.

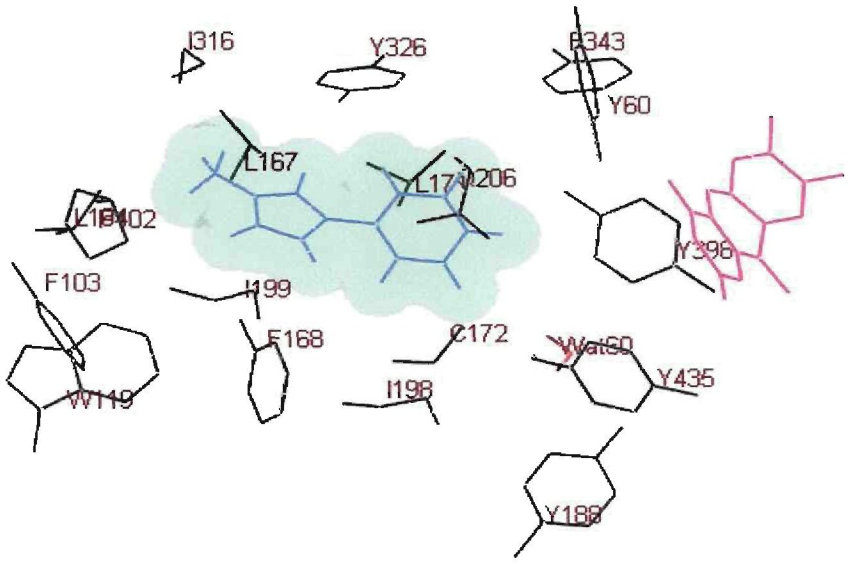

Figure 32. The binding mode of 1-methyl-3-phenylpyrrole (**8a**) to the active site of MAO-B.

4.3 Summary

In this chapter we have shown that all the N-methyl-2-phenylmaleimide analogues (**9a–g**) tested were found to be reversible competitive inhibitors of MAO-B, with the most potent inhibitor being the unsubstituted N-methyl-2-phenylmaleimide with a K_i value of 3.49 μM, approximately a 30 fold increase in potency compared to the unsubstituted N-methyl-3-phenylpyrrole which has a reported K_i value for the inhibition of baboon liver MAO-B of 118 μM.

N-methyl-2-phenylmaleimide (**9a**) and 1-methyl-3-phenylpyrrole (**8a**) were docked into the active site of recombinant human MAO-B. The results show that the carbonyl oxygens of the maleimide ring is stabilized by hydrogen bonding with Wat-60 and Tyr-435 in the substrate cavity of the enzyme while the phenyl ring extends into the entrance cavity. Similar interactions are not possible with 1-methyl-3-phenylpyrrole.

We therefore conclude that in general, N-methyl-2-phenylmaleimides inhibit MAO-B with enhanced potency compared to the pyrroles and H-bonding appears to be a major contributing factor towards ligand stabilization and inhibition potency.

CHAPTER 5.

CONCLUSION

The enzyme MAO-B is a well known target for the treatment of degenerative disorders. Inhibitors of MAO-B are used for the symptomatic treatment of Parkinson's disease and are also under investigation as potential neuroprotective agents. Also, MAO-B is the catalyst responsible for the oxidation of the pro-neurotoxin MPTP to its ultimately neurotoxic product MPP^+. Therefore, inhibitors of MAO-B have been found to prevent the neurotoxic action of MPTP.
The primary aim of this study was to test the hypothesis that N-methyl-2-phenylmaleimide anlaogues, which are structural analogues of known MAO-B inhibitors 1-methyl-3-phenylpyrroles, could act as more potent inhibitors of MAO-B due to the presence of carbonyl oxygen atoms that could act as hydrogen bond acceptors. Maleimides have long been known for their pharmaceutical value, as they have been found to act as antibacterial, antifungal, antinoceptive, anticonvulsant and antitumor agents. The possibility that N-methyl-2-phenylmaleimide analogues may act as potent inhibitors of MAO-B, could possibly lead to the discovery of new lead compounds for the treatment of Parkinson's disease.

To achieve this aim, a series of N-methyl-2-phenylmaleimide analogues (**9a-g**) were successfully synthesized and the structure and purity of the compounds were confirmed by ^1H and ^{13}C NMR. The series of N-methyl-2-phenylmaleimide analogues (**9a-g**) prepared were found to be reversible competitive inhibitors of MAO-B. The MAO-B assay results revealed that the unsubstituted N-methyl-2-phenylmaleimide was the most potent inhibitor, with an enzyme–inhibitor dissociation constant (K_i value) of 3.49 μM. This is 30 fold more potent than the 1-methyl-3-phenylpyrrole, the lead pyrrole compound for this study. The least potent inhibitor was found to be N-methyl-2-(3-trifluoromethylphenyl)maleimide with a K_i value of 10.99 μM.

Reversibility studies showed that N-methyl-2-phenylmaleimide (**9a**) was not a time dependent inactivator but acted reversibly with the enzyme MAO-B. This makes the maleimides examined here more desirable than irreversible inhibitors. Since inhibitors of MAO B are currently in use, and still being investigated for the treatment of neurodegenerative disorders, the results of this study contributes to the identification of new reversible inhibitors.

Another goal of this research was to investigate the binding mode of N-methyl-2-phenylmaleimide within the active site of the MAO-B enzyme and compare it with the 1-methyl-3-phenypyrroles.

Molecular docking revealed that N-methyl-2-phenylmaleimide analogues traverse both cavities of the enzyme and bind in a manner opposite to that of the pyrroles, in which the maleimide ring is bound in the substrate cavity of the enzyme while the phenyl ring is located in the entrance cavity. Hydrogen bonds were formed between the carbonyl oxygens of the maleimide ring and the amino acid residues within the susbstrate cavity, an interaction not possible with the pyrroles.

Thus, modifying the structure of the pyrroles to include hydrogen bond acceptors greatly improved binding affinity within the active site of the enzyme. Hydrogen bonding was an additional interaction to the hydrophobic interactions shown by the N-methyl-2-phenylmaleimide analogues, enhancing ligand stabilization, thus making them more potent inhibitors of MAO-B than the 1-methyl-3-phenylpyrroles.

BIBLIOGRAPHY

Alam, M. & Schmidt, W. J. 2002. Rotenone destroys dopaminergic neurons and induces parkinsonian symptoms in rats. *Behav. Brain Res.* 136:317–324.

Andricopulo, A. D., Willian Filho, A., Corrêa, R., Santos, A. R. S., Nunes, R. J., Yunes, R. A. & Cechinel Filho, V. 1998. Analgesic activity of 3,4-dicloromaleimides: structure activity relationships. *Pharmazie.* 53:493–498.

Averill-Bates, D. A., Agostinelli, E., Przybytkowski, E., Mateescu, M. A. & Mondovi, B. 1993. Cytotoxicity and kinetic analysis of purified bovine serum amine oxidase in the presence of spermine in Chinese hamster ovary cells. *Arch. Biochem. Biophys.* 300:75–79.

Ballard, P. A., Tetrud, J. W. & Langston, J. W. 1985. Permanent human parkinsonism due to 1-methyl-4-phenyl-1,2,3,6-tetrahydropyridine (MPTP): seven cases. *Neurology.* 35:949–956.

Bernheimer, H., Birkmayer, W., Hornykiewicz, O., Jellinger, K. & Seitelberger, F. 1973. Brain dopamine and the syndromes of Parkinson and Huntington. Clinical, morphological and neurochemical correlations. *J. Neurol. Sci. 20*:415–455.

Betarbet, R., Sherer, T. B., Mackenzie, G., Garcia-osuna, M., Panov, A. V. & Greenamyre, J. T. 2000. Chronic systemic pesticide exposure reproduces features of Parkinson disease. *Nat. Neurosci.* 3: 268–273.

Binda, C., Li, M., Hubalek, F., Restilli, N., Edmonson, D. E. & Mattevi, A. 2003. Insights into the mode of inhibition of human mitochondrial monoamine oxidase B from high resolution crystal structures. *Proc. Natl. Acad. Sci, USA,* 100:9750–9755.

Binda, C., Newton–Vinson, P., Edmondson, D. E. & Mattevi, A. 2002. Structure of human monoamine oxidase, a drug target for the treatment of neurological disorders. *Nat. Struc. Biology.* 9:22–26.

Binda C., Hubalek, F., Li, M., Edmondson, D. E. & Mattevi, A. 2004. Crystal structure of human monoamine oxidase B, a drug target enzyme monotopically inserted into the mitochondrial outer membrane. *FEBS Lett.* 564:225–228.

Birkmayer, W., Reiderer, P., Youdim, M. B. H. & Linauer, W. 1975. The potentiation of the anti-akinetic effect after L-dopa treatment by an inhibitor of MAO-B, L-deprenyl. *J. Neural. Transm.* 36:303–326.

Bissel, P., Bigley, M. C., Castagnoli, K. & Castagnoli, N., Jr. 2002. Synthesis and biological evaluation of MAO-A selective 1,4-disubstituted-1,2,3,6-tetrahydropyridinyl substrates. *Bioorg. Med. Chem.* 10:3031–3041.

Bove´, J., Prou, D., Perier, C. & Przedborski, S. 2005. Toxin-induced models of Parkinson's disease: *J. Am. Soc. Exp. NeuroTherapeutics.* 2:484–494.

Bradford, M. M. 1976. A rapid and sensitive method for the quantitation of microgram quantities of protein utilizing the principle of protein–dye binding. *Anal. Biochem.* 72:248–254.

Brinkley, B. R., Barham, S. S., Barranco, S. C. & Fuller, G. M. 1974. Rotenone inhibition of spindle microtubule assembly in mammalian cells. *Exp. Cell. Res.* 85:41–46.

Calne, D. B. 1989. Is "Parkinson's disease" one disease? *J. Neurol. Neurosurg. Psychiatry.* 52:18–21.

Calne, D. B. 1994. Is idiopathic parkinsonism the consequence of an event or a process? *Neurology.* 44:5–10.

Castagnoli, N. Jr., Chiba, K. & Trevor, A. J. 1985. Potential bioactivation for the neurotoxin 1-methyl-4-phenyl-1, 2,3,6-tetrahydropyridine (MPTP). *Life Sci. 36*:225–230.

Cechinel Filho, V., Bella Cruz, A., Nunes, R. J., Calixto, J. B., Moretto, E., Gonzaga, L., Corrêa, R. & Yunes, R. A. 1994. Atividade antimicrobiana de análogos da filantimida. *Rev. Latinoamer. Quim.* 23:116-122.

Chazot, P. L. 2001. Safinamide (Newron Pharmaceuticals). *Curr. Opin. Investig. Drugs.* 2:809–813.

Chen, J. F., Xu, K., Petzer, J. P., Staal, R., Xu, Y. H., Beilstein, M., Sonsalla, P. K., Castagnoli, K., Castagnoli, N. Jr. & Schwarzschild, M. A. 2001. Neuroprotection by caffeine and A_{2A} adenosine receptor inactivation in a model of Parkinson's disease *J. Neurosci.* 21:1–6.

Chiba, K., Trevor, A. J. & Castagnoli, N. Jr. 1984. Metabolism of the neurotoxic tertiary amine MPTP by brain monoamine oxidase *Biochem. Biophys. Res. Commun. 120*:574–578.

Chiba, K., Peterson, L. A., Castagnoli, K., Trevor, A. J. & Castagnoli, N. Jr. 1985. Studies on the molecular mechanism of bioactivation of the selective nigrostriatal toxin 1-methyl-4-phenyl-1,2,3,6-tetrahydropyridine (MPTP). *Drug Metab. Dispos.* 13:342–347.

Cotzias, G. C. & Dole, V. P. 1951. Microdetermination of monoamine oxidase in tissues. *J. Biol.Chem.* 190:665–672.

Dauer, W. & Przedborski, S. 2003. Parkinson's disease: Mechanisms and models. *Neurons.* 39:889–909.

Day, B. T., Patel, M., Calavetta, L., Chang, L. Y. & Stamler, J. S. 1999. A mechanism of paraquat toxicity involving nitric oxide synthase. *Proc. Natl. Acad. Sci. USA.* 96:12760–12765.

Dantas, Z. M. R., Lima, E. O., Vasconcelos Filho, P. A. & Cechinel Filho, V. 2000. Susceptibilidade *invitro* de espécies de *Candida* a maleimidas, naftalimidas e succinimidas. *Rev. Bras. Farm.* 81:31-35.

Dingemanse, J., Wood, N., Jorga, K. & Kettler, R. 1997. Pharmacokinetics and pharmacodynamics of single and multiple doses of the MAO-B inhibitor lazabemide in healthy subjects. *Br. J. Clin. Pharmacol.* 1:41–47.

Ebadi, M., Brown-Borg, H., Ren, J., Sharma, S., Shavali, S., El ReFaey, H. & Carlson, E. C. 2006. Therapeutic efficacy of selegiline in neurodegenerative disorders and neurological diseases. *Curr. Drug Targets.* 7:1513–1529.

Edmonson, D. E., Binda, C. & Mattevi, A. 2004. The FAD binding sites of human monoamine oxidases A and B. *Neurotoxicology.* 25:63–72.

Epstein, J. W., Mckenzie, T. C., Lovell, M. F. & Perkinson, N. A. 1980. Diels-Alder dimerization of 2-arylmaleimides. X-ray crystal structure of the dimer of 2-*p*–tolylmaleimide. *J.C.S. Chem. Comm.* 314–315.

Ferrante, R. J., Schulz, J. B., Kowall, N. W. & Beal, M. F. 1997. Systemic administration of rotenone produces selective damage in the striatum and globus pallidus, but not in the substantia nigra. *Brain Res. 753*:157–162.

Finberg, J. P., Wang, J., Bankiewich, K. S., Harvey-White, J., Kopin, I. & Golstein, D. S. 1988. Increased striatal dopamine production from L-DOPA following selective inhibition of monoamine oxidase B by R (+)–N-propargyl-1-aminoindan (rasagiline) in the monkey. *J. Neural. Transm. Suppl.* 52:279–285.

Flohe, L. 1978. Glutathione peroxidase: Fact and fiction. *Ciba Found Symp.* 65:95–122.

Gayoso, C. W., Lima, E., Leite de Souza, E., Valdir Cechinel Filho, V., Trajano, V. N, Pereira, F. & Igara Oliveira Lima, I. O. 2006. Antimicrobial effectiveness of maleimides on fungal strains isolated from onychomycosis. *Braz. Arch. Bio. Tech.* 49:661–664.

Gesi, M., Santinami, A., Ruffoli, R., Conti, G. & Fornai, F. 2001. Novel aspects of dopamine oxidative metabolism: confounding outcomes take place of certainties. *Pharmacol. Toxicol.* 89:217–224.

Gnerre, C., Catto, M., Leonetti, F., Weber, P. A., Altomare, C. & Carotti, A. & Testa, B. 2000. Inhibition of monoamine oxidases by functionalized coumarin derivatives: biological activities, QSARs, and 3D-QSARs. *J. Med. Chem.* 43:4747–4758.

Greene, J. G. & Greenmayre, J. T. 1996. Bioenergetics and glutamate excitoxicity. *Pro. Neurobiol.* 48: 613–634.

Hamani, C. & Lozano, A. M. 2003, Physiology and pathophysiology of Parkinson's disease. *Ann. N.Y. Acad. Sci.* 991:15–21.

Heikkila, R. E., Manzino, L., Cabbat, R. S. & Duvoisin, R. C. 1984. Protection against the dopaminergic neurotoxicity of 1-methyl-4-phenyl-1,2,3,6-tetrahydropyridine by monoamine oxidase inhibitors. *Nature.* 311:467–469.

Hubalek, F., Binda, C., Khalil, A., Li, M., Mattevi, A., Castagnoli, N. Jr. & Edmondson, D. E. 2005. Demonstration of isoleucine 199 as a structural determinant for the selective inhibition of human monoamine oxidase B by specific reversible inhibitors. *J. Biol. Chem.* 280:15761–15766.

Inoue, H., Castagnoli, K., Van der Schyf, C., Mabic, S., Igarashi, K. & Castagnoli, N. Jr. 1999. Species-dependent differences in monoamine oxidase A and B catalyzed oxidation of various C4 substituted 1-methyl-4- phenyl-1,2,3,6-tetrahydropyridinyl derivatives. *J. Pharmacol. Exp. Ther.* 291:2856–2864.

Javitch, J. A., D'Amato, R. J., Strittmetter, S. M. & Syner, S. H. 1985. Parkinsonism-inducing neurotoxin, 1-methyl-4-phenyl-1,2,3,6-tetrahydropyridine: uptake of the metabolite 1-methyl-4-phenylpyridine by dopamine neurons selective toxicity. *Proc. Natl. Acad. Sci.* USA . 82:2173–2177.

Jenner, P. 2003. Oxidative stress in Parkinson's disease. *Ann. Neurol.* 53:S23–S38.

Jenner, P.1998. Oxidative mechanisms in nigral cell death in Parkinson's. disease. *Mov Disord.* 13 (Suppl 1):24–34.

Jenner, P. & Olanow, C. W. 1996. Oxidative stress and the pathogenesis of Parkinson's disease. *Neurology.* 47:161–170.

Kalgutkar, A., Testa, B. & Castagnoli, N. Jr. 1995. Selective inhibitors of monoamine oxidase (MAO-A and MAO-B) as probes of its catalytic site and mechanism. *Med. Res. Rev.* 15:325–388.

Kearney, E. B., Salach, J. I., Walker, W. H., Seng, R. L., Kenney, W., Zeszotek, E & Singer, T. P. 1971. The covalently-bound flavin of hepatic monoamine oxidase. Isolation and sequence of a flavin peptide and evidence for binding at the 8α position. *Eur. J. Biochem.* 24:321–327.

Langston, J. W., Ballard, P. A., Tetrud, J. W. & Iwrin, I. 1983. Chronic parkinsonism in humans due to a product of meperidine analog synthesis. *Science.* 291:979–980.

Langston, J. W., Forno, L. S., Rebert, C. S. & Irwin, I. 1984. Selective nigral toxicity after systemic administration of 1-methyl-4-phenyl-1,2,3,6-tetrahydropyridine (MPTP) in the squirrel monkey. *Brain Res.* 292:390–394.

Langston, J. W. 1985. The case of the tainted heroin. *Science.* 25:34–40.

Langston, J. W. 1990. Predicting Parkinson's disease. *Neurology.* 40:70–76.

Lee, F. J., Liu, F., Pristupa, Z. B. & Niznik, H. B. 2001. Direct binding and functional coupling of alpha-synuclein to the dopamine transporters accelerate dopamine-induced apoptosis. *FASEB. J.* 15:916–926.

Lima, E. O., Queiros, E. F., Andricopulo, A. D., Nunes, R. J., Yunes, R. A., Correa, R., Cechinel Filho, V. 1999. Evaluation of antifungal activity of N-aryl-maleimides and N-phenylalkyl-3-4-dichloromaleimides. *Biol. Soc. Chile Quim.* 44:185-189.

Manning-Bog, A. B., Mccormack, A. L., Li, J., Uversky, V. N., Fink., A. L & Di Monte, D. A. 2002. The herbicide paraquat causes up-regulation and aggregation of alpha-synuclein in mice: paraquat and alpha-synuclein. *J. Biol. Chem.* 277:1641–1644.

Marsden, C.D. 1983. Neuromelanin and Parkinson's disease. *J. Neural. Transm. Suppl.* 19:121–141.

Mckenzie, T. C., Epstein, J. W., Fanshawe, W. J., Dixon, S. J., Osterberg, A. C, Wennogle, L. P., Regan, B. A., Abel, M. S. & Meyerson, L. R. 1984. 5-Aryl-3-azabicyclo[3.2.0]heptan-6-one ketals, compounds with morphine-like analgesic activity. *J. Med. Chem.* 27:628–632.

Miller, J. R. & Edmondson, D. E. 1999. Structure–activity relationships in the oxidation of *para*–substituted benzylamine analogues by recombinant human liver monoamine oxidase A. *Biochemistry.* 38:13670–13683.

Mizuno, Y., Sone, N., Suzuki, K. & Saitoh, T. 1988. Studies on the toxicity of 1-methyl-4-phenylpyridinium ion (MPP^+) against mitochondria of mouse brain. *J. Neurol. Sci.* 86:97–110.

Nicklas, W. J., Vyas, I. & Heikkila, R. E.1985. Inhibition of NADH-linked oxidation in brain mitochondria by 1-methyl-4-phenyl-pyridine, a metabolite of the neurotoxin, 1-methyl-4-phenyl-1,2,3,6-tetrahydropyridine. *Life Sci.* 36:2503–2508.

Novaroli, L., Daina, A., Favre, E., Bravo, J., Carotti, A., Leonetti, F., Catto, M., Carrupt, P. A. & Reist, M. 2006. Impact of species-dependent differences on screening, design and development of MAO-B inhibitors. *J. Med.Chem.* 49:6264–6272.

O'Brien, E.M., Kiely K.A. & Tipton, K.F. 1993. A discontinuous luminometric assay for monoamine oxidase. *Biochem. Pharmacol.* 46:301–1306.

Ogunrombi, M. O., Malan, S. F., Terre'Blanche, G. T., Castagnoli, N. Jr., Bergh, J. J. & Petzer, J. P. 2008. Structure–activity relationship in the inhibition of monoamine oxidase B by 1-methyl-3-phenylpyrroles. *Bioorg. Med.Chem.* (In press).

Olanow, C. W. 1990. Oxidation reactions in Parkinson's disease. *Neurology.* 40:32–37.

Ono, T. 1975. A new colorimetric assay for monoamine oxidase in serum and its clinical application. *J. Lab. Clin. Med.* 85:1022–1031.

Petzer, J. P., Steyn, S., Castagnoli, K. P., Chen, J., Schwarzchild, M. A., Van der Schyf, C. J. & Castagnoli, N. Jr. 2003. Inhibition of monoamine oxidase B by selective adenosine A_{2A} receptor antagonists. *Bioorg. Med. Chem.* 11:1299–1310.

Pitts, S. M., Markey, S. P., Murphy, D. L. & Weisz, A. In MPTP: *A neurotoxin producing a Parkinsonian syndrome.* Markey, S. P.; Castagnoli, N.; Trevor, A. J.; Kopin, I. J.; Ed.; Academic Press: New York, 1986; pp 703–716.

Pontes,V., Z. B.; Lima, E. O., Cechinel Filho, V. 2007. Profile of susceptibility *in vitro* of *Trichosporon asahii* and *Trichosporon inkin* strains against cyclic imides. *Braz. J. Pharm. Sci.* 43:237-239.

Przedborski, S. & Ischiropoulos. H. 2005. Reactive oxygen and nitrogen species: weapons of neuronal destruction in models of Parkinson's disease. *Antiox. Redox. Signal.* 7:685–693.

Przedborski, S. & Vila, M. 2003. The 1-methyl-4-phenyl-1,2,3,6-tetrahydropyridine mouse model: a tool to explore the pathogenesis of Parkinson's disease. *Ann. N.Y. Acad. Sci.* 991:189–198.

Rabey, J. M., Sagi, I., Huberman, M., Melamed, E., Korczyn, A., Giladi, N., Inzelberg, R., Djaldetti, R., Klein, C. & Berecz, G. 2000. Rasagiline Mesylate, a new MAO-B inhibitor for the treatment of Parkinson's disease: A double-blind study as adjunctive therapy to Levodopa. *Clin. Neuropharm.* 23: 324–330.

Ramsay, R. R., Krueger, M. J., Youngster, S. K., Gluck, M. R., Casida, J. E & Singer, T. P. 1991. Interaction of 1-methyl-4-phenylpyridinium ion (MPP^+) and its analogs with the rotenone/piericidin binding site of NADH dehydrogenase. *J. Neurochem.* 56:1184–1190.

Ramsay, R. R., Salach, J. I. & Singer, T. P. 1986. Uptake of the neurotoxin 1-methyl-4-phenylpyridine (MPP^+) and its relation to the inhibition of mitochondrial NADH-linked substrates by MPP^+. *Biochem. Biophys. Res. Commun. 134*:743–748.

Ramsay, R. R & Singer, T. P. 1986. Energy-dependent uptake of N-methyl-4-phenylpyridinium, the neurotoxic metabolite of 1-methyl-4-phenyl-1,2,3,6-tetrahydropyridine, by mitochondria. *J. Biol. Chem.* 261, 17: 7585–7587.

Reiderer, P., Lachenmayer, L. & Laux, G. 2004. Clinical applications of MAO- inhibitors. *Curr. Med. Chem.* 11:2033–2043.

Reiderer, P. & Youdim, M. B. 1986. Monoamine oxidase activity and monoamine metabolism in brains of parkinsonian patients treated with 1-deprenyl. *J. Neurochem.* 46:1359–1365.

Rodwell, A. & Kennely, V. W. 2000. Enzymes: Kinetics. In Harper's Biochemistry. 25th Edition. David A. Barnes (Ed), APPLETON & LANGE. Stanford, Connecticut. pp 95–97.

Salach, J. I. & Weyler, W. 1987. Preparation of the flavin-containing aromatic amine oxidases of human placenta and beef liver. *Methods Enzymol.* 142:627–637.

Salach, J. I., Singer, T. P., Castagnoli, N. Jr. & Trevor, A. 1984. Oxidation of the neurotoxic amine 1-methyl-1,2,3,6 tetrahydropyridine (MPTP) by monoamine oxidases A and B and suicide inactivation of the enzymes by MPTP. *Biochem. Biophys. Res. Commun.* 125:831–835.

Sauer, H. & Oertel, W. H. 1994. Progressive degeneration of nigrostriatal dopamine neurons following intrastriatal terminal lesions with 6-hydroxydopamine: a combined retrograde tracing and immunocytochemical study in the rat. *Neuroscience.* 59:401–415.

Schumacher, H., Smith, R. L & Williams, R. T. 1965a. The metabolism of thalidomide: the spontaneous hydrolysis of thalidomide in solution. *Br. J. Pharmacol.* 25:324–327.

Schumacher, H., Smith, R. L & Williams, R. T. 1965b. The metabolism of thalidomide: the fate of thalidomide and some of its hydrolysis products in various species. *Br. J. Pharmacol.* 25:338–351.

Silverman, R. B., Hoffman, S. J. & Catus, W. B. 1980. A mechanism for mitochondrial monoamine oxidase catalyzed amine oxidation. *J. Am. Chem. Soc. 102*:7126–7128.

Silverman, R. B. 1996. In Contemporary Enzyme Kinetics and Mechanism. 2nd edition, Purick D.L (Ed.) Academic Press, San Diego. pp 291–334.

Singer, T. P. & Ramsay, R. R. 1990. Mechanisms of the neurotoxicity of MPTP. An update. *FEBS Lett.* 274:1–8.

Singer, T. P., Ramsay, R. R., Mckeown, K., Trevor, A. & Castagnoli, N. Jr. 1988. Mechanisms of the neurotoxicity of 1-methyl-4-phenylpyridinium (MPP^+), the toxic bioactivation product of 1-methyl-4-phenyl-1,2,3,6-tetrahydropyridine (MPTP). *Toxicology.* 49:17–23.

Smeyne, R. J. & Jackson-Lewis, V. 2005. The MPTP model of Parkinson's disease. *Rev. Mol. Brain Research.* 62:57–66.

Stacy, M. & Jankovic, J. 1993. Current approaches in the treatment of Parkinson's disease. *Ann. Rev. Med.* 44:431–440.

Stevanato R., Vianello, F. & Rigo, A. 1995. Thermodynamic analysis of the oxidative deamination of polyamines by bovine serum amine oxidase. *Arch. Biochem. Biophys.* 324:374–378.

Talpade, D. J., Greene, J. G., Higgins, D. S, Jr. & Greenamyre, J. T. 2000. In vivo labeling of mitochondrial complex I (NADH:ubiquinone oxidoreductase) in rat brain using [(3)H]dihydrorotenone. *J Neurochem.* 75:2611–2621.

Thebault, J. J., Guillaume, M. & Levy, R. 2004. Tolerability, Safety, Pharmacodynamics and Pharmacokinetics of Rasagiline: A potent, selective and irreversible monoamine oxidase type B inhibitor. *Pharmacotherapy.* 24:1295–1305.

Trevor, A. J., Singer, T. P., Ramsay, R. R. & Castagnoli, N. Jr. 1987. Processing of MPTP by monoamine oxidase: Implications for molecular toxicology. *J. Neural. Transm. Suppl.* 23:73–89.

Ungerstedt, U. & Arbuthnott, G. 1970. Quantitative recording of rotational behaviour in rats after 6-hydroxydopamine lesions of the nigrostriatal dopamine system. *Brain Res.* 24:485–493.

Ungerstedt, U. 1968. 6-Hydroxydopamine induced degeneration of central monoamine neurons. *Eur. J. Pharmacol.* 5:107–110.

Vlok, N., Malan, S. F., Castagnoli, N. Jr, Bergh, J. J & Petzer, J. P. 2006. Inhibition of monoamine oxidase B by analogues of the adenosine A_{2A} receptor antagonist (E)-8-(3-chlorostrylcaffeine). *Bioorg. Med. Chem. 14*:3512–3521.

Vyas, I., Heikkila, R. E. & Nicklas, W. J. 1986. Studies on the neurotoxicity of 1-methyl-4-phenyl-1,2,3,6-tetrahydropyridine: inhibition of NAD-linked substrate oxidation by its metabolite, 1-methyl-4-phenylpyridinium. *J. Neurochem. 46*:501–507.

Waldmeier, P.C. 1987. Amine oxidases and their endogenous substrates. *J. Neural Transm. Suppl.* 23: 55–72.

Walker, M. C. & Edmondson, D. E. 1994. Structure–activity relationships in the oxidation of benzylamine analogues by bovine liver mitochondrial monoamine oxidase B. *Biochemistry. 33:*7088–7098.

Weyler, W., Hsu, Y. P. P. & Breakefield, X. O. 1990. Biochemistry and genetics of monoamine oxidase. *Pharmcol. Ther.* 47:391–417.

Williams, C. H & Lawson, J. 1999. The behaviour of arylpyrrolines with monoamine oxidase. *J. Neurobiology* (Bp). 7:225-233.

Wu, D. C., Teismann, P., Tieu, K., Vila, M., Jackson-Lewis, V., Ischiropoulos, H. & Przedborski, S. 2003. NADPH oxidase mediates oxidative stress in the 1-methyl-4-phenyl-1,2,3,6-tetrahydropyridine model of Parkinson's disease. *Proc. Natl. Acad. Sci. U. S. A.* 100:6145–6150.

Youdim, M. B. & Green, A. R. 1975. Biogenic monoamine metabolism and functional activity in iron–deficient rat; behavioural correlates. *Ciba Found Symp.* 51:201–22.

Youdim, M. B. H., Collins, G. G. S., Sandler, M., Bevan Jones, A. B., Pare, C. M. B. & Nicholson, W. J. 1972. Biological Sciences: Human brain monoamine oxidase: Multiple forms and selective inhibitors. *Nature.* 236:225–228.

Youdim, M. B. H., Edmondson, D. & Tipton K. F. 2006.The therapeutic potential of monoamine oxidase inhibitors. *Nat. Rev. Neurosci.* 7:295–309.

Youdim, M. B. H. 1988. Platelet monoamine oxidase B: Use and misuse. *Cellular & Mol. Life Sci.* 44:137–141.

Youdim, M. B. & Bakhle, Y. S. 2006. Monoamine oxidase: isoforms and inhibitors in Parkinson's disease and depressive illness. *Br. J. Pharmacol.* 147 (Suppl 1):S287–S296.

Zhou, M. & Panchuk-Voloshina, N. 1997. A one-step fluorometric method for the continuous measurement of monoamine oxidase activity. *Anal. Biochem.* 253:169–174.

ANNEXURE

Spectral Data

^{1}H NMR, ^{13}C NMR

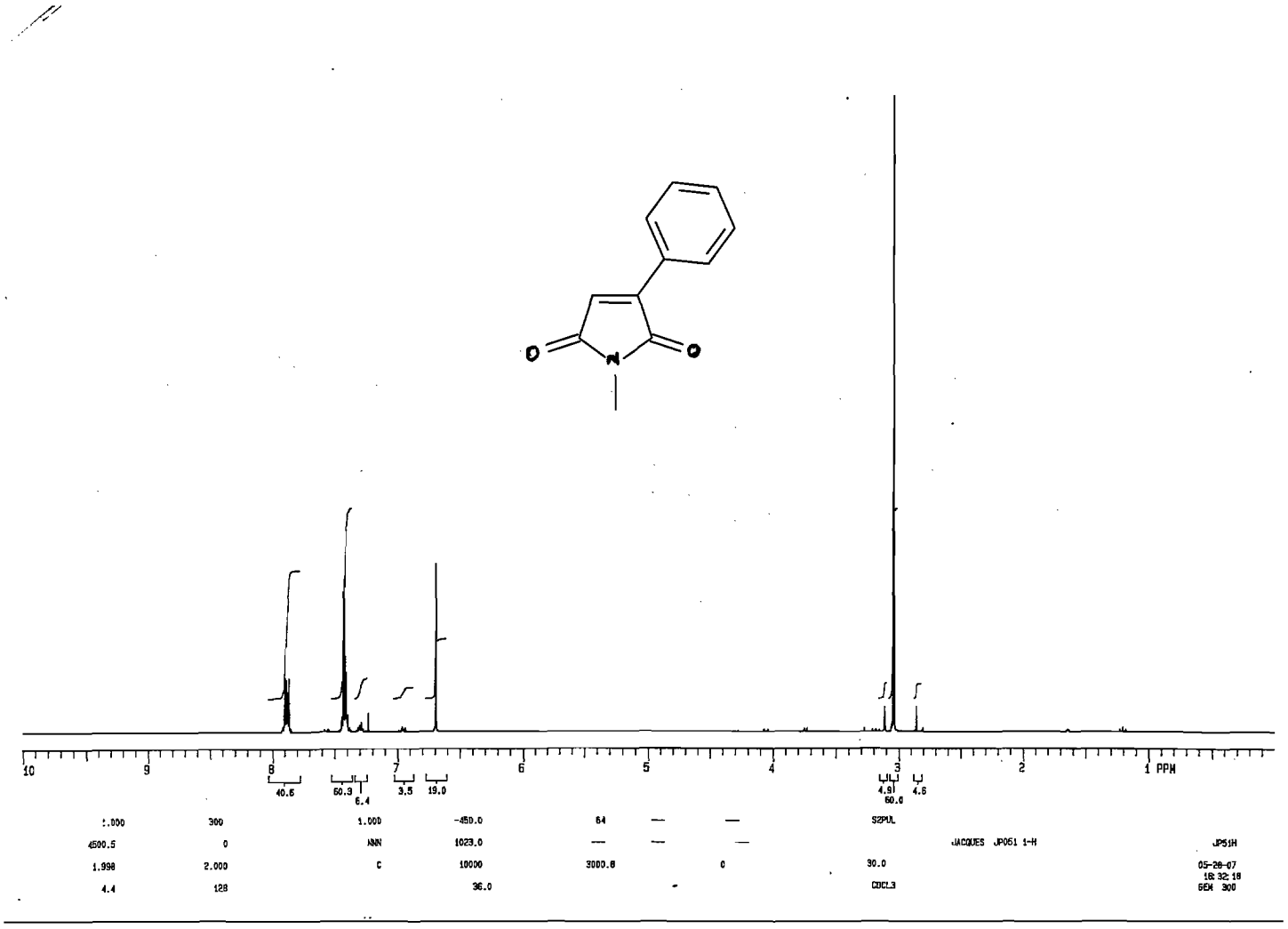
O
N
O
10
9
8
7
6
5
4
3
2
1 PPM
40.6
60.9
6.4
3.5
19.0
4.9
60.0
4.6
1.000 300 1.000 -450.0 64 — — S2PUL
4500.5 0 NNN 1023.0 — — — JACQUES JP051 1-H JP51H
1.998 2.000 C 10000 3000.8 0 30.0 05-28-07
4.4 128 36.0 CDCL3 16:32:18
GEM 300

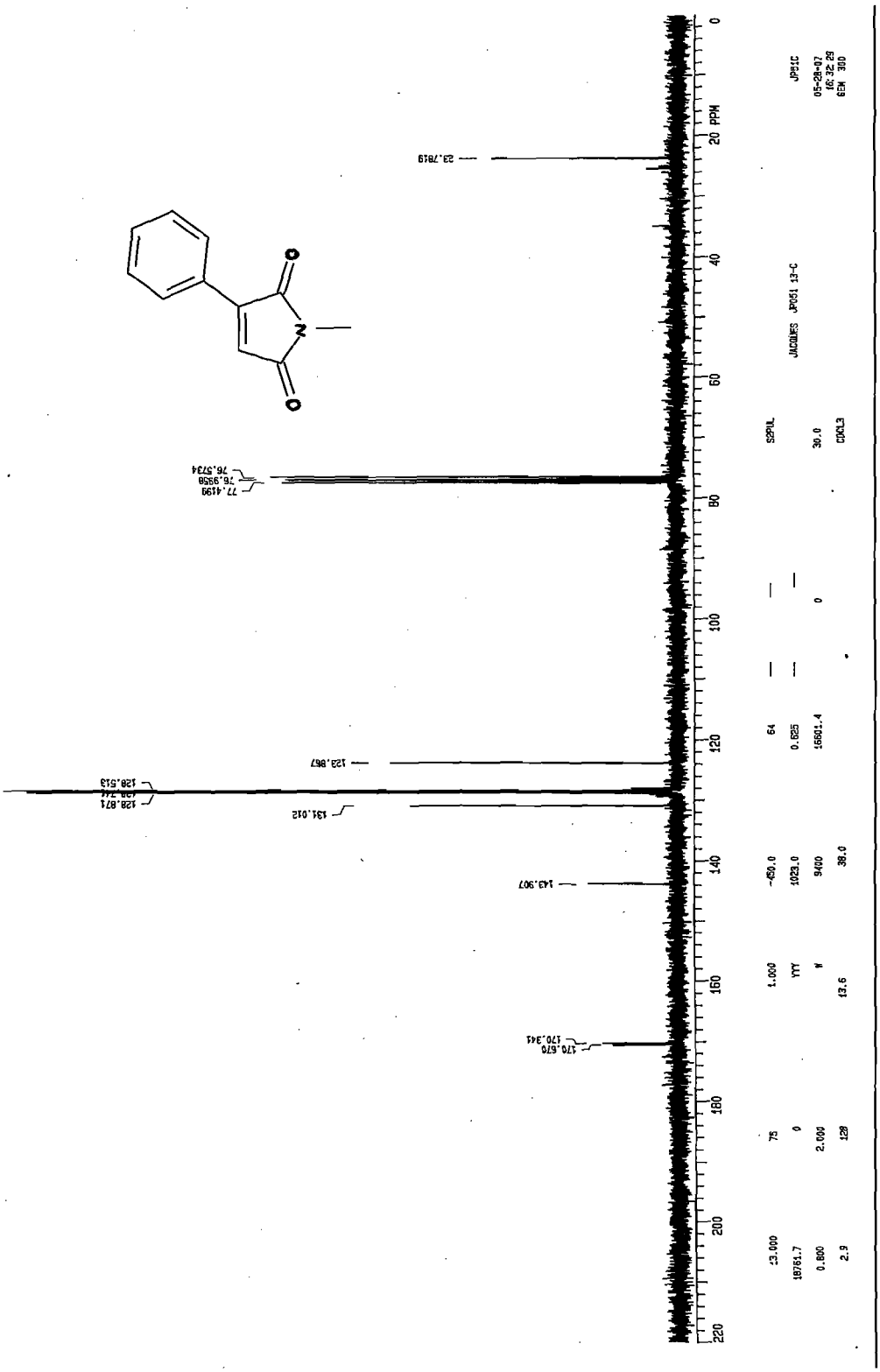
23.7819
77.4199
76.9958
76.5734
123.867
128.513
128.871
128.744
131.042
143.907
170.670
170.344
O
N
O
0
20 PPM
40
60
80
100
120
140
160
180
200
220
SCPUL
JACQUES JP051 13-C
JP51C
05-28-07
16:32:29
EEM 300
CDCL3
30.0
64
0.825
16601.4
0
-450.0
1023.0
9400
38.0
1.000
YYY
N
13.6
75
0
2.000
128
23.000
18761.7
0.800
2.9

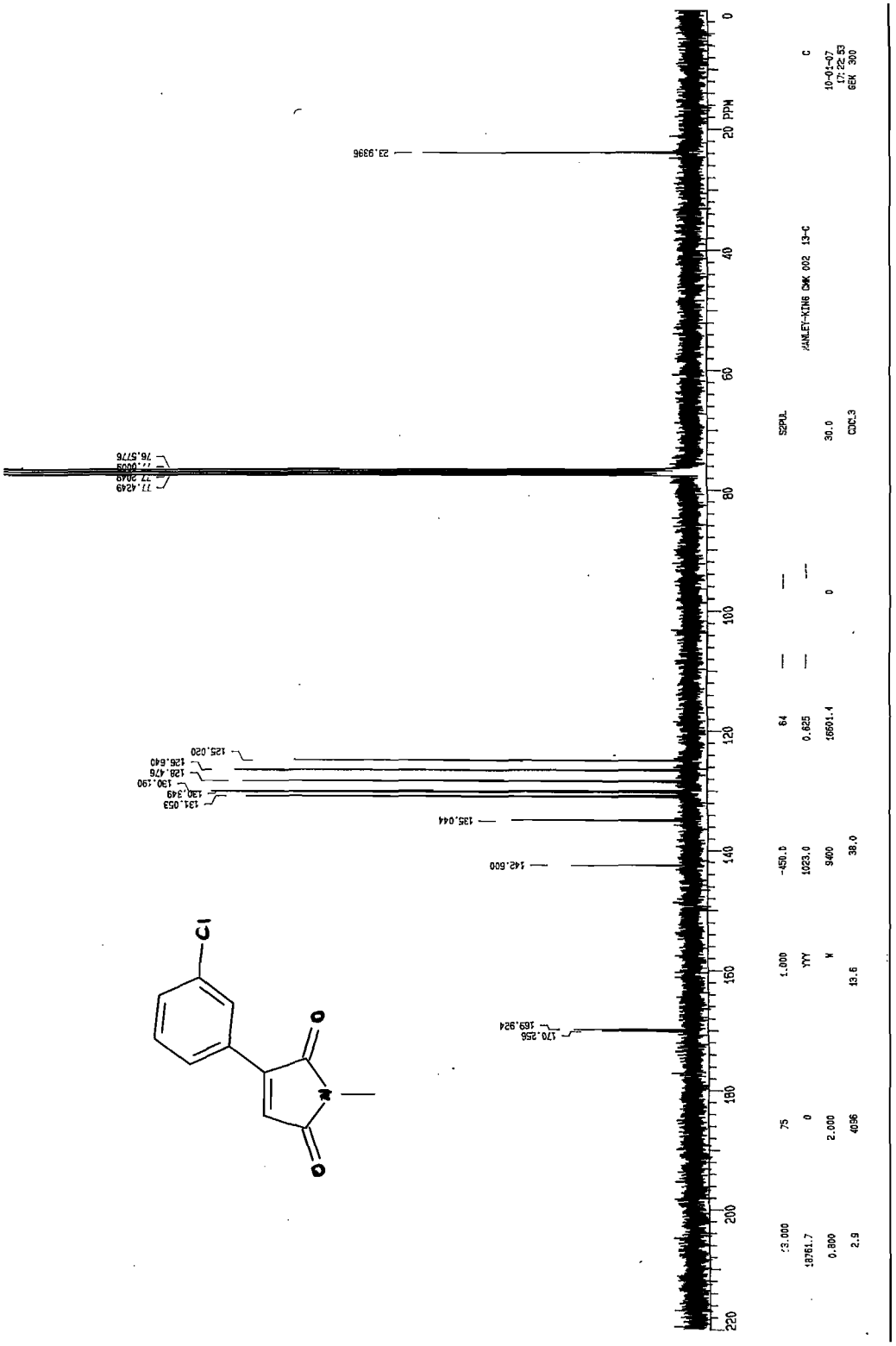
23.9386
76.5776
77.0059
77.2049
77.4249
125.020
126.640
128.476
130.290
130.349
131.053
135.044
142.600
169.924
170.256
0
20 PPM
40
60
80
100
120
140
160
180
200
220
Cl
O
N
O
SGPUL
64
0.625
16601.4
1.000
YYY
1023.0
9400
38.0
13.6
75
0
2.000
4096
13.000
18761.7
0.800
2.9
STANLEY-KING CHK 002 13-C
30.0
CDCL3
10-01-07
17:22:53
GEN 300
C

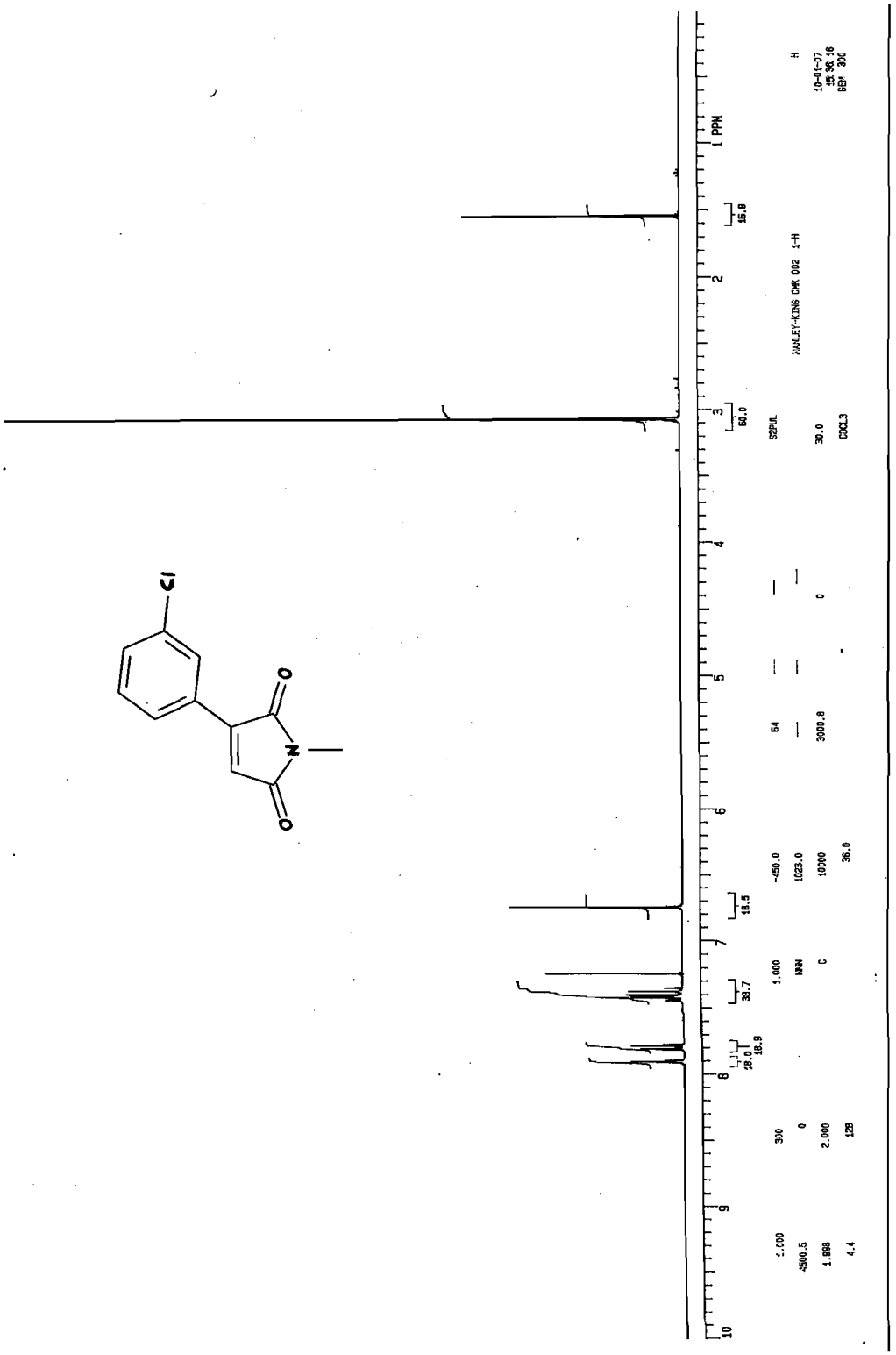
Cl
O
N
O
1 PPM
10-01-07
15:36:16
DEP 300
HANLEY-KING CHK 002 1-H
SZPUL
COCL3

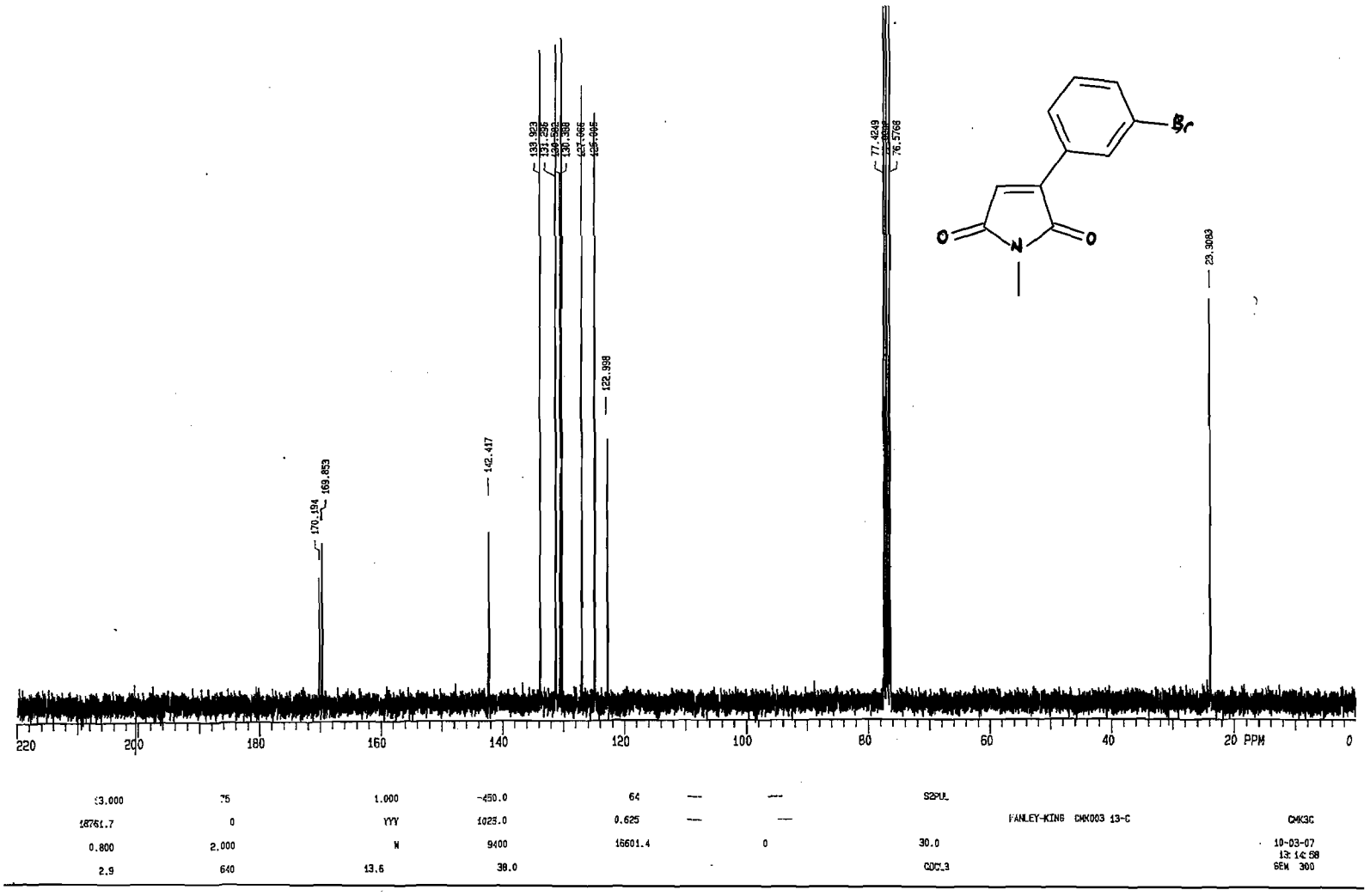
170.194
169.853
142.417
133.923
131.256
130.388
127.466
125.865
122.998
77.4249
76.5768
29.3083
Br
O
N
O
220
200
180
160
140
120
100
80
60
40
20 PPM
0
13.000 75 1.000 -450.0 64 S2PUL
16761.7 0 YYY 1023.0 0.625 FANLEY-KING CMK003 13-C CMK3C
0.800 2.000 N 9400 16601.4 0 30.0 10-03-07
2.9 640 13.6 38.0 CDCl3 13:14:58
SEM 300

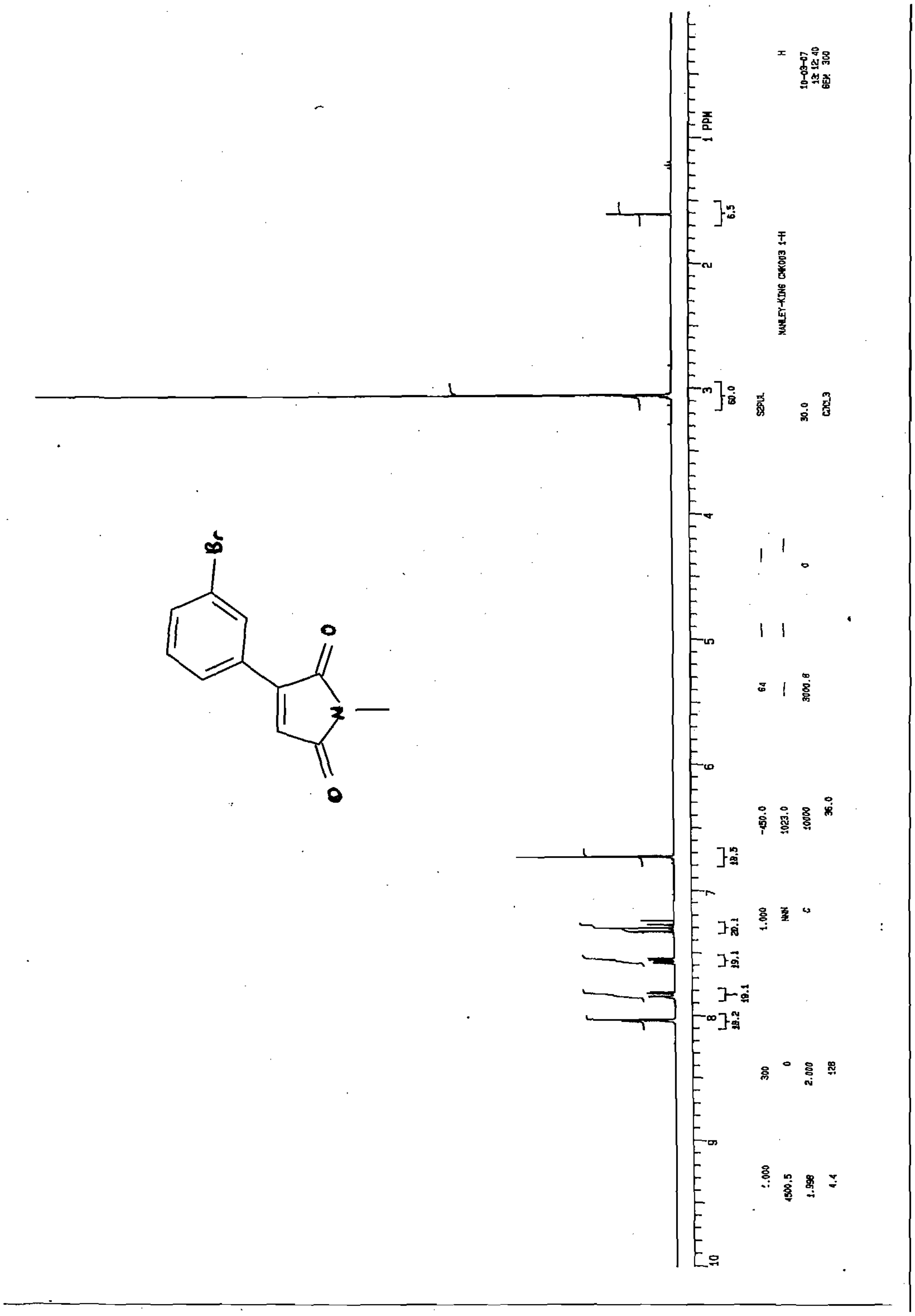
Br

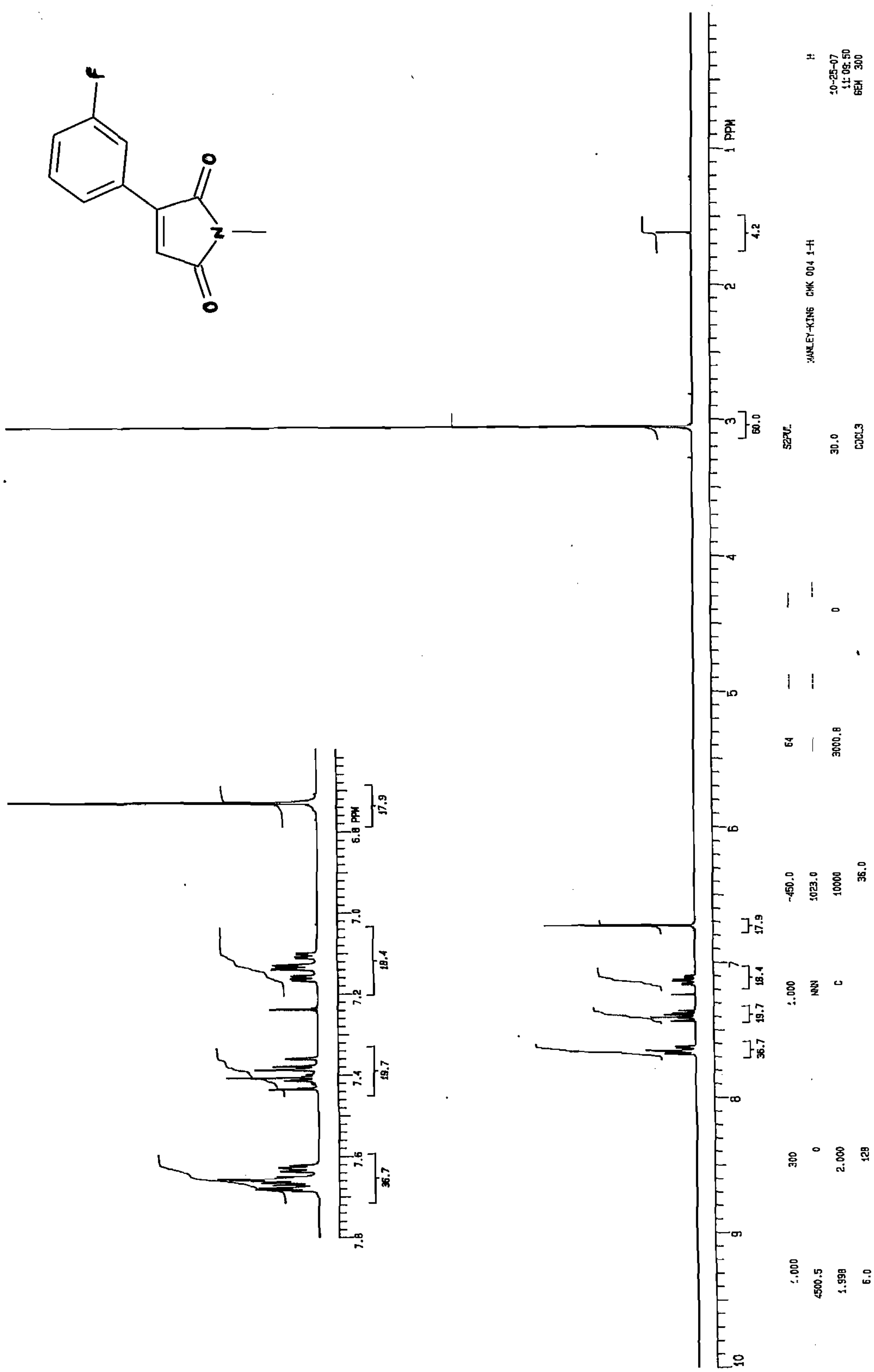

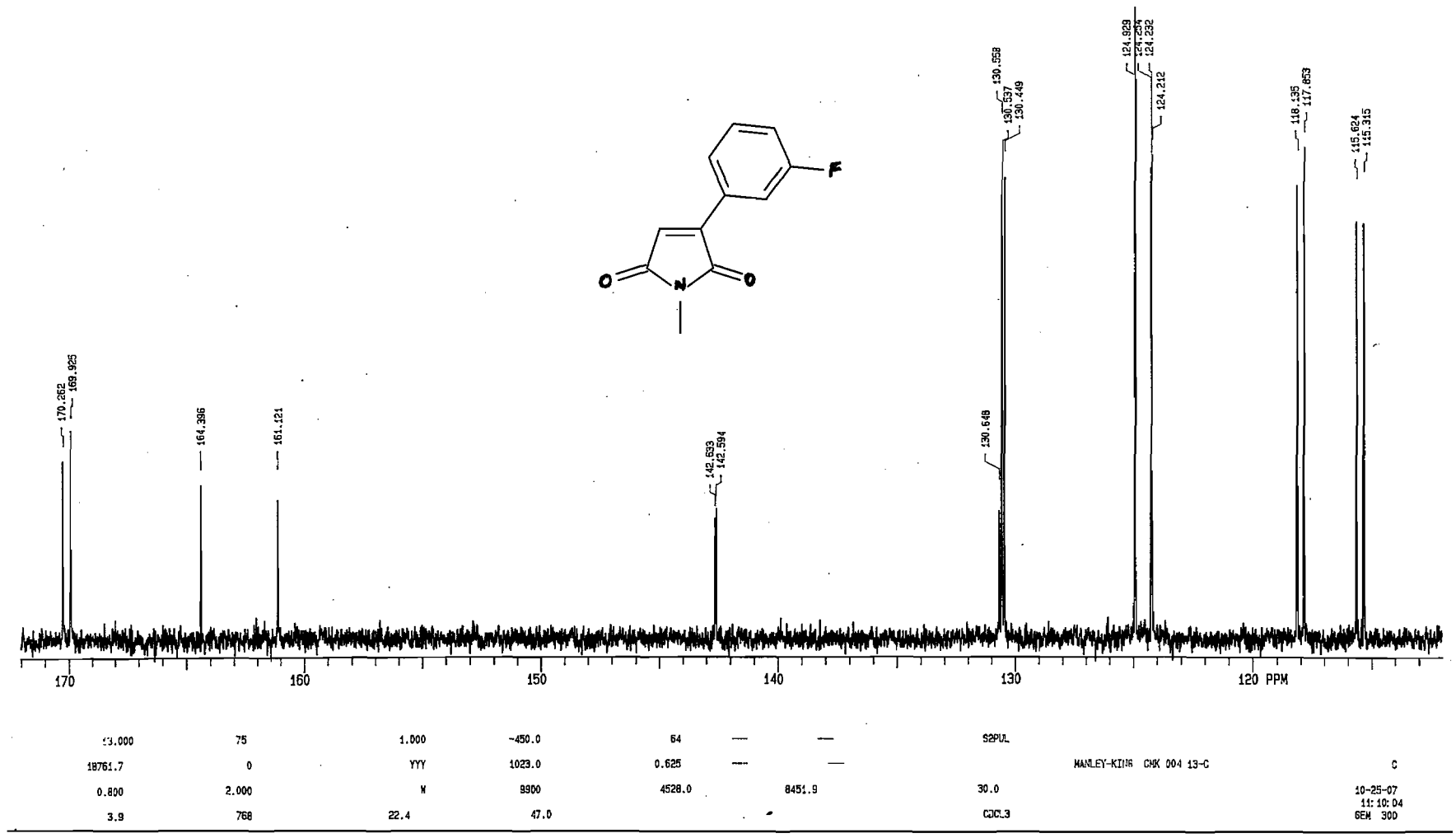
170.262
169.925
164.396
161.121
142.633
142.594
130.648
130.558
130.537
130.449
124.929
124.584
124.232
124.212
118.135
117.853
115.624
115.315
F
O
N
O
170
160
150
140
130
120 PPM
13.000 75 1.000 -450.0 64 S2PUL
18761.7 0 YYY 1023.0 0.625 MANLEY-KING CMK 004 13-C C
0.800 2.000 N 9900 4528.0 8451.9 30.0 10-25-07
11:10:04
3.9 768 22.4 47.0 CDCL3 GEM 300

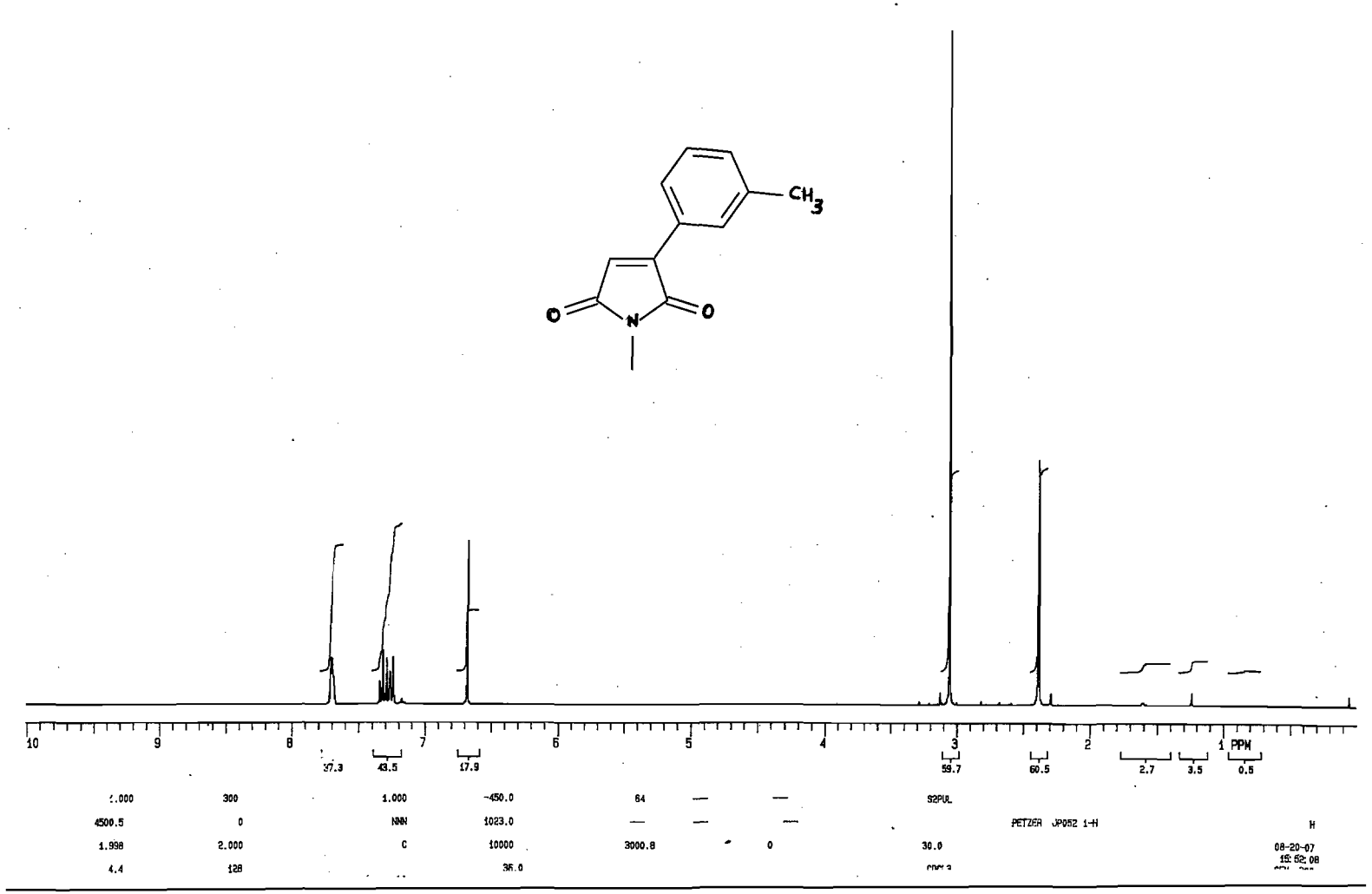
CH3
O
N
O
10
9
8
7
6
5
4
3
2
1 PPM
27.3
43.5
17.9
59.7
60.5
2.7
3.5
0.5
1.000 300 1.000 -450.0 64 S2PUL
4500.5 0 NNN 1023.0 PETZER JP052 1-H H
1.998 2.000 C 10000 3000.8 0 30.0
4.4 128 36.0
08-20-07

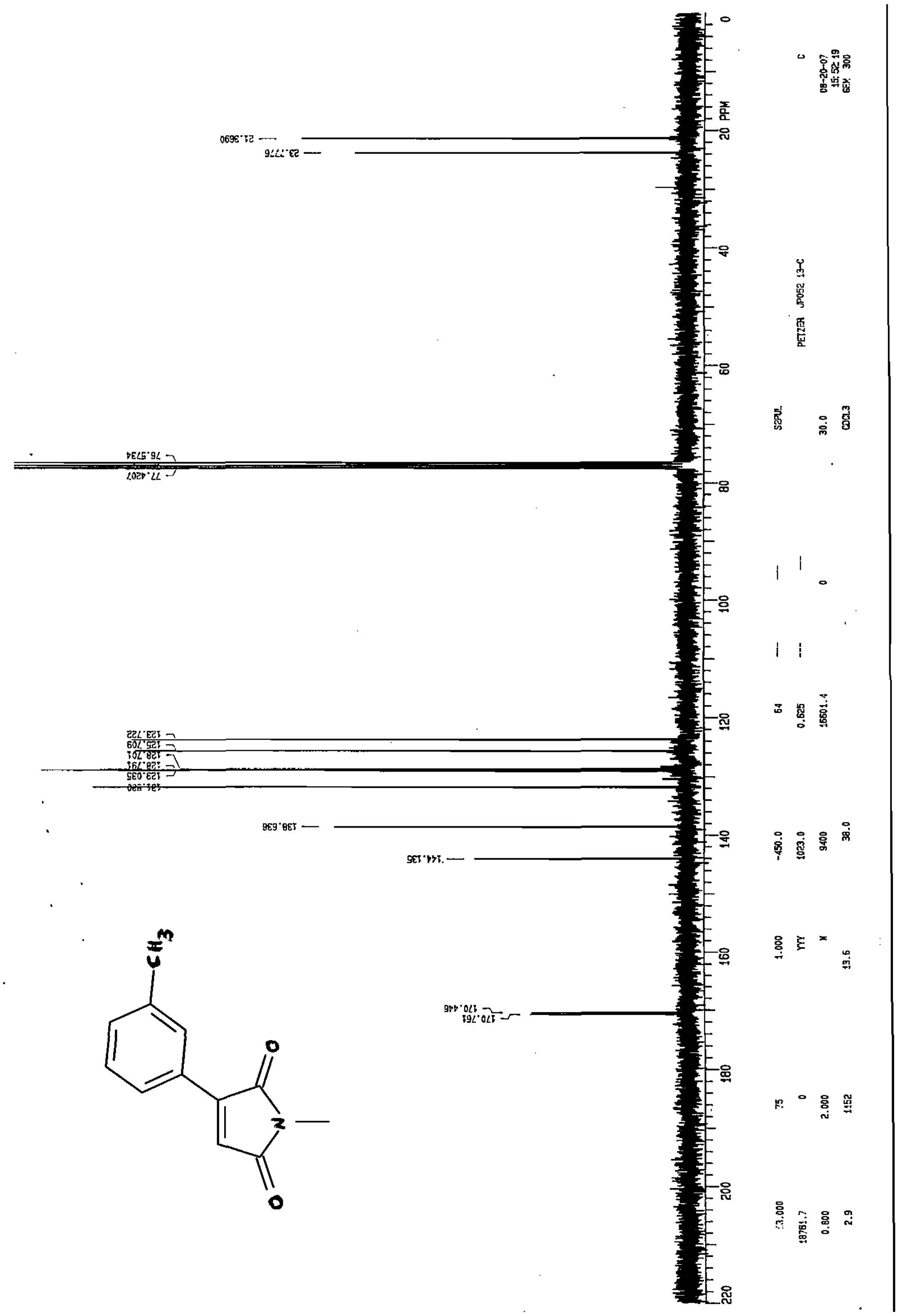

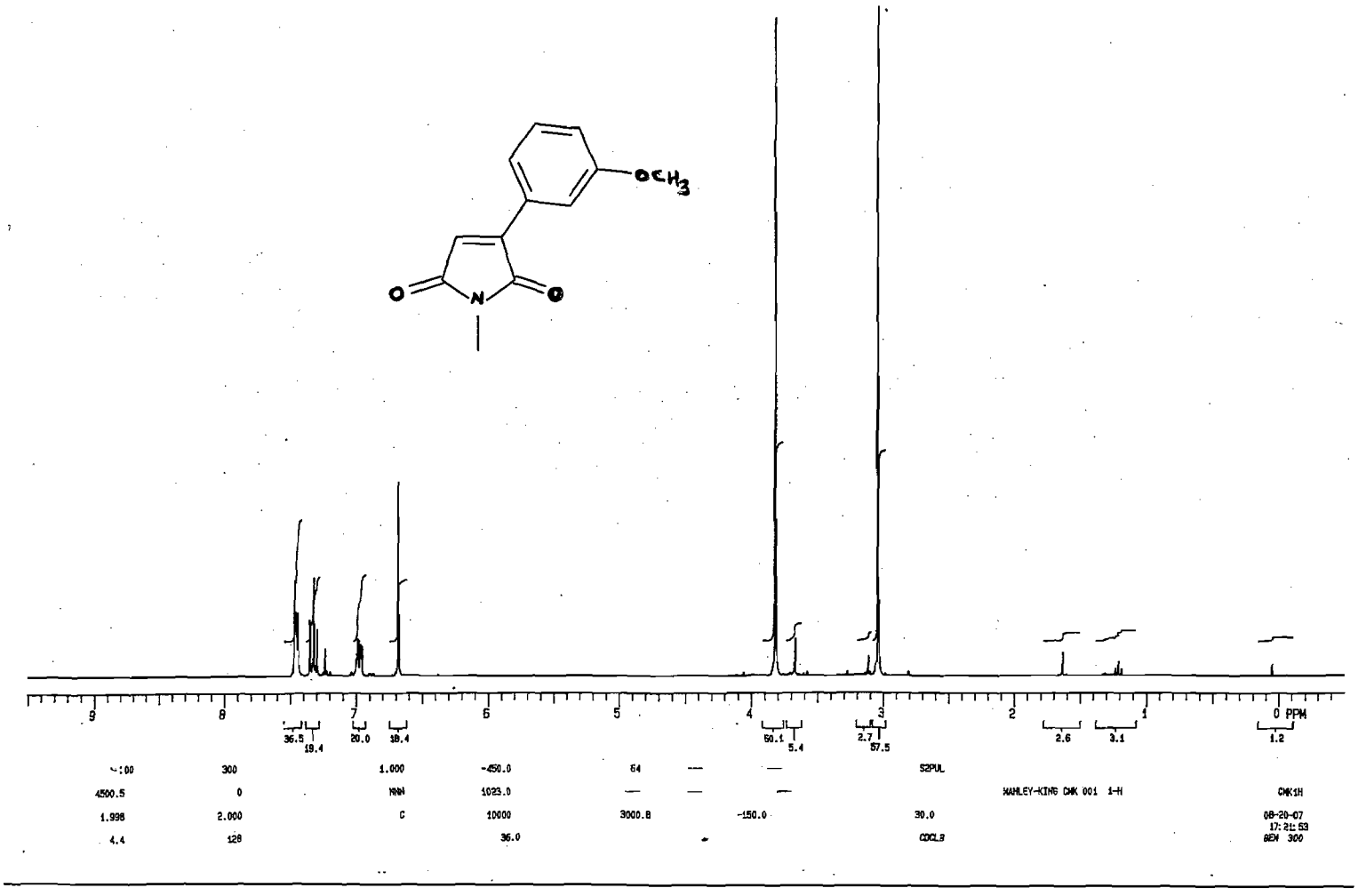
OCH3
O
N
O
9
8
7
6
5
4
3
2
1
0 PPM
36.5
19.4
20.0
18.4
50.1
5.4
2.7
57.5
2.6
3.1
1.2
300
1.000
-450.0
64
S2PUL
4500.5
0
MNN
1023.0
MAHLEY-KING CMK 001 1-H
CMK1H
1.998
2.000
C
10000
3000.8
-150.0
30.0
08-20-07
17:21:53
4.4
128
36.0
CDCL3
BEM 300

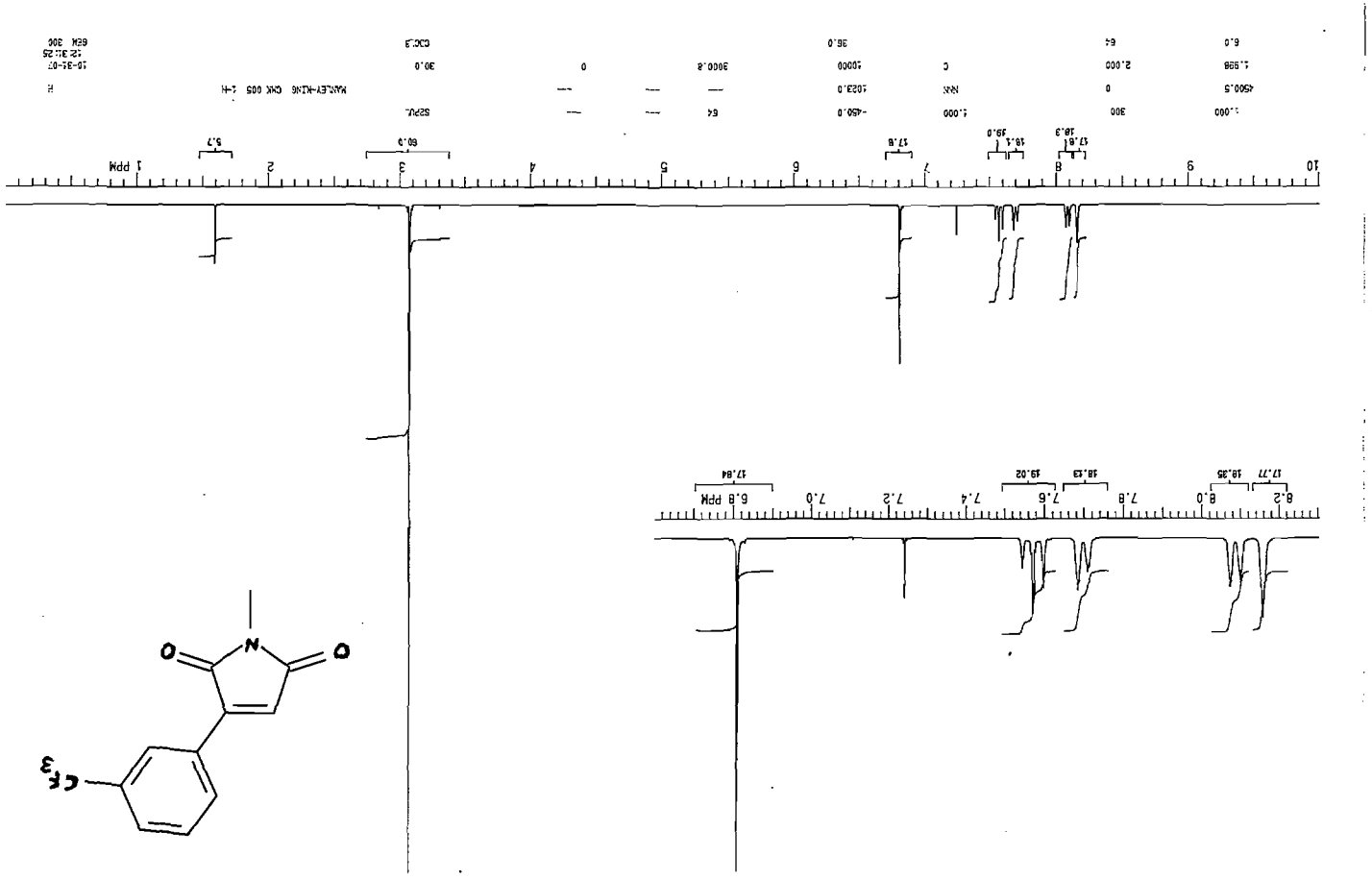
O
N
O
CF3